(JPL CONTRACT NO. 950239)

DOCUMENT NO. 64SD540

9½-FOOT DIAMETER MASTER AND MIRROR

FINAL REPORT

Prepared for

CALIFORNIA INSTITUTE OF TECHNOLOGY
(JET PROPULSION LABORATORY)
4800 OAK GROVE DRIVE
PASADENA, CALIFORNIA

MARCH 20, 1964

GENERAL ELECTRIC

A Department of the Missile and Space Division

JPL

CONTRACT NO. 950239

DOCUMENT NO. 64SD540

(NASA CR53813; 64SD540) OTS: $ cite only see cover

9½-FOOT DIAMETER MASTER AND MIRROR

FINAL REPORT

This work was performed for the Jet Propulsion Laboratory, California Institute of Technology, sponsored by the National Aeronautics and Space Administration under Contract NAS7-100.

Prepared for

CALIFORNIA INSTITUTE OF TECHNOLOGY
(JET PROPULSION LABORATORY)
4800 OAK GROVE DRIVE
PASADENA, CALIFORNIA

MARCH 20, 1964

auth → J. J. Guy, Project Manager, Solar Concentration Project

20 mar. 1964 221p rpls

105 58 42

① GENERAL ELECTRIC Co.
② A Department of the Missile and Space Division
Valley Forge Space Technology Center
P.O. Box 8555 • Philadelphia 1, Penna. Pa.

TABLE OF CONTENTS

TABLE OF CONTENTS (Continued)

TABLE OF CONTENTS (Continued)

LIST OF ILLUSTRATIONS

LIST OF TABLES (Continued)

LIST OF TABLES

LIST OF ILLUSTRATIONS (Continued)

LIST OF ILLUSTRATIONS (Continued)

1. INTRODUCTION

Spincasting is not new or novel. The principle has been known since Newton's laws were first applied to derive the basic theories of hydrodynamics, and even before that parabolic shapes of spinning liquids were noted by many mathematicians In 1901 Albert Krank of Warkaue, Grand Duchy of Finland, Imperial Russia, was granted a U.S. patent for a method of capturing a liquid paraboloid in solid form. In 1908 the famed American physicist, R.W. Wood[1], observed the stars and planets in his spinning dish of mercury, the first scientific approach using spincasting for high precision optics.

The history of more recent applications of spincasting to end item requirements was begun in 1952 at the Aeronautical Electronic and Electrical Laboratory, U.S. Naval Air Development Center, Johnsville, Pennsylvania, where spincastings with epoxies, phenolics and polyester resins were spun on a 78-rpm record turntable. Paraboloids formed were used for X-band antennas. This work was followed by many other scientific contributors, George Haas[2], William Erbe[3], A. P. Bradford[4], Saxton and Kline[5] and many others. General Electric became interested in the process in 1958 as applied to the manufacturing of large, highly accurate tooling for the development of solar collectors.

Since the immediate advantage of spincasting is that the initial paraboloid formed is a theoretically perfect parabola (whereas in machining processes involving cutting, hewing, and grinding the object only approaches the parabolic shape), spincasting has been evaluated and chosen as a worthy development to replace mechanical processes. This is not to say that spincasting has been without problems. Starting in 1958, GE funded a plastic development program to solve the major problems associated with finding materials that would capture the true parabolic shape of a

spinning liquid. The problem was to find materials or combinations of materials that would be transformed into solids during spinning from the liquid stage with a minimum of shrinkage, surface deformation, and surface finish loss.

At present plastic technology and engineering has been able to develop plastics that will keep their surface finish (to less than 1/2 rms) and design spincasting equipment which will give slope errors of less than 2 minutes of arc over 98% of the area. Eventually smaller slope errors can be achieved by further sophisticating the spincast mechanisms. The tooling produced by spincasting is adaptable to many processes such as electroforming and stretchforming. In both electroforming or stretchforming, the process involves the following steps:

a. Spincast a female master.

b. Electroform into the female master a male replica. For less stringent accuracy the replica of the female spincasting can be developed by plastic lay-ups or casting a plug within the female shape.

c. From the male replica, a second-generation replica is electroformed or the male replica can be used as a dye to stretch-form the second-generation mirror.

The success of the spincasting program offers new breakthroughs not only in the development of solar concentrators but in the areas of optics, IRs, radio telescopes and radar antennas.

On 30 August 1962 work was started on contract JPL 950239 to produce from the plastic spincast female mold a male nickel electroforming from which a nickel electroformed 9 1/2-ft collector would be fabricated. Both the nickel electroformed male master (permanent tooling) and nickel mirror were delivered to the Jet Propulsion Laboratory on 25 November 1963. This work was performed in three phases as defined in the JPL work statement whose abstract is as follows:

> "General Electric will design, fabricate and optically inspect a spincast female master suitable for reproducing a 9.5-foot diameter male paraboloidal mirror master. This male master shall be suitable for the reproducing of light-weight, high-quality paraboloidal solar concentrators with the

design objective of collector absorber efficiencies of seventy-five percent (75%) when operating a 2000°K black-body cavity. This will be accomplished in two (2) phases as follows:

"(1) Phase I

A. Design and fabricate a spincast mold back-up structure.

B. Spincast a female mold master.

C. Perform optical inspection of the spincast female mold master.

D. Design and fabricate a male back-up structure.

"(2) Phase II

A. Electroform a male mirror master.

B. Design and fabricate a mirror back-up structure.

"After the completion of Phase II, General Electric will replicate in Phase III a concentrator by electroforming a thin skin over the male master, separating, inspecting and aluminizing same as follows:

"(1) Phase III

A. Electroform mirror.

B. Optically inspect mirror.

C. Aluminize mirror.

"At the conclusion of this program data will enable the correlation of:

1. Optical testing to calorimetric testing.
2. Replication of spincasting by electroforming.
3. Replication of electroforming by electroforming.

"This will be provided when the following action and interactions are completed:

1. Optical inspection of the female spinning.
2. Optical inspection of the female electroforming against the same standard used in the inspection of the female spinning.
3. Calorimetric testing of finished mirror by JPL."

At the writing of this report only the calorimetric testing of the finished mirror remains (presently in progress at JPL). Optical data has shown that replication of a

plastic spincasting by electroforming and replication of an electroforming by electroforming for the purpose of producing solar concentrators of high accuracy is now well within the state of the art. The successful completion of this program has opened the door to collectors of any size requiring highly accurate parameters.

1.1 REFERENCES

1. R.W. Wood, Astrophysical Journal, XXIX. 164-176, (March 1909).
2. George Hass and James R. Jenness, Jr., Journal of the Optical Society of America, 48:86-87 (1958).
3. George Hass and William W. Erbe, Journal of the Optical Society of America, 44:669-671, (1954).
4. A.P. Bradford, W.W. Erbe, and G. Hass, Journal of the Optical Society of America, 49:990-991, (1959).
5. J.H. Saxton and D.E. Kline, Journal of the Optical Society of America, 60, 1103-1111, (1960).

2. SUMMARY

2.1 SPINCASTING

Phase I of this program consisted of providing a high-quality spincasting which could be electroformed. The spincasting program was successfully completed after the 10th pour of resin. Originally only three pours were planned.

Prior to the first pour the mold is placed on the turn table and sealed to prevent the entry of dirt; the first coat is placed on the spinning structure to fill the unevenness of the spin structure and gather dust. The second and third coats are poured to bring the surface up to its finish and slope specification. Once the mold is opened, this procedure must be repeated; however, in some instances only two coats are required.

After the third pour of the Phase I program, the mold was opened and optically inspected. Although the inspection indicated that the mold was within specification (i.e., its geometry was within specified tolerances), a haze and faint radial line (orange peel) condition on the surface of the mold was noted. A design review was held and it was decided to make minor modifications to the design of the system and spin again. Pours 4 and 5 were made, and the mold was again opened for inspection. Pour No. 5 was observed to be poorer in quality than pour No. 3 and marked with strong haze and stronger radial lines emanating from the center and continuing to the periphery. The lines had the appearance of bicycle-wheel spokes. General Electric asked that the contract be temporarily stopped and that GE be given 12 weeks to solve the problem on company funds; permission was granted. An ensuing development and investigation program determined the cause of the haze and orange-peel problem. The orange-peel effect was caused by torsional vibration and the haze by flow-additive

breakdown. Spincasting was again resumed. After pour No. 8, the mold was opened and inspected; a highly satisfactory end product without haze or radial lines was observed. Unfortunately, all pours were made on top of each other producing a resin structure 0 5/8-in. thick. While machining the outer edge for electroforming attachments, the plastic delaminated from the substrate, cracking in the process. All plastic was removed from the aluminum substrate, a bonding agent that would adhere both to the aluminum and the plastic was painted onto the substrate. Pours No. 9 and 10 were made. Pour No. 10 was entirely successful and the program was continued. To ensure process repeatability and to verify controls several spincastings have been made after Pour No. 10; all spinings have been without problems.

2.2 ELECTROFORMING

The electroforming tasks in this program are divided into two phases: 1) fabrication of the nickel male master and 2) fabrication of the female mirror.

2.2.1 MALE MASTER

While the problem of electroforming the male master to optical accuracies is a formidable new requirement imposed upon an old process, it becomes compounded when dealing simultaneously with very large shapes and with relatively unstable substrates. To illustrate this point, one only has to consider the small, one-inch laser corner cubes which were unsuccessfully electroformed even in well-controlled laboratory cells despite numerous industry-wide attempts, and despite the use of ideally inert glass or metal substrates. The major difficulty in obtaining optical quality reproduction is the presence of poorly-understood electroforming stresses; these are not only difficult to control but previously could not even be measured more accurately than $\pm$600 psi. This wide range is commonly called a "zero" stress region (although this much stress can ruin the optics). A breakthrough development in stress work occurred with the development by GE-MSD of

an order-of-magnitude more accurate stress measuring device which is also sufficiently rapid to be used as a process control throughout the entire process. The new stress device was first put to practical use in the present program; its highly satisfactorily performance was demonstrated both by control samples and depth-of-thickness measurements at the completion of the process. Since stresses are an overriding function of current density which in turn determines the depth of thickness obtained in a given time interval, direct comprehension of the method was possible and the program demonstrated that predetermined—including true zero—stress values are now within easy reach of the electroforming process, regardless of the sizes involved.

The last remaining problem to the fabrication was the chemical instability of the substrate. The critical period occurred during the preparation cycle, when the substrate had to undergo exposures to various cleaning, sensitizing, silvering and electroforming chemicals. These processes had to be identified and changed on numerous occasions hand-in-hand with the spincasting development work described in Section 5.

Finally when mutually compatible processes were formulated and the fabrication started, it was found that difficulties arose from an unexpected factor—the slow cooling rate of the spincast structure—which was $5^{o}F$ too high. Surface temperature of the epoxy during silvering nearly ruined the specularity of the surface area and left permanent blemishes on the resulting mirror. Looking back the solution to this problem appears simple, and more experience with this process would easily have avoided the problem.

During the process an anode was accidentally dropped on the mold surface causing an ugly blemish; however, this sort of accident should be comparably easy to avoid in future work by using better trained workmen.

Despite such minor accidents, the process dramatically demonstrated that the truly formidable difficulties which stood in the way of optical electroforming, i.e., distorting stresses and control over large areas, can well be solved.

2.2.2 FEMALE MIRROR

The electroforming of the mirror was less difficult since the substrate at this time was metallic nickel. Cell geometry and stress control solution was already on hand from experience with the master; the anode design was such as to preclude any accidental falling of objects onto the surface.

The separation techniques using a silverfilm as a parting layer performed gratifyingly well and a major problem was not encountered in this phase.

3. CONCLUSIONS AND RECOMMENDATIONS

3.1 ELECTROFORMING AND HANDLING

As with any research and development program technology, challenges must be met. This program had very few technology problems. One human error which left its mark on the end item - the 9 1/2' solar concentrator - was the improper silvering due to underestimation of the heat capacity of the epoxy mold (See Section 6.1.) This silver had to be removed by acid which in turn etched the surface of the plastic casting. This etching in turn degraded the specularity of both the master and finished collector. The reason for etching was analyzed and corrected; it would not be a problem on future spincasting. A minor but esthetically objectionable degradation occurred when a 19-lb electrode was dropped accidently onto the spincasting while electroforming of the male master was underway. This unfortunate accident made a radial spoke identation into the male master where it became a permanent record of the accident. Damage to the mirror occurred in shipping due to improper cushioning procedure; also it is planned to stress relieve the torus in any future work to minimize distortion to the peripheral areas.

It is recommended that the follow-on to this program be that of developing and making thin-skin, full-size, flight-weight collectors from the tooling produced under this contract. It would be advantageous however to first produce a new male electroformed paraboloid with a more specular finish free of any idendations using new tooling which has taken advantage of the technology developed to correct items that caused degradation. More perfect tooling would enable the pulling of thinner metal skins and could be used for both aluminum and nickel electroforming developments.

3.2 SPINCASTING

The time-consuming, expensive method of grinding accurate paraboloidal glass masters presents severe limitations where either large diameter surfaces or "fast

paraboloids" (deep-dish paraboloids) are required. In the process of spincasting, the paraboloidal shape is generated solely through the interaction of gravity and centrifugal forces. The basic simplicity of the process is particularly attractive where glass grinding is most difficult. The simplicity of spincasting remains the same whether fabricating small-diameter, large-diameter, shallow or deep-dish paraboloids.

To date GE-MSD has fabricated spincast paraboloids up to 35 feet in size where:

a. Angular shape errors have been held within 1.9 minutes of arc over 99.7% of the total area.

b. Surface smoothness has been held well below a 2-micro-inch finish (RMS). Indeed numerous paraboloids have been spincast with a surface smoothness of less than one-micro-inch finish over the entire surface.

By combining presently available material formulations with existing processing techniques, there is considerable justification to believe that surface errors can be maintained closer than 45 seconds of arc over 98% of the surface area.

The following recommendations have evolved from the data obtained and the observations made during spincast processing of the JPL 9-1/2 ft. diameter mold.

a. Processing:

Improved accuracy of slope error and increased surface specularity may be obtained with no change in the materials formulation by:

1. Utilizing a cover of uniform material and a paraboloidal shape which is uniformly spaced one and one-half inches from the cast epoxy surface.

2. Allowing the cover to remain sealed for a minimum of 48 hours at 70 to 75^{o}F after mold rotation is stopped.

b. Materials Formulation

The addition of a wetting agent solved the problem of haze discoloration, but it also increased the propensity to form unacceptable entrapped gas bubbles on the surface. Additional sampling work should be evaluated utilizing other wetting agents in order to reduce surface tension and further minimize the bubble problem.

c. Spincast Mold Substructure

Owing to its superior resistance to electroform solutions, stainless steel is highly recommended for use in the fabrication of spincast mold substrates. The surface of the stainless structure should be base coated with a material compatible with and more flexible than the spincast material. The purpose of the base coat should be that of a primer to promote adhesion and also to act as a flexible buffer to minimize the effect of thermal differential expansion between the stainless and spincast epoxy layers.

d. Spintable

Piggy-back mounting of the 9-1/2-ft JPL mold on the 30-ft space simulator structure increased the system rotatory moment of inertia approximately eight times. As a result, actual vibration measurements showed that torsional vibration of the mold-spintable system decreased significantly. It is recommended that balanced systems of high-rotatory moment of inertia be used in the casting of all spincast molds.

During operation of the spintable, intermittent variation in drive-motor input current induced a visible, significant increase in spintable oscillation as observed on the table dial indicators. Installation of a voltage-stabilizing transformer on the power input line to the Kinatrol spintable drive motor would alleviate this condition.

Both the standard Kinatrol 1% speed regulator and the more complicated 0.1% speed regulating system are presently installed at the spincast facility. To ensure the capability to continue table rotation, a throw switch should be installed to change the system circuit from the 0.1% control to the 1% speed control. Thus any malfunction of the more complicated electronic feedback system could be traced and corrected while the spintable continued to rotate under control of the standard Kinatrol system.

3.3 OPTICAL INSPECTION TOWER

The location of the immobile optical inspection tower directly over the spintable precludes use of the available overhead crane. At present the truss supporting the optical tower is rigidly mounted to the bridge crane rails. By changing the rigid mount to a rail mount, the entire optical tower could be made to traverse the crane

rails thereby granting use of the existing crane to the spincast facility. Suitable clamping devices would enable the optical tower to be placed and remain rigidly in position above the spintable for normal optical inspection.

4. SYSTEMS CONSIDERATIONS

4.1 MIRROR ACCURACIES REQUIRED TO ACHIEVE A 75% COLLECTOR-ABSORBER EFFICIENCY

Prior to the start of this contract, a theoretical study was made of the effects of mirror inaccuracy and orientation-angle error on collector-absorber efficiency for a collector operating in free space in the vicinity of earth. In these calculations the effects of mirror inaccuracy were determined by a method considered to be quite precise while the effects of orientation angle error were determined in an approximate, but conservative, manner. Both procedures are discussed in more detail in Sections 4.2 and 4.3 of this report.

Results indicate the following requirements must be met in order to achieve a collector-absorber efficiency of 75%.

a. Assuming Zero Orientation Angle Error — Assuming that the mirror has a Gaussian distribution of angular errors over its surface, the 3σ value* of angular error must be less than 12 minutes. (See Figure 4.1-1.)

b. Including Effects of Orientation Angle Error — Figure 4.1-2 shows collector-absorber efficiency as a function of orientation angle error for various 3σ values of mirror error and a mirror rim angle of 45 degrees. (As will be discussed in more detail in Sections 4.2 and 4.3, a mirror of this rim angle gives performance which, for all practical purposes, can be considered to be equal to the optimum performance for the conditions considered here.)

   It can be concluded from this figure that achievement of 75% collector-absorber efficiency requires that both the 3σ value of mirror error and the orientation angle error be somewhat less than 6 minutes.

*3σ is defined as the slope error which is not exceeded over 99.74% of the area.

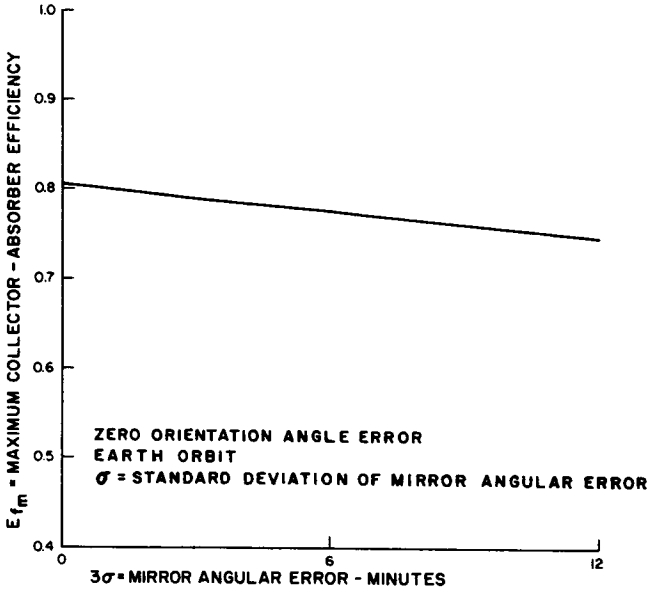

Figure 4.1-1. Maximum Collector-Absorber Efficiency

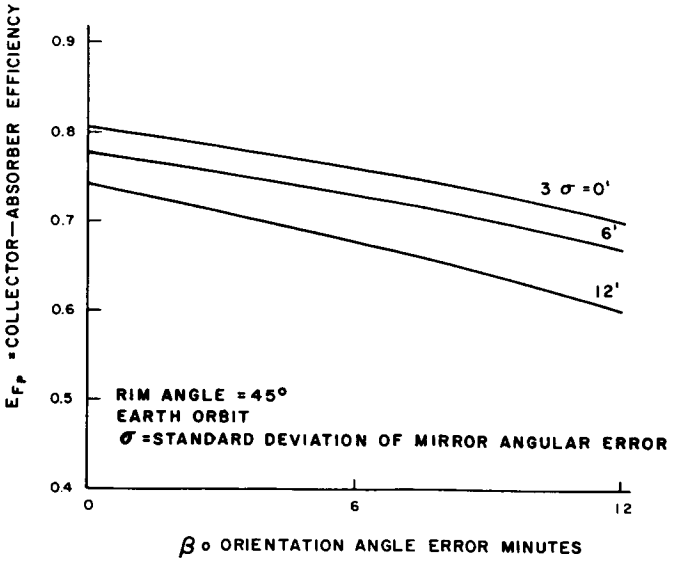

Figure 4.1-2. Peak Collector-Absorber Efficiency

Key assumptions involved in arriving at the preceding conclusions are:

a. Solar constant is 0.14 watt/cm^2.

b. Mirror reflectivity is 90%.

c. Five percent of the mirror area, based on rim diameter, is ineffective due to blockage by struts, absorber, holes, etc.

d. The absorber behaves as a black-body cavity having an emissivity and absortivity of 1.0 with a temperature of 2000 K.

e. The mirror angular errors are assumed to have a Gaussian distribution centered about zero error.

f. Thermal distortion of the mirror is assumed either to be zero or to be compensated for in the design.

g. The orientation angle error is assumed to be invariant with time.

h. Collector-absorber efficiency is defined as the ratio of the net power absorbed in the cavity to the solar power intercepted by a circle having a diameter equal to that of the collector.

4.2 OPTIMUM RIM ANGLE DETERMINATION

A theoretical investigation was made to determine the values of collector rim angle which result in maximum collector-absorber efficiency for various mirror error angles and orientation error angles. (Collector rim angle is defined as the angle between the axis of symmetry of the mirror and a line drawn from the focal point to a point on the rim.) The investigation (including the effects of orientation angle error) was not completed in the desired detail, but rather complete results were obtained for zero orientation angle error. These results, and the procedure used in obtaining them, will be discussed here.

The fact that an optimum rim angle exists as a function of mirror error angle, orientation error angle, and cavity temperature can be shown qualitatively. It is well known that, for a given mirror and orientation angular error, the minimum aperture diameter which will pass all of the energy reflected from the collector

occurs when the collector rim angle is slightly less than 45 degrees; the actual value of this rim angle being given by:*

$$\phi = 45^{o} - 1/2\ (B_S + 2B_C + B_O),$$

where:

ϕ is the collector rim angle;

B_S is the half angle subtended by the sun (about 16 minutes at the earth);

B_C is the maximum mirror error angle, assumed to occur at the rim;

B_O is the orientation angle error.

On the other hand, the optimum aperture diameter for a given collector, angular errors, and generator cavity temperature will be something less than that diameter which passes all of the reflected energy from the collector. This occurs because of the trade off between energy entering the aperture and that reflected and re-radiated back out through the aperture as aperture diameter is varied. Moreover, the higher the cavity temperature, the smaller this optimum diameter will be, with the other items constant. Furthermore, in considering the nature of the flux distribution in the plane of the aperture for geometrically perfect collectors having zero orientation angle error, the peak flux density, occurring within the sunspot diameter, increases as the rim angle increases. As one goes to higher and higher cavity temperatures, the optimum rim angle for maximum net energy to the generator will, therefore, increase for collectors having zero geometric orientation angle errors. On the other hand, effects of geometric and orientation angle errors increase with rim angle. It is apparent that detailed analysis is required to determine the optimum rim angle for a specific case, but generally, it can be said that it should not be less than about 45 degrees and will be something more than that as the cavity temperature is increased.

The procedure used in determining the optimum rim angle and the resultant collector-absorber efficiency, for the conditions of this report, was as follows:

*Semiannual Technical Summary Report, Solar Thermionic Electrical Power System, 29 February 1960 to 30 June 1960, Contract No. AF 33(616)-7008.

1. The flux distribution in the plane of the aperture was determined for rim angles of 45^{o}, 51^{o}, 57^{o}, and 64^{o} and for various values of mirror angular error assumed to be constant over the entire collector. The calculation was carried out on an IBM 7090 computer using a procedure developed on another program. It takes into account the distribution of solar intensity across the sun's disc but assumes zero orientation angle error. It also assumed that mirror errors occur only in the meridional plane and not in the circumferential direction. This latter assumption is made based on results of optical inspections of fabricated parts.

   Typical results from this calculation for a rim angle of 45^{o} are shown in Figure 4.2-1, where the collector-aperture geometric efficiency, η_{cg}, is plotted as a function of the ratio of the radial dimension, X, in the plane of the aperture to the mirror diameter, D_c. The collector-aperture geometric efficiency is here defined as the ratio of the energy entering the aperture to the energy reflected from the collector, assuming no blockage of the reflected energy due to struts, etc. It is obtained by integration of the flux density in the plane of the aperture.

   (After the calculations for this report were well underway, some inaccuracies were discovered in the flux distribution for mirror angular errors of 2, 4, and 6 minutes at the low values of X/D_c. Inasmuch as the maximum collector-absorber efficiencies occur at relatively high values of X/D_c, it is believed that these inaccuracies have only a minor effect on results, and so they were not corrected.)

2. A Gaussian distribution of mirror error angles was then assumed, centered about zero error angle. (This assumption is believed to be reasonable based on past experience of this company in manufacturing mirror masters.) For any given 3σ value defining the magnitude of the error distribution, the resulting collector-aperture geometric efficiency was then determined, wherein values such as those shown on Figure 4.2-1 were weighted according to the Gaussian distribution and then used as input data.

   Collector-aperture geometric efficiency for a rim angle of 45 degrees and three values of the standard deviation of mirror error is shown in Figure 4.2-2. Similar curves were obtained for the other rim angles.

3. The collector-absorber efficiency was then calculated for each rim angle and various values of mirror error from the relation for a black-body cavity of:

$$E_f = \eta_{cg}\ \eta_r\ \eta_a - \frac{\sigma T^4}{qs}\left(\frac{D_a}{D_c}\right)^2$$

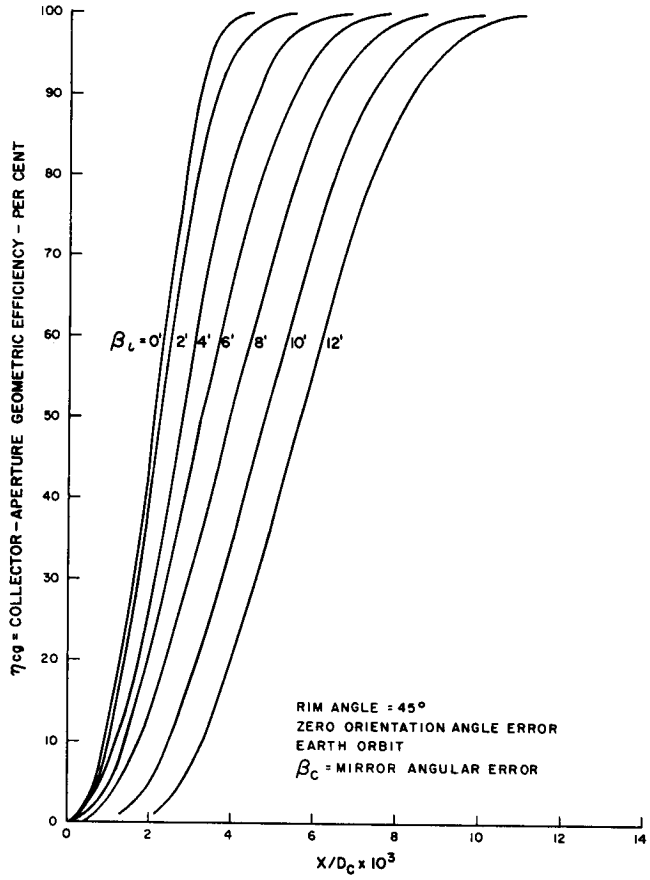

Figure 4.2-1. Collector-Aperture Geometric Efficiency for Constant Monitor Error Angle

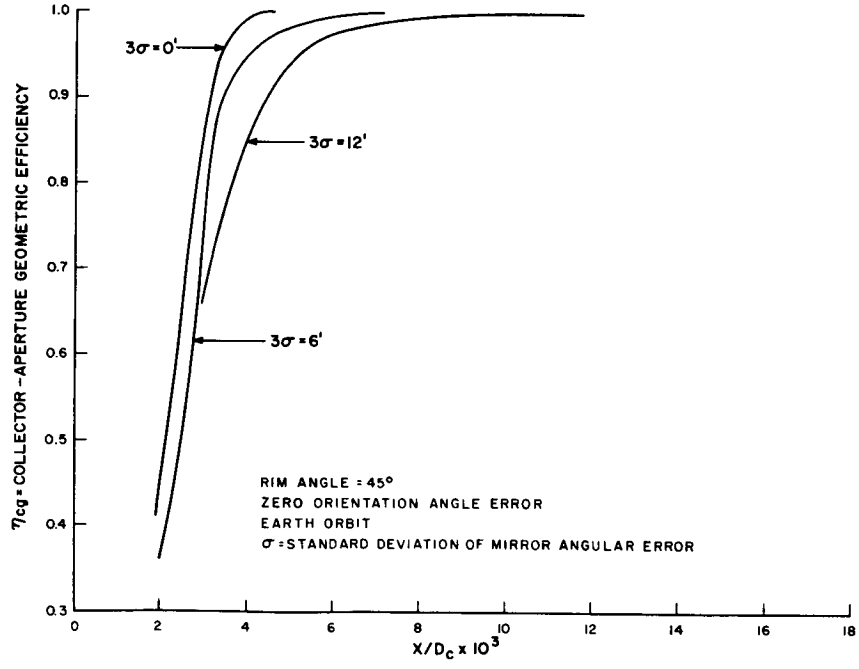

Figure 4.2-2. Collector-Aperture Geometrical Efficiency for Gaussian Distribution of Mirror Angular Error

Where:

E_f is the collector-absorber efficiency;

η_{cg} is the collector-aperture geometric efficiency;

η_r is the mirror reflectivity (0.9);

η_a is the mirror effective area factor (0.95);

q_s is the solar constant (0.14 watt/cm^2 at earth);

σ is the Stefan-Boltzmann constant q (5.67×10^{-12} watt/cm^2 -$^oK^4$);

T is the cavity temperature (2000K);

D_a is the aperture diameter;

D_c is the mirror diameter.

Typical results for a 45-degree rim angle are shown in Figure 4.2-3.

4. Peak values of collector-absorber efficiency were then selected from Figures such as 4.2-3 and results are shown on Figure 4.2-4 as a function of rim angle for various values of mirror error.

5. Finally, a cross-plot of the maximum values of Figure 4.2-4 results in Figure 4.1-1 which has been previously referred to and which gives the maximum obtainable efficiency as a function of mirror error angle for zero orientation angle error.

Reviewing the results just presented, the most striking feature is the relative insensitivity of collector rim angle. Referring to Figure 4.2-4, it is seen that this efficiency is essentially constant for rim angles between 45 and 57 degrees but thereafter begins to fall off. As a matter of fact, the accuracy of the calculations is not considered to be sufficient to detect, in this range, the actual value of the optimum rim angle as a function of mirror error angle.

This is not only an interesting result, but useful in the sense that it means that for absorber temperatures of 2000K or less, one has considerable freedom in the choice of rim angle from an efficiency standpoint. Anticipating somewhat the results from the study of orientation angle error, it means that final choice of rim angle in a given case will probably, therefore, be determined from structural or packaging considerations.

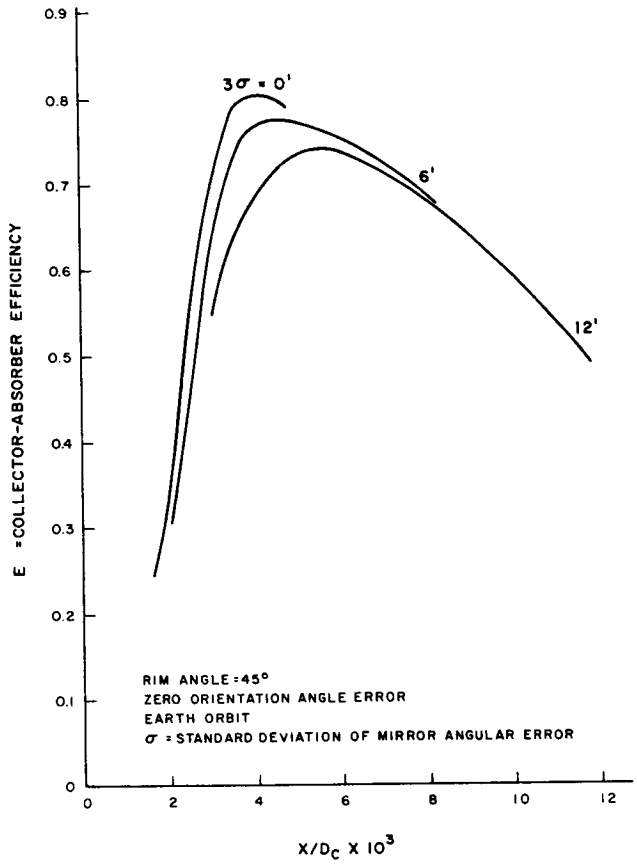

Figure 4.2-3. Collector-Absorber Efficiency

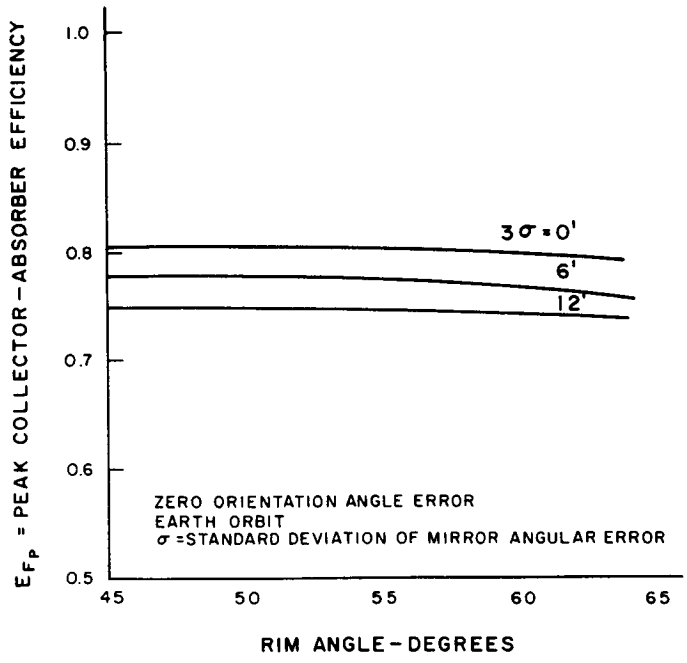

Figure 4.2-4. Peak Collector-Absorber Efficiency

4.3 MISORIENTATION STUDY RESULTS

An approximate, but conservative procedure was used in the analysis of the effect of orientation angle error. In this procedure, the results such as shown on Figure 4.2-2 were shifted to the right by an amount equal to twice the radial displacement in the aperture plane of a ray from the rim of the collector which is misoriented by the amount of the orientation angle error. Calculations for collector-absorber efficiency were then carried out as before, resulting in curves such as shown on Figure 4.3-1, which apply for a 45-degree rim angle and a perfect collector.

This procedure is conservative in that, except for the extreme case where the collector-aperture efficiency approaches, in the limit, 100%, the collector-aperture efficiency curve will not be shifted as far to the right as used in the calculations. Actual efficiency values would, therefore, be somewhat higher than shown in Figure 4.3-1.

By determining curves such as Figure 4.3-1 for a number of rim angles and selecting the peak values of efficiency, Figure 4.3-2 results. This Figure shows the peak collector-absorber efficiency as a function of the rim angle for various orientation angle errors and for a perfect collector. Similar curves could be calculated for other mirror error angles.

Again, the relative insensitivity of collector-absorber efficiency to rim angle will be noted. It is to be expected, however, that results at higher values of mirror error would show somewhat more sensitivity.

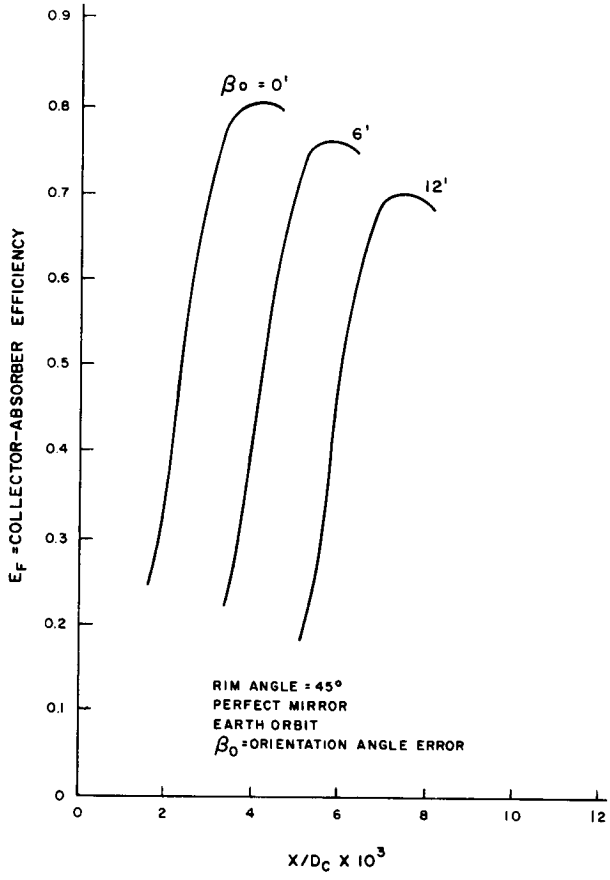

Figure 4.3-1. Collector-Absorber Efficiency

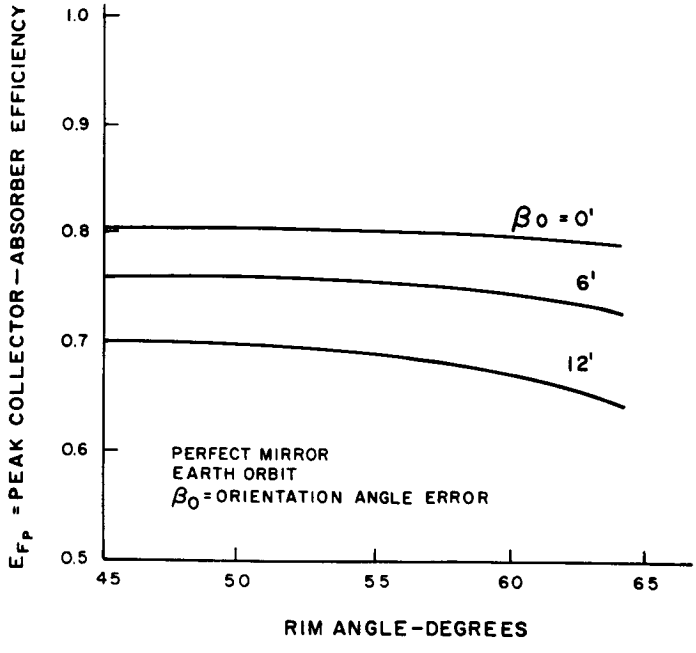

Figure 4.3-2. Peak Collector-Absorber Efficiency

5. FEMALE SPINCAST MASTER

5.1 BACK-UP STRUCTURE DESIGN

5.1.1 DESIGN PHILOSOPHY

A three-point suspension design was used for the spincasting back-up support structure. This design makes the structure statically determinate for all loading conditions: spincasting, handling and electroforming. By placing the support points and sling pick-up points exactly vertically above and below each other, equal deflections and stresses of the structure are assured regardless of whether the structure is supported from below or suspended from above. The statical determinacy makes shimming of the structure on the spintable or in the electroforming tank unnecessary. There is no change in the epoxy surface from the condition of spincasting through handling and shipping to placing it on the floor of the electroforming tank.

The structure is designed so that the addition of weight caused by plating the male nickel master on the epoxy and placing the male back-up structure onto this will cause a distortion of the female master surface not to exceed one minute of slope. For handling purposes, an epoxy tensile stress limit of 2000 psi was set. A 6g vertical load was assumed during shipping of the spincast master to the electroforming vendor. Figures 5.1-1a and b show details of the structure. Figure 5.1-2 shows the triangular support by which it was mounted to the spintable. The structural analysis is shown in Appendix E.

Aluminum was chosen for fabricating the structure to keep the weight to a minimum. Because aluminum can be attacked by the electroforming solution if not properly protected, no tubes or similar shapes were used which would make it difficult to apply the stop-off. All handling hooks and support legs were fabricated from stainless steel to eliminate the necessity of protecting these critical areas.

Late in the program it was found that cathodic protection of the aluminum structure was sufficient to prevent corrosion damage. This alleviated the masking requirement. Still, fairly good masking techniques are recommended to preserve current distribution and protect nickel.

5.1.2 DESCRIPTION OF THE STRUCTURE

The mold support structure was a paraboloidal dish reinforced by an egg crate structure, shown in Figure 5.1-3. The three corners of this triangular channel structure served both as lifting points for the structure during handling and as mounting points when the structure was placed on the spin table or in the electroforming bath (Figure 5.1-4).

The egg crate was fabricated by positioning all of the cut pieces on a specially constructed flat table and tack welding them together. The triangular channel structure was then tack-welded to the egg crate. Each petal of the dish was intermittently welded on one side to each radial rib. The petals were welded together and the welds were ground flush. The entire assembly was then completely welded and stress relieved. Forming of the petals was done by a trial and error method on a vibrating single plane die-type machine using a plaster mold as a checking template.

Because air pockets would be formed when the structure was lowered into the electroforming bath, holes were drilled in each circumferential rib to permit the air to escape. These holes are not shown on (Figure 5.1-1), but are visible in Figure 5.1-3.

Dimensional checks after heat treating showed the dish to be well within the ±1/4-in. tolerance specified on the drawing. This tolerance is not a requirement for spincasting, but was used to keep the number of epoxy pours to a minimum. The spincasting of epoxy will form a true paraboloid of revolution regardless of the shape on which it is poured. However, because of the tendency of the epoxy base to "show through" on the surface, if the initial shape is far removed from the desired shape, more pours will be required to obtain an acceptable surface.

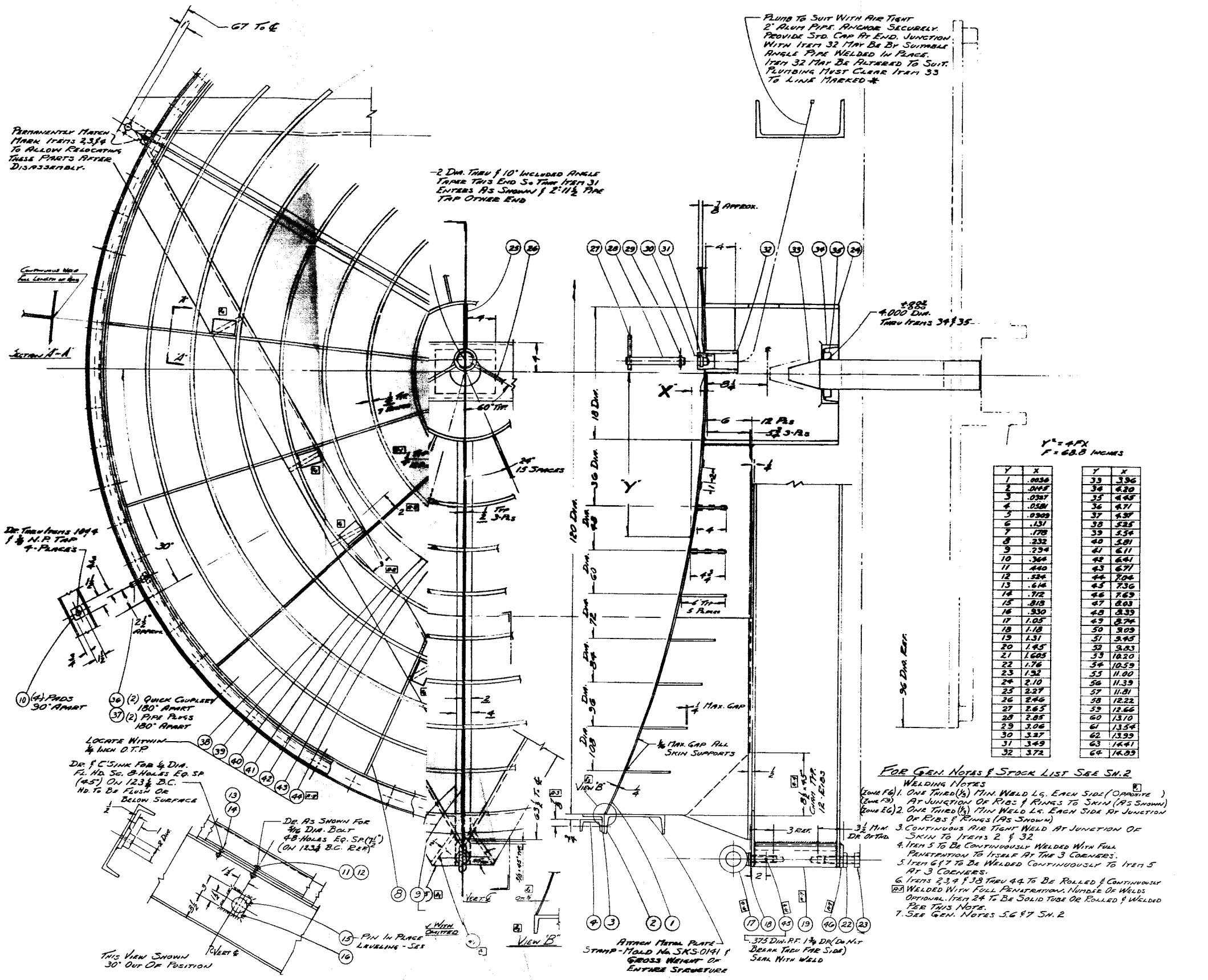

Y	X
1	.0036
2	.0145
3	.0327
4	.0581
5	.0909
6	.131
7	.178
8	.232
9	.294
10	.365
11	.440
12	.526
13	.616
14	.712
15	.813
16	.930
17	1.05
18	1.18
19	1.31
20	1.45
21	1.605
22	1.76
23	1.92
24	2.10
25	2.27
26	2.46
27	2.65
28	2.85
29	3.06
30	3.27
31	3.49
32	3.72

Y	X
33	3.96
34	4.20
35	4.45
36	4.71
37	4.97
38	5.25
39	5.54
40	5.81
41	6.11
42	6.41
43	6.71
44	7.06
45	7.36
46	7.69
47	8.03
48	8.39
49	8.74
50	9.09
51	9.45
52	9.83
53	10.20
54	10.59
55	11.00
56	11.39
57	11.81
58	12.22
59	12.66
60	13.10
61	13.54
62	13.99
63	14.41
64	14.89

Figure 5.1-1a. Spincasting Mold

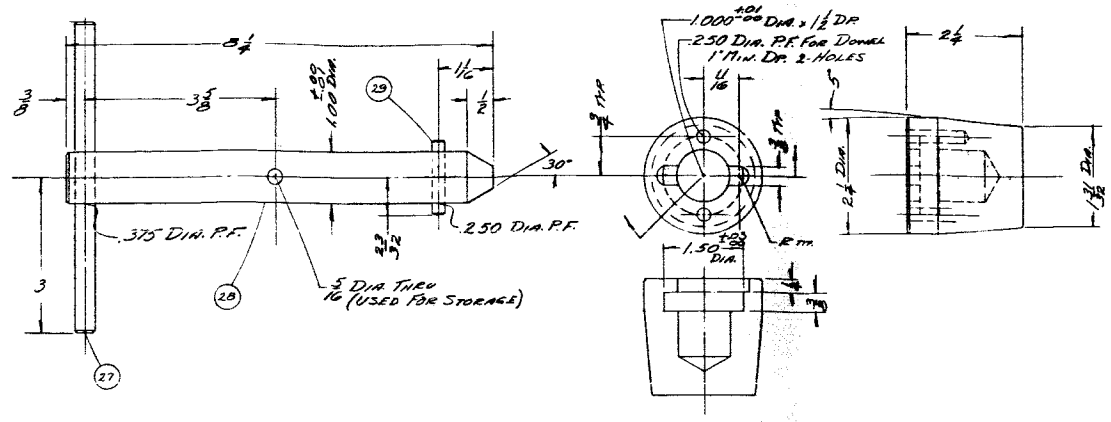

ITEM 31 MATL. H.R.S.

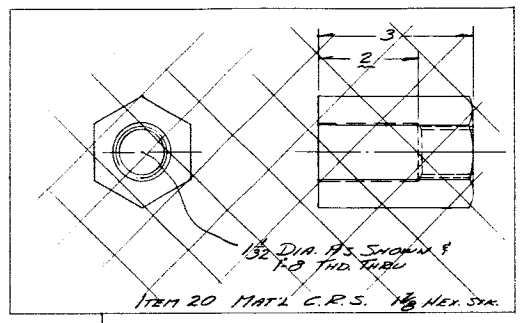

ITEM 20 MATL C.R.S. 1⅞ HEX. STK.

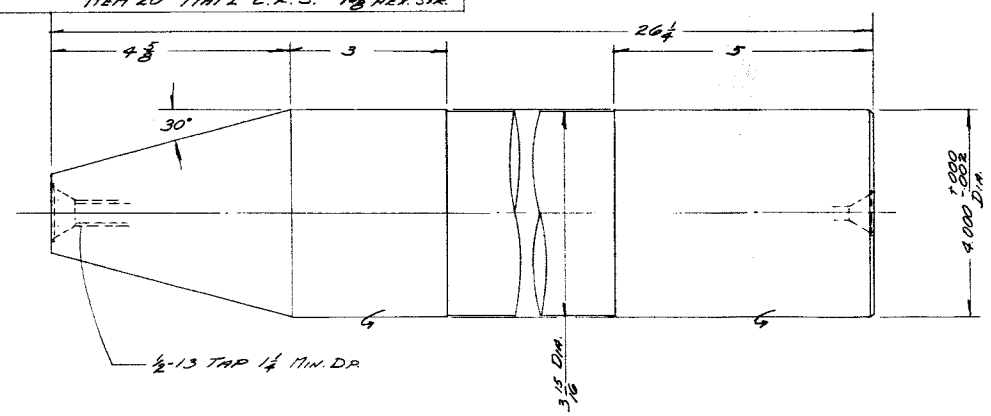

ITEM 33 MATL H.R.S.
CARB. HDW. & GR. 4.000 DIA.

GENERAL NOTES

F.) 1. STAMP NO. 3, 4, 5, 6, 7, 8, 9, 10, 11, 12, 13 MUST BE VISIBLE AFTER WELDING THE FINISHED STRUCTURE.

2. THE CREATED STRUCTURE MUST PASS THRU A DOORWAY 12 FEET WIDE x 11 FEET HIGH.

3. THE FINISHED STRUCTURE MUST BE SUPPORTED BY THE (3) LIFTING POINTS (EYE BOLTS) OR THE (3) SUPPORT POINTS (HEX HD. BOLTS) AT ALL TIMES.

4. THE PARABOLOIDAL SURFACE (SKIN) MUST BE MADE FROM A ONE PIECE SPUN DISH OR U.S. EQUIVALENT.

5. ALL WELDING TO BE COMPLETED BY THE INERT GAS SHIELDED ARC METHOD.

6. STRESS RELIEVE ENTIRE STRUCTURE AFTER ALL WELDING TO INSURE DIMENSIONAL STABILITY OF THE SURFACE.

7. AFTER STRESS RELIEF, THE CONTINUOUS SKIN SURFACE (ITEM 41) MUST APPROXIMATE A TRUE PARABOLOIDAL SHAPE WITHIN A TOLERANCE OF ± 1/8 INCHES. THE SURFACE MUST BE SMOOTH (RMS 250 OR BETTER) AND FREE FROM LOCALIZED BUMPS OR DISTORTIONS IN EXCESS OF 1/32 OF AN INCH.

8. ATTACH METAL PLATE INDICATING GROSS WEIGHT OF ENTIRE STRUCTURE AS SHOWN.

9. LOCATE (3) LEVELING BUTTONS (ITEM 18) ON STRUCTURE AS SHOWN SO THAT A PERPENDICULAR TO THE AXIS OF THE MEAN PARABOLOIDAL SURFACE CAN BE ACCURATELY DETERMINED.

10. NUTS & BOLTS TO BE MEDIUM CARBON STEEL OR EQUIVALENT. THE BASIC WELDED STRUCTURE TO BE 6061 ALUM ALLOY OR EQUIV. OTHER ITEMS AS SHOWN.

B-11 11. AFTER STRESS RELIEF, STATIC BALANCE ENTIRE STRUCTURE ABOUT THE CENTER POINT UNTIL THE ADDITION OF NO MORE THAN TWO POUNDS OF WEIGHT IS SUFFICIENT TO ATTAIN FINAL BALANCE. STATIC BALANCE ADAPTER HARDWARE TO BE PROVIDED BY G.E.

12. CRATE TO BE SUPPLIED BY G.E.

F.) 13. THE DISH (SKIN) MAY BE FABRICATED FROM (16) SIXTEEN PIECES OR LESS - PROVIDING A CONTINUOUS WELD IS USED AT THE FINAL JOINTS. EQUAL WELDS ARE TO BE PLACED OVER BOTH EDGES AS SHOWN IN ZONE F-13 SHEET 1

Item	Req	Matl	Finished Size	Description
			FINISHED SIZE BILL OF MATERIAL	
48	12		½ x 4½ x 7	E.A.
47	6		½ x 5½ x 7	E.A.
46	3		½ x 2 x 3½	PAD
B-2 45	9	ALUM	⅜ DIA. x 1¾ LG.	PIN
44	1		¼ x 4 x 115 APP.	RING
B-9 43	1		¼ x 4¾ x 150 APP.	RING
42	1		¼ x 6 x 188 APP.	RING
41	1		¼ x 6 x 226 APP.	RING
40	1		¼ x 6 x 265 APP.	RING
39	1		¼ x 6 x 302 APP.	RING
38	1		¼ x 6 x 340 APP.	RING
37	2	COMM	SCHRADER No. 306 1C-12-⅜ H.P.T.m.	QUICK COUPLER
36	2	STL.	⅜ STD. SQ. HD. N.P. PLUG	PLUG
35	1		1 x 6 x 8	PAD
34	1		.8 x .475 x 18 LG.	CHANNEL
33	1	H.R.S.	4 DIA. x 26 LG.	CENTERING PIN
32	1		2 I.D. x 3 O.D. x 4½ LG.	DRAIN TUBE
31	1	H.R.S.	2¼ DIA. x 3½ LG.	PLUG
30	2	COMM.	¼ DIA. x 1 LG.	DOWEL
29	1	COMM.	¼ DIA. x 1⅛ LG.	DOWEL
28	1	C.R.S.	1 DIA. x 8½ LG.	SHANK (WRENCH)
27	1	C.R.S.	⅝ DIA. x 6 LG.	HANDLE (WRENCH)
26	2		¼ x 4 x 8½	E.B.
25	1		½ x 4 x 5⅛	E.B.
24	1		18 I.D. x 19.0 O.D. x 18¼ LG.	TUBE
23	3		1-8 x 4	HEX. HD. BOLT
A-8 22	3		1-8 "	HEX. JAM NUT
21	3		½ x 2 x 3	BLOCK
A-7 20	3	C.R.S.	1⅞ HEX x 3 LG.	SPACIAL NUT
B-5 19	3		2 x 3½ x 11½	BLOCK
B-6 18	3	20 DURO RUBBER	1.0 I.D. x 2 O.D. x 3/16 TH.	WASHER
B-3 17	3	COMM. SN.	WILLIAMS WILDRIG WILDLESS THREADED SHOULDER BOLT NR. 10 - 1 DIA. x 3 LG.	
16	3		½ x 3 x 3	PAD
15	3	ALUM	2 DIA. x 1 LG.	BUTTON
14	8		½-20	HEX. NUT
13	8		½-20 x 1½ LG.	FL. HD. BOLT
12	48		¾-16	HEX. NUT
11	48		⅜-16 x ½ LG.	HEX. HD. BOLT
10	4		½ x 1½ x 1½	PAD
9	12		½ x 2 x 3 x 3 LG.	ANGLE (CLIP)
B-6 8	12		½ x 19½ x 50½	E.B.
B-8 7	3		½ x 4 x 54⅛	PLATE
B-7 6	3		½ x 19½ x 54	E.B.
F-1 5	3		12 SIMS ½ x 12 LG. APP.	CHANNEL
4	1		3 x 20.8 " x LG. T. SUT (APP. 288°)	CHANNEL
12 3	1		2½ x 3 x 153 " x LG. T. SUT (APP. 186°)	ANGLE
F-1 2	1		8.1 x 47.8 " x LG. T. SUT (APP. 330°)	CHANNEL
1	1		¼ TO SEE SH 1 NOTE 4 THIS SH.	SKIN

Figure 5.1-1b. Spincasting Mold

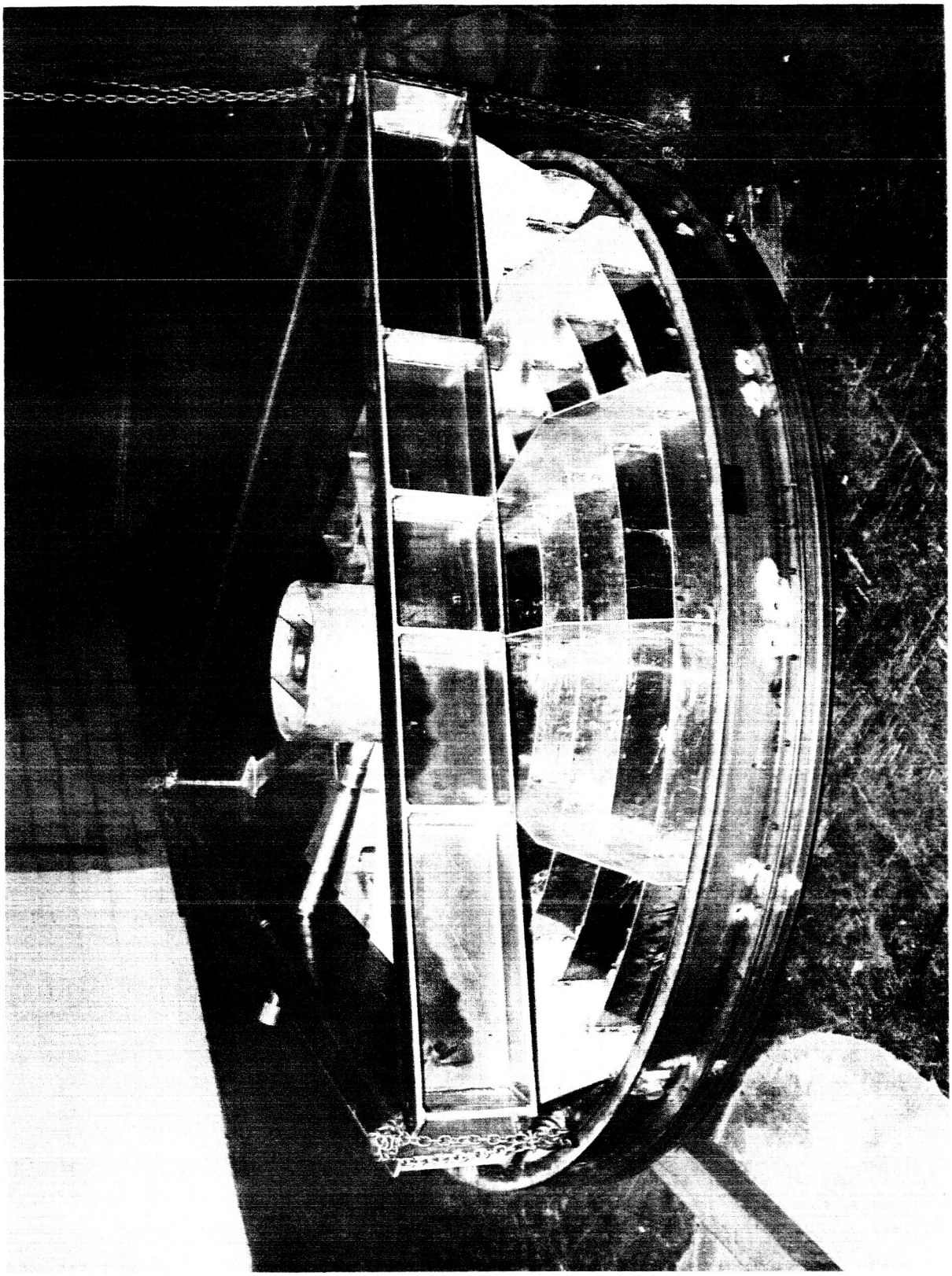

Figure 5.1-3. Spincast Mold Back-Up Structure

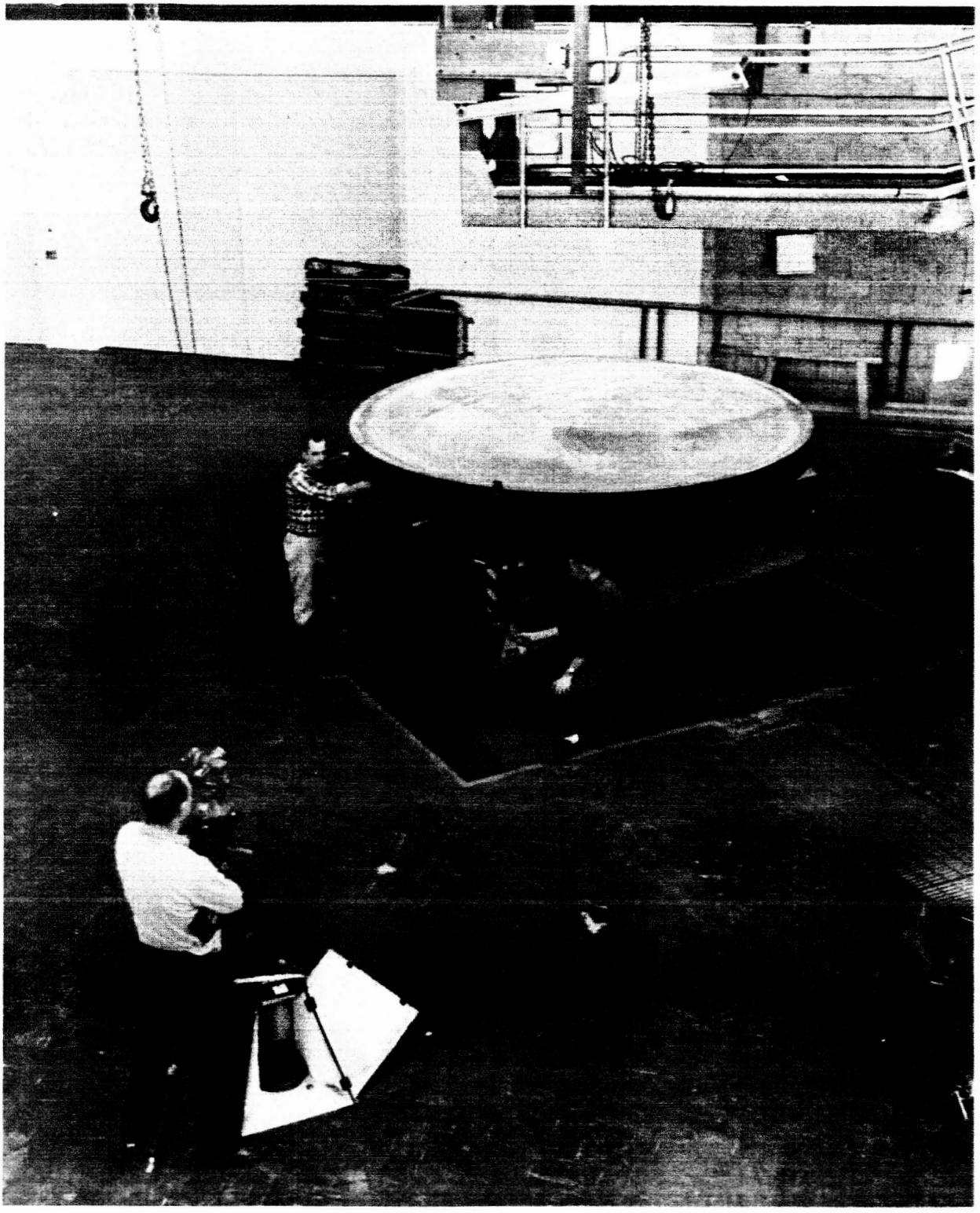

Figure 5.1-4. Spincast Mold Mounted on Spintable

5.1.3 PROTECTION AGAINST CHEMICAL ATTACK

Prior to mounting the aluminum structure and mold on the spintable it was protected against chemical attack by the electroforming bath. The detailed procedure is described in Appendix A.

5.2 SPINCASTING POUR NOS. 1 THROUGH 7

5.2.1 FACILITIES AND EQUIPMENT

A. Spintable System

1. Machine Design

The spincasting machine (Figures 5.2-1 and 5.2-2) consists of an extremely rigid frame, 8-feet square and 4-feet high, filled with concrete to act as a ballistic mass. A steel shaft, 12 inches in diameter and 62 inches long, is mounted within a cylindrical steel housing in the center of the frame. The shaft supports a stiff, tapered-rib, cast-steel table, 8 feet in diameter, upon which is mounted related tooling for spincasting. The upper section of the shaft is supported by an axial thrust bearing and a radial thrust bearing. Its lower section is supported by a tapered roller bearing which provides both radial thrust and axial preloading of the shaft assembly. Specifications for the three bearings are:

Bearing Type	Dimensions (inches)		Basic Dynamic Load Rating
	OD	ID	
Axial thrust	15	9-1/2	165 tons at 850 rpm
Radial thrust	16	10-1/4	96 tons at 850 rpm
Tapered roller	15-1/8	7-7/8	105 tons at 850 rpm

The drive unit for this machine is a 5-hp, 440-volt 60-cycle General Electric Kinatrol (Eddy current coupling) variable-speed motor. This motor is rated at 100 to 1675 rpm with a maximum output torque of 15.7 ft-lb. The motor shaft

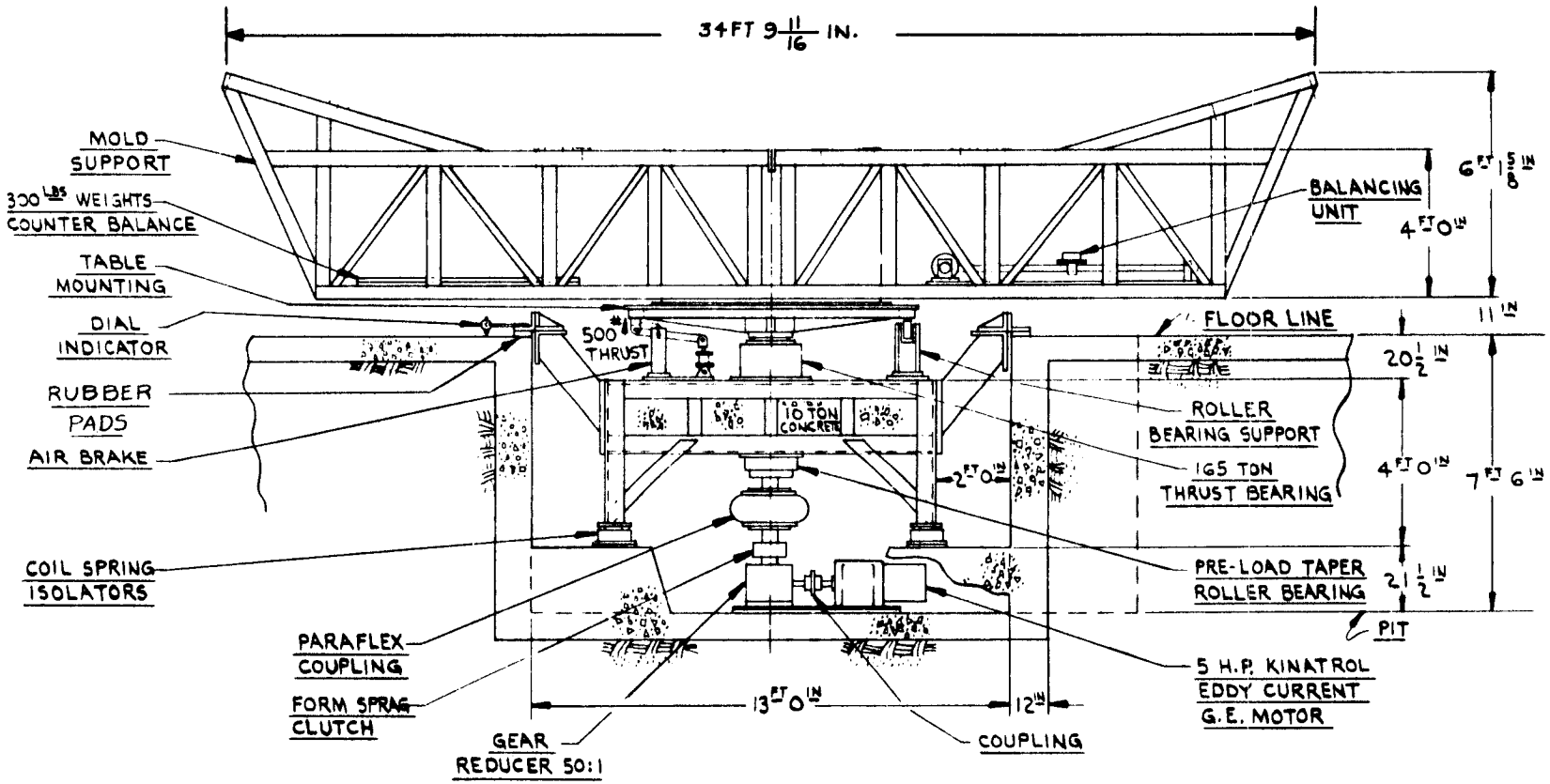

Figure 5.2-1. Spincast Machine Cross Section

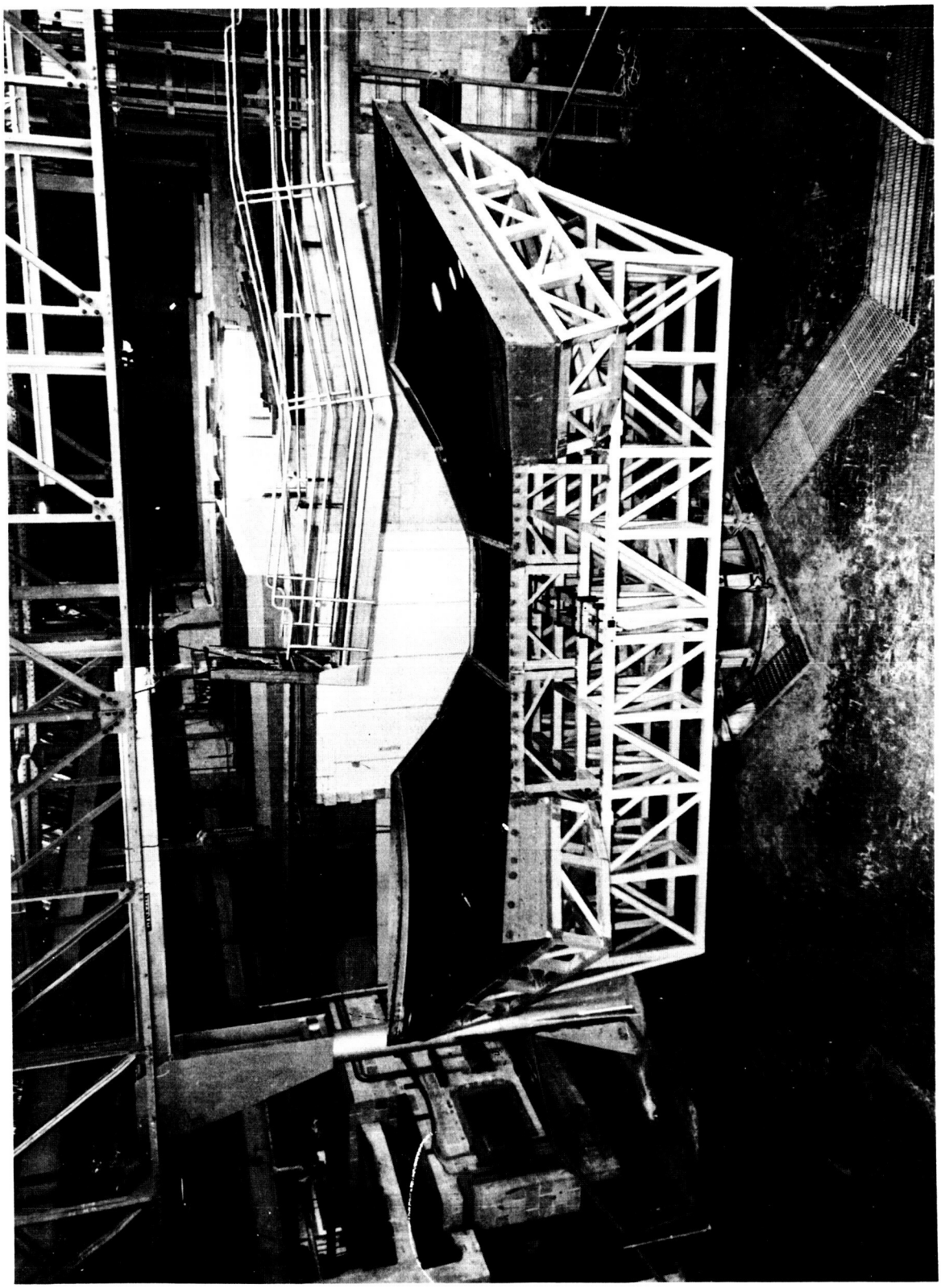

Figure 5.2-2. Spincast Facility Showing Spintable, 35-foot Trusses, GE Space Simulator Mirror Molds, Overhead Walkway, and Optical Inspection Tower.

drives through an Eberhart Denver 50:1 speed reducer gearbox, then through a Formsprag overriding camtype clutch, and finally through a Paraflex vibration-absorbing coupling which is connected to the spintable drive shaft. The machine is not fastened to the floor; each of its four support legs is mounted on Korfund Vibro Isolators individually rated at 10,000 pounds capacity.

Under conditions of mold imbalance, sudden braking, or rapid acceleration the high inertia of the rotating system might induce rotation or lateral translation of the spintable frame since the table legs are mounted on unrestrained Korfund vibro-isolators. To prevent such an occurrence, sturdy outriggers are attached to all four sides of the table frame. One-eighth inch clearance is held from the vertical concrete side walls of the spin pit, and two-inch clearance is set between the horizontal face of the outrigger and the concrete floor. Two-inch thick rubber mounts can be placed between the horizontal section of the outrigger and the floor. These rubber mounts were not used during any pours for this program. They were, however, employed during the vibration investigation. Four five-inch diameter dial indicators were mounted on the spin table frame at two locations 90^{o} apart and on a 10-foot diameter to detect vertical and horizontal deflections.

Three copper slip rings are mounted to the table drive shaft for reversible operation of a motor driven weight balancing unit. This allows correction of vertical deflections in excess of 0.001 inch through electrical actuation of the balance weight while the spin table continues to rotate without interruption. As an additional safety precaution, eight adjustable roller bearings mounted on equally spaced support brackets are affixed to the spintable frame to support the cast-steel table beneath its 8-foot diameter outer rim. A running clearance of 0.020 inches was set between each roller and the rim of the table at the minimum point of table runout.

The vertical shaft of the spintable was carefully aligned in a true vertical plane both before and after placement of the mold. The mold substructure and truss were also aligned and leveled in a true horizontal plane. Extreme care was exercised to achieve accurate leveling, as this affects the mold balance during casting of epoxy and the quality of material dispensed. Obviously, the accuracy of the final master surface depends on the accuracy with which the spin axis of the assembly coincides with the local vertical. The check-out system is described in detail in Appendix C.

2. Speed Sensing and Control

Checkout tests revealed that local line variations in voltage had a significant effect upon spintable speed. At certain times of day, intermittent line loads produced speed variations of ±0.5%. In order to minimize manual readjustment of the ten-turn control potentiometer during the continuous phase monitoring of spin casting, additional drive system speed regulation controls were added prior to the start of this program. This addition to the Kinatrol eddy-current coupling drive motor consisted of a GE Thyratron controlled speed regulated feedback system which utilizes a cog belt driven tachometer generator to sense motor-shaft output speed. A small area of reflective tape was placed on the outer rim of the table. As the table rotated, the tape reflection tripped a photo-electric lamp which was pre-focused on it. The electric pulse generated by the interrupted light beam was picked up through an amplifier and fed into a Hewlett Packard counter which was set at a standard time frequency count of 1,000 counts per second. Direct reading of the table rotation was considered necessary since the unidirectional action of the Formsprag clutch permits slip between table and drive shaft. After considerable adjustment and several minor circuit modifications were completed, the installation provided a rated speed control accuracy of ±0.1%. A second tachometer generator built into the Kinatrol unit was wired to a pointer-type tachometer to give a second, though rough, means for visual observation of rpm.

3. Standby Equipment

In the event of an emergency shutdown, it is necessary to either remove all resin from the mold within 15 minutes or less, or to make quick repairs and resume spintable rotation within that time span. Failure to promptly remove a large mass of resin concentrated at the center section of the mold can create an exothermic reaction which could severely damage the mold.

To prevent a delayed shutdown the following spare parts were available at the spin-cast site:

1. Pre-baked thyratron tubes stored in an upright position
2. Electrical fuses and electronic tubes
3. Tachometer head photocell bulbs

In the event the table could not be made operational within 15 minutes, equipment was on hand to drain the resin from the mold.

4. Overhead Walkway

To make the mold center accessible for epoxy casting and visual observation, an overhead walkway was installed. It is hinged on a support structure beyond the mold edge and suspended on a chain hoist above the mold center to provide height adjustment.

B. Metering and Mixing Equipment

1. Considerations

a. Uniform Mixing — Extreme importance was placed on uniform mixing of the epoxy materials. The casting of thin coatings over large areas presents a configuration that is especially vulnerable to non-uniform blending of reactive constituents. Since the cast surface must have an optical finish, uniform mixing becomes even more critical.

b. Exclusion of Bubbles — Air inclusions are common to the mixing of viscous materials, but in this application they could not be tolerated. Although previous materials development efforts had produced a formulation which was highly insensitive to the propagation of air inclusions, it was decided to include additional provisions to eliminate the occurrence of bubbles in the process equipment.

c. Contamination by Exposure to Air — The basic material used was an amine-cured epoxy. Amines are noticeably hygroscopic and absorb atmospheric moisture quite readily. Previous experience indicated that this acquired moisture produces a film on the cured epoxy surface which detrimentally affects its optical properties. This consideration pointed up the desirability of employing a closed system in the processing and delivery of reactive material onto the mold surface.

2. Description of Metering-Mixing Equipment

To combat the above problems, the process is built around a metering-mixing system which automatically proportions, meters, mixes, and dispenses measured quantities of blended material under fluid pressure. Two reservoirs, capable of storing and de-aerating a 40-gallon working quantity of any reactive component, are connected with the system; one houses the resin and the filler components, the other stores the catalyst. The resin container is equipped with an agitator to keep fillers and resin in uniform suspension during de-aeration. Figure 5.2-3 shows a photograph of this equipment.

The metering components are positive-acting, piston-type metering elements capable of maintaining volumetric accuracy within 0.5% for each liquid constituent. The metering elements are integrated by electropneumatic controls in a double-feedback arrangement for simultaneous proportional metering. This type of control yields pulsating streams of material which are in the required proportion at any time during the metering. As a result, homogeneity of the final mix is assured.

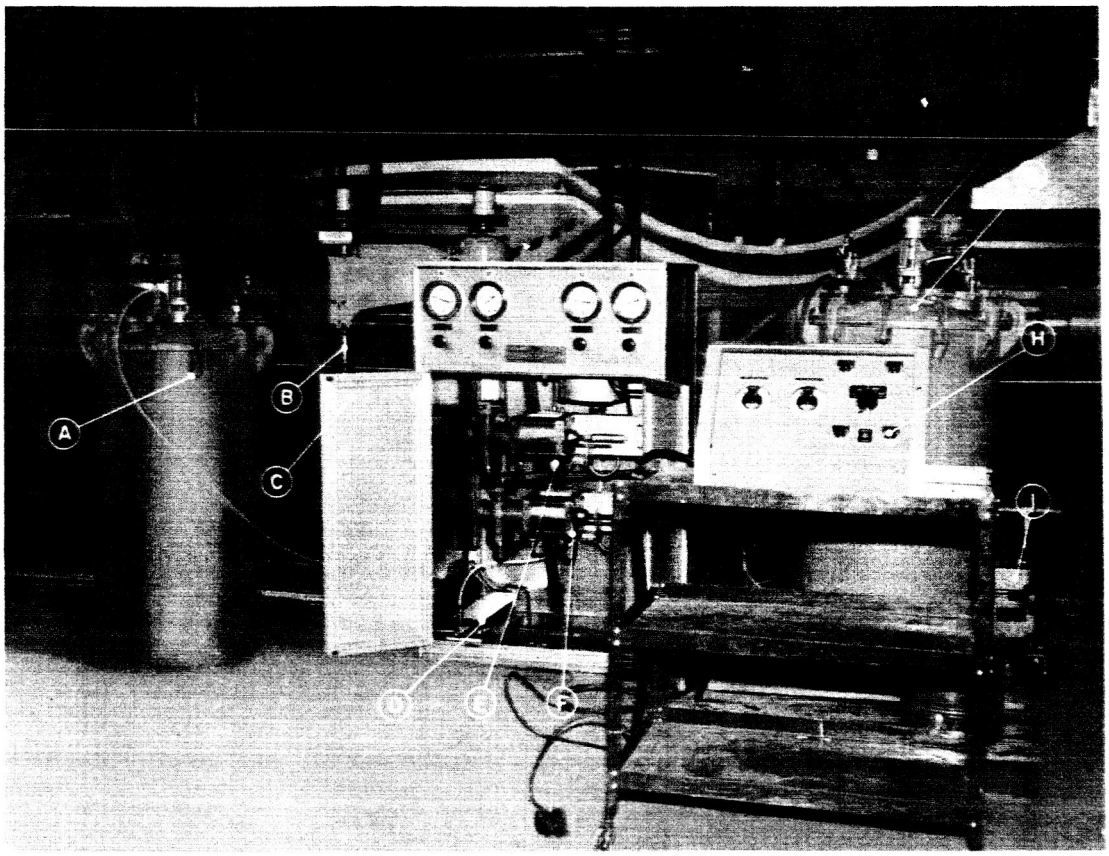

A. Pressurized hardener reservoir
B. Mixer reactor
C. Mixer outlet
D. Solvent purge pump
E. Resin metering element
F. Hardener metering element
G. Combination vacuum and pressure resin reservoir with agitator
H. Control box
I. Vacuum pump

Figure 5.2-3. Proportional Metering-Mixing Equipment

The metering elements feed into a mixer-reactor through check valves. The mixer device has a small volume for mixing which, by reason of a high rate of shear, permits thorough blending within the shortest possible time. Other mixer-reactor features eliminate stagnation areas. Thus the overall design permits processing of materials with a short pot life.

The metering-mixing system dispenses material under hydraulic pressure. Inasmuch as the dispensing point for spincasting is 30 feet away from, and 6 to 10 feet higher than, the material processing point, the dispensing hydraulic pressure could be used as the driving force in moving catalyzed material to the feed point. This was done by running polyethylene tubing from the dispensing head in the metering-mixing machine to the feed point by way of the overhead catwalk.

Cleaning of the reactive mix from the mixer-reactor and outlet was accomplished by a solvent purge. A solvent reservoir and purge pump feed the solvent to the mixer-reactor and outlet line, flushing out all reactive materials from the system. In this operation, the bulk of cleaning is done with a closed solvent can, so that the arrangement is well within the established safety limitations.

3. Batch Mixing Equipment

Special attention is required to obtain and maintain good filler dispersion since the filler tends to settle in the resin. A Gifford-Wood Eppenbach Laboratory mixer was used successfully for initial dispersion of filler in the resin, reducing the settling rate of the filler by providing good initial wetting. The Eppenbach unit was used for mixing the filler with a small quantity of resin prior to charging the storage tanks.

The required storage capacity for the resin containers was calculated to be 13 gallons for a 1/4-inch coating of the entire mold surface. An available vacuum-pressure tank (100 psi) of 55-gallon capacity containing a stainless-steel liner was used for storage, allowing 100% free board above the resin for the evacuation of

air. The tank was equipped with Lightning mixers of 3-HP capacity, running at 350 rpm, which were specified to handle resin viscosities from 500 to 50,000 cps and to disperse the filler. The mixer shafts, carrying propeller mixers, are located off the center axis and at a 10^{o} angle in the tank to also allow for proper mixing of resins which are considerably more viscous than those presently employed for spincasting.

A 20-gallon capacity stainless-steel tank was provided for catalyst storage. To avoid undissolved particles of dye, the dye was dissolved overnight and filtered before charging into the catalyst tank.

Nitrogen was used to pressurize both tanks to feed the materials to the metering pumps. Contact of the materials with air was minimized to prevent absorption of moisture. The only materials used in contact with resin and catalyst throughout the mixing machine were stainless-steel, teflon and polyethylene.

C. Small Spincast Facility

A small development spin casting facility was also used for this program. The facility with half of the safety guard removed and a typical mold mounted is shown in Figure 5.2-4. This facility can accommodate molds up to 7 feet in diameter and up to 1500 pounds in weight. The operating speed range is from 10 rpm to 125 rpm.

Although the small table has neither vibration damping nor an accurate speed mechanism, it has been used to obtain quality spincastings. (See Figure 5.2-5.)

In addition to the above facility, successful use was made of two record-player turntables. They are relatively small, limited to 4 speeds and mold diameters up to 2 feet. Both units were used in conjunction with the large development facility to evaluate resin formulations during dynamic casting studies. Results were excellent; many high quality surfaces were cast.

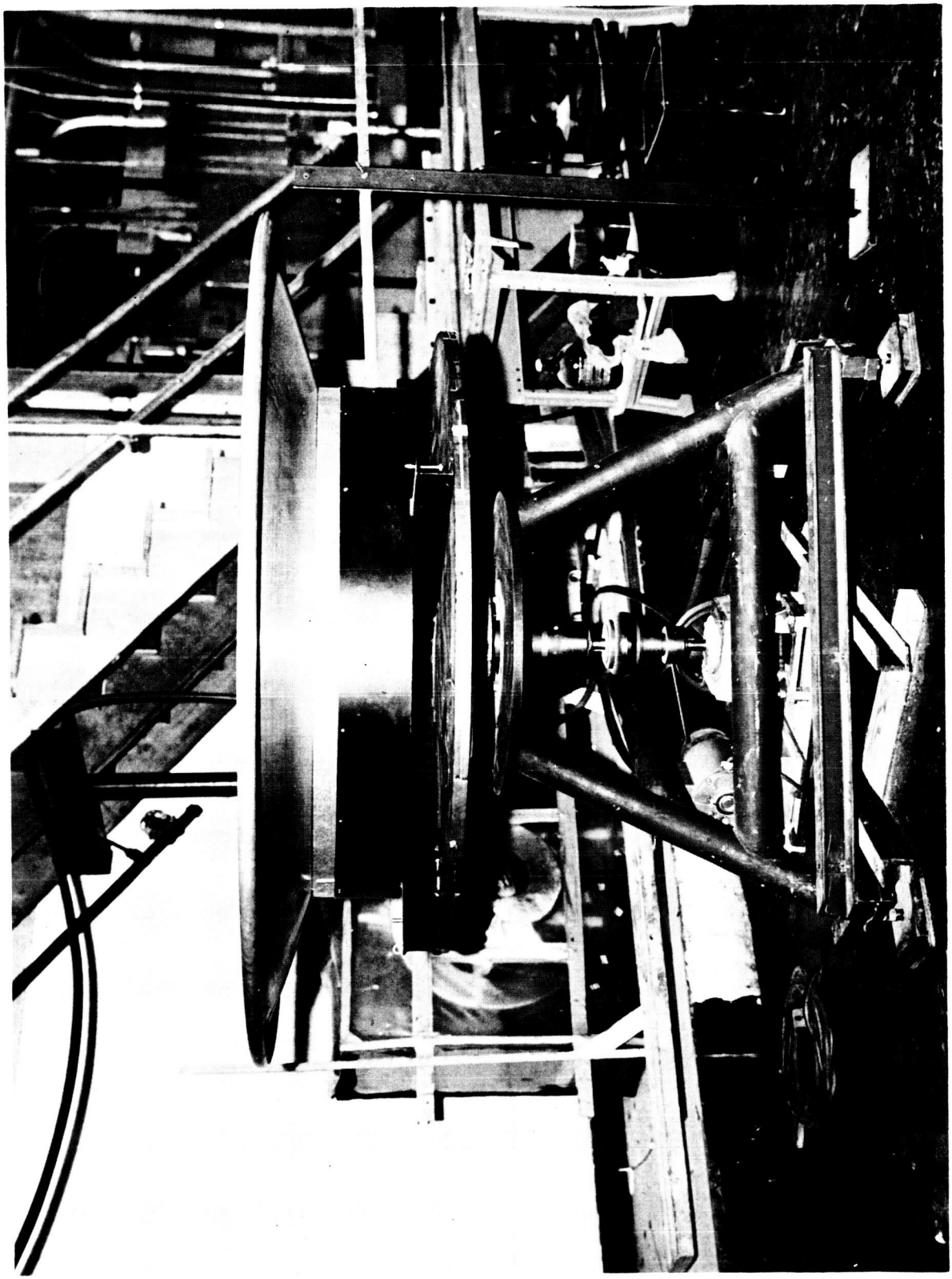

Figure 5.2-4. Development Spincasting Facility

Figure 5.2-5. Five-foot Diameter Spincasting Made on Small Spintable

5.2.2 PREPARATION FOR SPINCASTING

A. Alignment of Spintable

The spintable shaft was aligned in a vertical plane within 0.002 FIR runout for one full 360^{o} revolution. Repeat measurements were made with a precision machinists level (0.005 in. per foot graduations) placed at the outer periphery of the eight-foot table diameter. The runout of the spintable shaft as measured near the slip rings with a dial indicator was 0.0003 FIR maximum.

B. Calculation of Rotating Speed

Focal length of the paraboloid and rotational speed during spincasting are related by the following equation:

$$f = \frac{450g}{\pi^2 N^2}$$

where

F = Focal length,

N = Revolutions per minute,

g = Acceleration of gravity.

For the spincast mirror the desired focal length was 68.8 inches. The g value equals 32.1587 feet/sec/sec as measured at the Franklin Institute, Philadelphia, Pa. less than 6 miles from the spincasting facility. Figure 5.2-6 shows a plot of this equation.

$$N = \frac{1}{\pi}\sqrt{\frac{450g}{F}} = \frac{1}{3.14159}\sqrt{\frac{450 \times 32.1587 \times 12}{68.8}}$$

$$N = 15.9920 \text{ RPM} = \text{required spintable speed}$$

$$\text{Counter Setting} = \frac{60}{N} \times 1000 \frac{\text{counts}}{\text{sec}} = \frac{60,000}{15.9920} = 3752$$

Set counter at 3,752 counts per revolution.

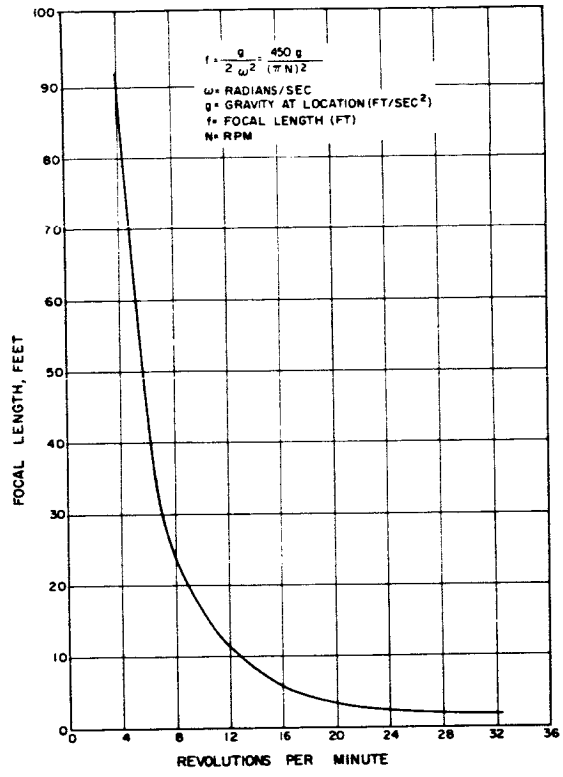

Figure 5.2-6. Focal Length vs. Spin Speed

C. Material Handling and Safety Precautions

1. Important Precautions

a. Sensitization to Materials — In order to prevent sensitization (contact dermatitis) and to promote safe usage of the materials employed in this operation, the following precautions should be observed:

1. Use SBS-40 medicated skin cream on hands, arms, face or other exposed areas of the skin whenever working in the spincast area.
2. Wash thoroughly after exposure to any of these materials, and reapply the protective cream.
3. Maintain good housekeeping in the area. Keep all working surfaces and tools clean and uncontaminated by the offending materials.
4. Remove any loose catalyzed resin from the area.
5. Use face respirators when handling large quantities of amine hardener, and wear protective gloves.

b. Material Cleanliness — Extreme care must be taken at all times to prevent contamination of the spincast materials. Material containers, stirrers, funnels and anything coming in contact with the materials must be thoroughly clean. Materials must always be handled and stored in covered air-tight containers. Caution must be exercised at all times to prevent contact between epoxy components and materials which might be reactive and, therefore, affect the quality of the spincast surface.

2. Safety Equipment

Flame-arrester-type containers were used for handling Ketone solvents and a sniffer alarm, installed in the spin pit, was regulated to ring if solvent fumes attained one-fifth of the concentration level required for an explosion to take place. Cleaning rags and waste materials were placed in covered metal containers and later moved outside the building to an approved storage area. A rigid tubular safety railing was erected around the periphery of the rotating mold and a centrally located eyewash fixture was installed for emergency use.

Other items which could be classified under safety equipment were: an underground spin pit walkway to permit in-operation access to the table drive motor; vertical deflection dial indicators which were used in conjunction with an electrically powered weight device; two independent speed sensing devices; and a spintable brake which required engagement of two separate switches to actuate.

3. Operational Safety

The great size and mass of equipment used in this operation may be more fully appreciated when one visualizes that the rotating mold is roughly equivalent in size to half of a normal-size house. With this thought in mind it becomes more apparent that great care must be exercised and all safety precautions must be strictly observed throughout all phases of spin-cast processing. In addition to the equipment checkout procedures, the following safety rules were observed:

a. A minimum of two men remained on duty at all times throughout spintable operation.

b. Smoking was not permitted when dispensing or solvent cleaning operations were in process, and a no-smoking rule prevailed at all times in the immediate area of material dispensing equipment.

c. Whenever the spintable was in motion, the speed controls were constantly monitored and the overhead catwalk was restricted to a maximum of three personnel.

5.2.3 SPINCAST POUR NOS. 1, 2, AND 3

The 9-1/2 ft mold was mounted to the spintable on triangular frame adapter No. SKS0147. The first five coats were spincast with GE standard formulation No. 1017Z7. (See Figure 5.2-7.)

In order to prevent dust from settling on the cured surface, the first three coats were visually inspected through the cover. Some haze discoloration was observed on spincast coat Nos. 1 and 2 in the vicinity of the pouring chute periphery. The polypropylene cover made visual observation difficult, and the spiral chute also restricted visibility such that the geometrical pattern of the discoloration was not readily discernible. Pour No. 2 had faint radial lines around the outer periphery of the mold. In preparation for the third spincast coat, a second layer of polypropylene was used to cover the mold surface. Hardener soaked pads were placed between the two layers of the cover. It was thought that the cover was not completely air tight and the addition of a second layer plus the hardener pads would tend to improve the quality of the cast surface. A sketch and description of the spincast surface resulting from the third coat is shown in Figure 5.2-8.

Upon discovery of the third coat spincast surface imperfections, a conference of all the people at GE-MSD who were connected with the present and experienced with previous spincast fabrications was convened in order to determine the cause for these imperfections. After review of a large list of possible causes had been made, the following four possibilities remained.

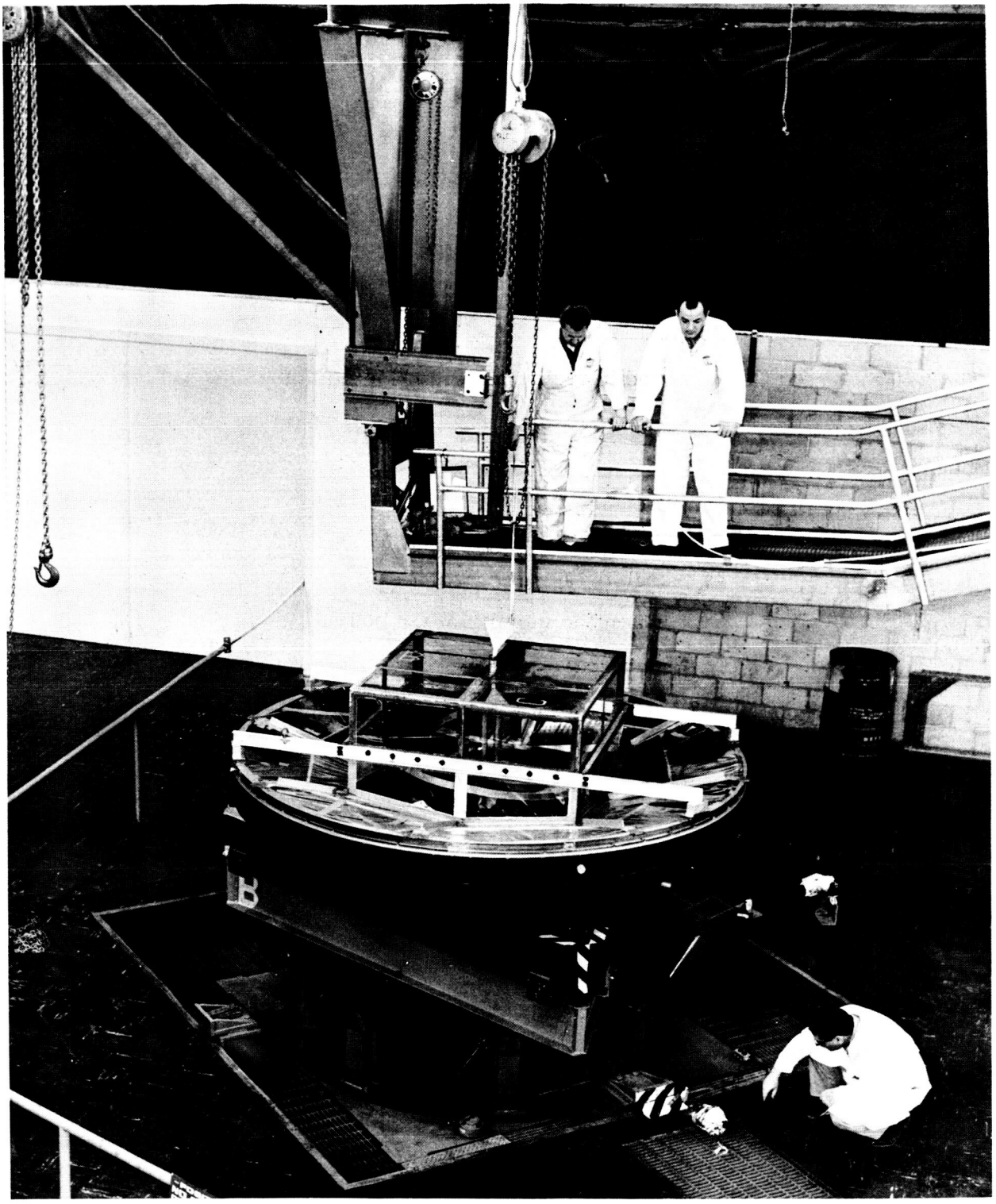

Figure 5.2-7. Spincasting of Pour No. 3

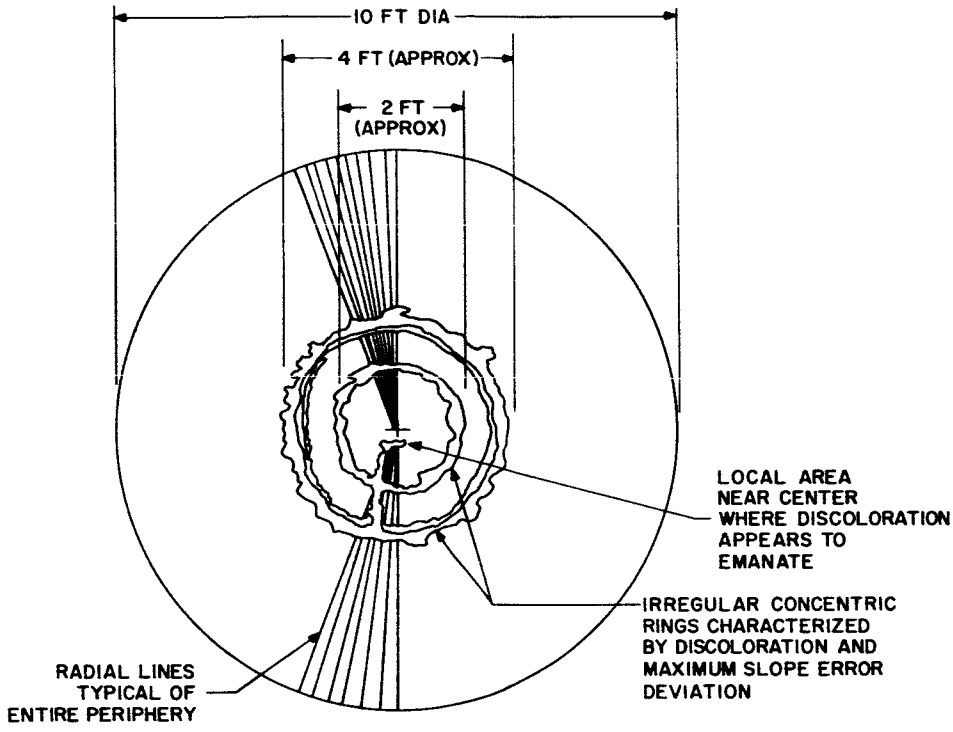

Figure 5.2-8. Surface of Third Spincasting

1. A mild chemical reaction between the epoxy materials and the polypropylene cover.
2. Partially polymerized material remaining from a previous pour dislodged from the pouring chute while dispensing epoxy.
3. Possible contamination from the lubricants used in the mixing machine or the resin mixing tank.
4. Separation of epoxy formulation ingredients during transport from mixer to mold and consequent flotation on the mold surface.

The corrective action taken was:

1. The polypropylene cover was replaced by a cover made of highly transparent plexiglass sheets bonded to an aluminum frame.
2. The pouring chute was eliminated and the epoxy was poured directly from the mixing machine through a long tube into the mold. (See Figure 5.2-9.)

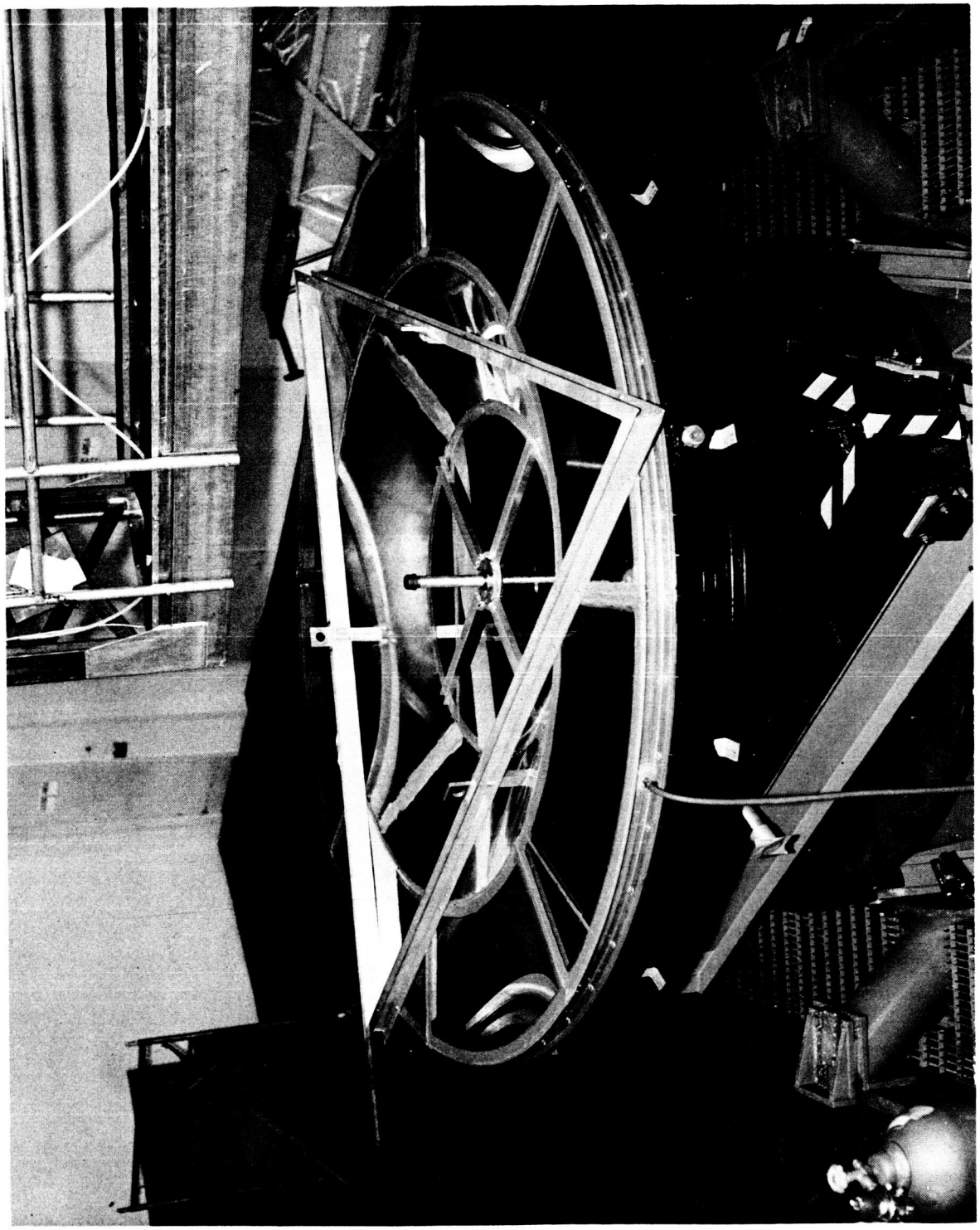

Figure 5.2-9. Spincasting Arrangement Used for Pour Nos. 4 and 5

3. The mixing machine was disassembled and the possibility of lubriplate contamination from the packing of the resin tank mixer shaft was established. A special seal adapter was fabricated to prevent lubricants from coming in contact with resin material.

4. Spectrographic analysis was made of scrapings taken from the cured mold surface and also of samples taken from the mixing machine and resin tank. Conclusive evidence of the problem mechanism was not obtained.

5.2.4 SPINCAST POUR NO. 4

After pouring the mold, a series of concentric rings and numerous small swirls all within four feet of each other were observed on the cast surface at the mold center. Within two hours a clear area covering 10 inches in diameter appeared at the center of the mold and moved radially outward at a very slow rate. Ten hours later the clear area extended to a 2-1/2-foot-diameter circle which blended at its periphery into a ring with visually noticeable optical aberrations, similar to that observed on the third spincast pour. After curing, the surface of the fourth pour was visually inspected through the plexiglass aluminum cover revealing:

a. Faint radial lines in the outer periphery.

b. Two concentric rings of discoloration located in approximately the same position as and similar in description to coat No. 3.

c. Severe radial lines within the central 4-foot diameter.

d. Some randomly spaced dust dimples in the cured surface.

e. Several randomly spaced areas containing a depressed swirl pattern of perhaps 3-inches diameter.

5.2.5 SPINCAST POUR NO. 5

Immediately after imperfections were observed on the cured surface of the fourth coat, another detailed design review meeting was held and the following changes were established as part of the procedure for the fifth pour.

a. To increase mixing dwell time, the 100cc high-shear mixing head was replaced with a 200cc mixing head of different design which had been used successfully on the GE 35-foot space simulator mold.

b. Material volumetric metering dispensing pumps were slowed down 50% on the forward (dispensing) stroke to give a longer dwell period for material to mix in the 200cc mixing chamber.

c. The hardener was handled with additional precautions to absolutely minimize exposure to atmosphere.

d. Material dispensing funnel was filled prior to insertion in the rotating mold, kept filled throughout dispensing, and removed with material remaining in the funnel.

e. The centrally positioned RTV-60 drain plug was cut flush to the top surface of the mold and covered with bondmaster epoxy.

f. Filler material was heated to 375°F in a recirculating air oven for 3 hours to remove any traces of water vapor, immediately removed and stored in a vacuum container at 1.0mm of mercury absolute pressure.

g. The spincast mold was purged 11-1/2 hours with hi-pure (99.996% by volume) nitrogen. The nitrogen replaced helium which was previously used.

h. Material was skimmed from the top of the resin tank after stirring.

i. An automatic recording camera was used to record speed control counter readings for 16 continuous hours beginning 2 hours after pouring.

Visual inspection of the fifth coat through the plexiglass cover revealed surface texturing (mild orange peel) and radial lines. (See Figure 5.2-10.) The cover was removed and an optical inspection performed the results of which are discussed in Section 5.5. The general appearance of the surface is shown in Figure 5.2-11.

Prior to and during the fifth spincast pour, a series of 69 samples was statically cast under different conditions. A matrix chart of the test results was prepared in an effort to uncover factors contributing to the problem of poor surface quality. A second matrix chart was prepared which provided detailed data taken from the 9-1/2-foot mold spincast pour Nos. 1 through 5, and also data taken from the successful GE 35-foot space simulator mold. See matrix charts (Tables 5.2-1 and 5.2-2) I and II. After the fifth spincast coat was cast, a 10-week development

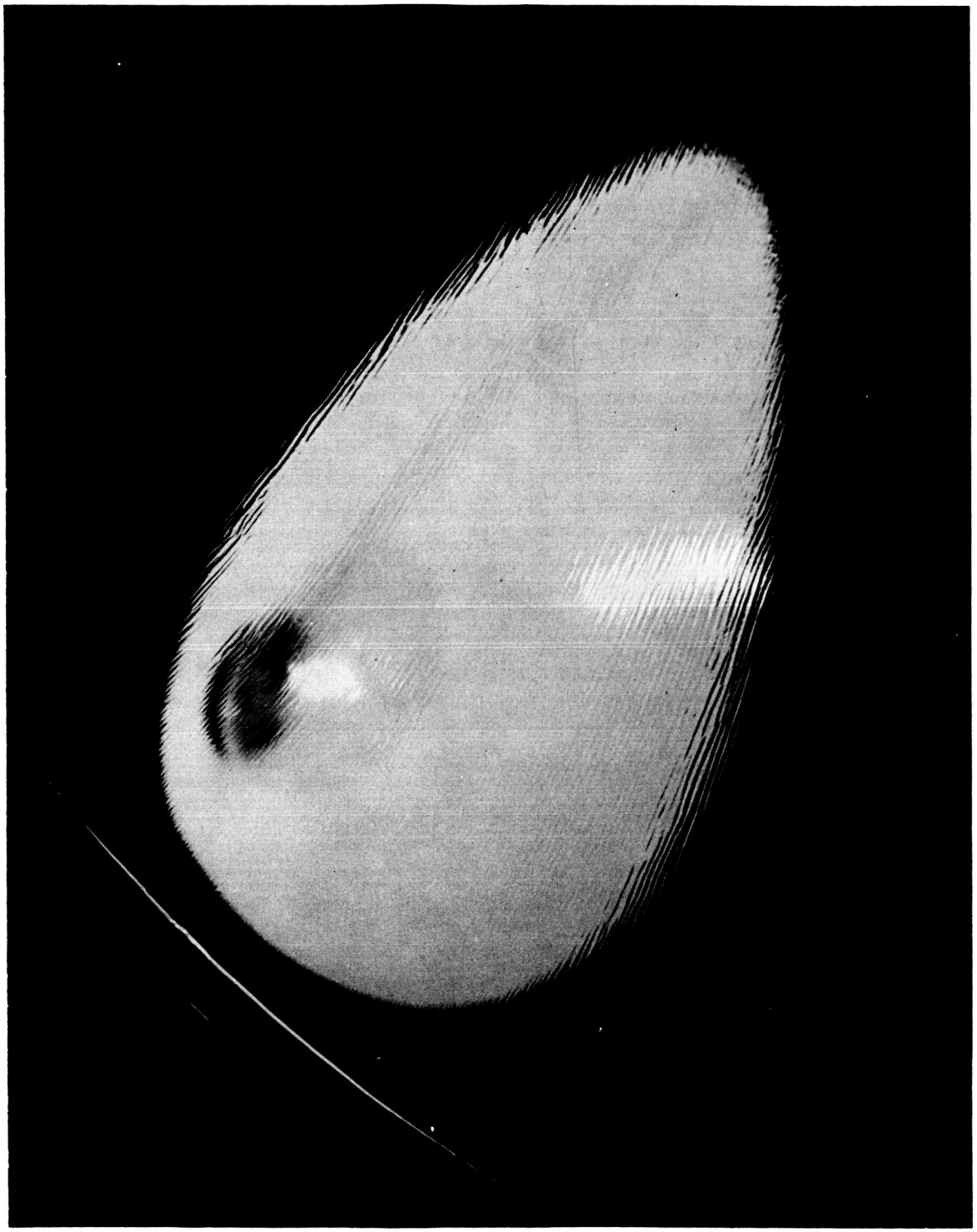

Figure 5.2-10. Radial Lines in Outer Portion of Pour No. 5

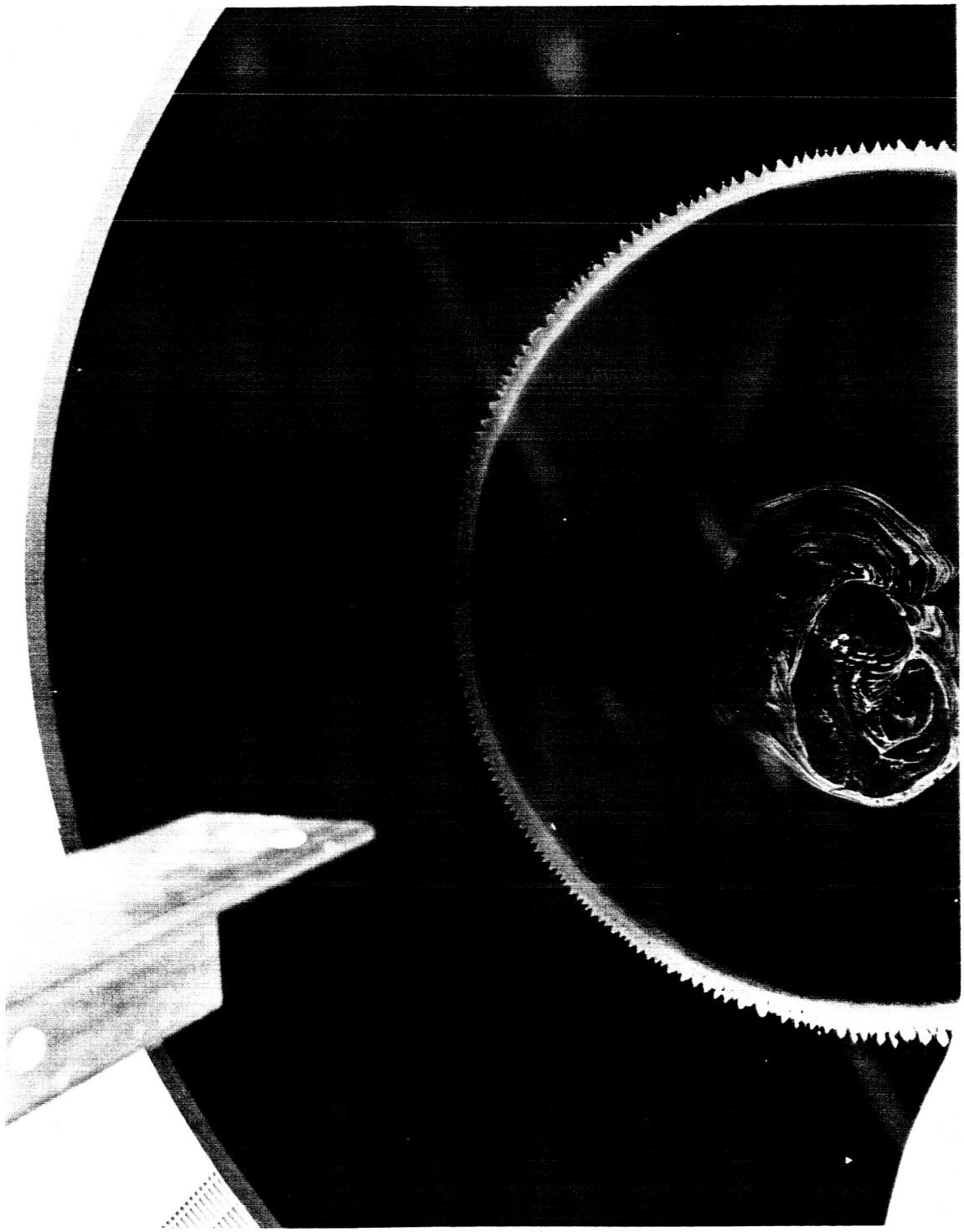

Figure 5.2-11. Surface Defects in Pour No. 5

TABLE 5.2-1. SPINCAST MATRIX

Process Data	Prep. for Pour 1	Pour 1	Pour 2	Pour 3	Pour 4	Pour 5	35 ft GE Space Simulator Mold	Remarks
100 cc High Shear Mixer, RPM		1740	1750	2000	2200	2150	2150	
200 cc Blender Mixer, RPM		Δ	Δ	Δ	Δ			
Mixer Head Water Cooled		13	13	7.5	6.1	9.1	54	
Total Gallons Poured		.25	.25	.14	.12	.17	.25	
Thickness of Material Poured		.27	.31	.31	.31	.31	1.41	
Rate of Pouring, GPM		1.85	1.60	1.60	1.60	1.5 to 1.8		Different Pumps
Pump Speed, Seconds Per Stroke		16.9	17.1	17.0	16.6	16.9	16.5	
Hardener to Resin Ratio		Δ	Δ	Δ	Δ	Δ	Δ	
Use of Pour Tube and Funnel						Δ		Bubbles on Removal
Funnel Filled at Start, Removed Filled						Δ		
Filler Heated to 375°F, 3 Hrs							Δ	
Filler Heated to 300°F, 8 Hrs		Δ	Δ	Δ			Δ	
Spiral Chute Used			Δ	Δ		Δ		
Continuous Funnel Flow Throughout Pour		Δ	Δ	Δ	Δ	Δ	Δ	
Formulation 1017Z7		Δ	Δ	Δ	Δ	Δ		
Dye Reagent Grade, Matheson-Coleman-Bell							Δ	
Dye Commercial Grade		Δ	Δ	Δ	Δ			
Toluene Cleaned Lines, Mixer Head						Δ	Δ	
Mek Cleaned Lines, Mixer Head					Δ			
Flushed Epoxy Surface with Reagent Isopropanol					Δ			
Flushed Epoxy Surface with Genosol "D"							Δ	
Wiped Aluminum Substrate & Flushed with MEK	Δ							
Halogen Leak Test, Freon				Δ	Δ			
Purged Mold with Helium, Hours		3	4	4	6		3	
Purged Mold with Nitrogen, Hours						11		
Skimmed Top of Resin Reservoir Before Evacuating						Δ		
Resin Reservoir Dipstick Close to Bottom of Tank		Δ	Δ	Δ	Δ			
Resin Reservoir Dipstick Raised 3 in. from Bottom						Δ	Δ	(Filler Settling)
RTV-60 Mold-Released Periphery		Δ	Δ	Δ	Δ	Δ		
Polyethylene Double Back Tape Around Periphery							Δ	
RTV-60 Plug 2-1/2 in. from Center		Δ	Δ	Δ	Δ			
RTV-60 Plug Removed						Δ		
Plexiglass-Aluminum-Bondmaster Cover					Δ	Δ	Δ	
Polypropylene Taped Cover		Δ	Δ					
Polypropylene + Polyethylene Cover		Δ	Δ	Δ				
Crystallization of Hardener Noticed				Δ	Δ	Δ	See Note 1	1
Mold Side Closing First During Pour		B	B	B	B	B		
Dispersion of Filler in Resin with Homo-Mixer		Δ	Δ	Δ	Δ	Δ	Δ	Same Mixer
Average Height of Cover to Epoxy Surface, Inch		9	8.8	8.6	5.9	5.7	5.5	
Supplemental Hardener Pads Added in Region of Chute & Cover				Δ				
Resistance to Cleaning Solutions				Poor			Good	

Notes:
1. Crystallization of hardener noticed at bottom of reservoir upon removing year-old hardener for GE Space Simulator 35-foot mold.
2. Emission spectrograph analyses have been made of:
   a) Cured epoxy at center, 4-ft dia, 10-ft dia of JPL mold (Check also made to detect lubriplate grease or bellows oil)
   b) Cured epoxy at center, and 12-ft dia of 35-ft GE Space Simulator mold
   c) Droplets on cured RTV-60 peripheral ring of JPL mold.
3. Screen sieve analyses have been made to compare filler used for JPL mold to GE Space Simulator mold.
4. On Pours 4 & 5 filler & resin were batch mixed with homo-mixer for much longer time than on previous pours. Haze in control samples has been continually increasing. This suggests that haze becomes greater as Eppenbach mixing is improved.
5. Polypropylene cover did not maintain tight seal during spincasting.
6. On Pour 5 camera limit switch hit "C" clamp. Radial lines appeared stronger on 5th pour than on other pours.

TABLE 5.2-2. SPINCAST EPOXY SAMPLE MATRIX CHART

Sample Description		Quantity Cast Total	Container Geometry			Amount of Haze			Surface Quality				Remarks
			10-1/2-in. Dia Pyrex	9 in. x 13 in. Stainless	6 in. Dia Lids	None	Slight	Great	Poor	Fair	Good	Excellent	
1 1017Z5	(H.M. 4 min) T. Parry's old mix	2	Δ				Δ			Δ			
2 1017Z0	(H.M. 10 min) matl from barrels	7	4		3	Δ			Δ				Orange peel
3 1017Z7	(H.M. 10 min) matl from barrels	3			Δ		Δ		Δ				Less orange peel than item 2
4 1017Z7	Machine mixed 100 cc high shear head 2000 RPM (after pour 3)	36	Δ				Δ		Δ				All 36 are uniform, orange peel (masking tape)
5 1017Z7	(H.M. 10 min) material from pump test ports	4	2	2				Δ	Δ				Orange peel
6 1017Z7	Machined, mixed 200 cc blender 2150 RPM (2 before 3 after pour 5)	5	Δ					Δ	Δ				Orange peel & alligatoring
7 1017Z7	(H.M. 10 min) Resin skimmed from top reservoir, hardener from test port	5	Δ				Δ		Δ				Strong orange peel
8 1017Z7	(H.M. 10 min) Resin from bottom of reservoir thru dipstick	3	Δ					Δ	Δ				Dipstick 3 inches from bottom
9 1017Z7	After pour 3 machine-mixed 100 cc high shear head 2000 RPM with 3 x 3 in. RTV-60 cast into epoxy	4		Δ			Δ		1	1	2		

NOTES:
1 Metal containers seem to repel haze at periphery consistently
2 Pyrex containers repel haze at periphery inconsistently
3 Amount of haze appears to be directly proportional to filler concentration
4 H.M. samples were hand mixed by R. Fuse

program was performed and funded by GE in order to determine the causes of the surface defects in the spincasting, and to develop remedies to overcome them. Weekly interim progress reports were sent to JPL during the course of this program. At the conclusion of this program, a verbal report was presented by General Electric personnel to JPL at Pasadena.

5.2.6 SPINCAST POUR NO. 6

As a result of the development program the spincast formulation was altered, the room ambient temperature was maintained between 72 and 79°F throughout the pour and cure cycle. The 100cc mixing head was set at 1000 rpm with a Strobotac; 1100 strokes were dispensed which represented 9-1/2 gallons and a 3/16-in. thick coat.

In order to reduce the vibrations of the table which were believed to cause radial ripples, a heavy 35-ft truss structure was added to the assembly between the spintable and the mold (Figure 5.2-12). This structure had been used during the manufacture of the GE Space Simulator Mirror Spincasting (Figure 5.2-2). Details of the vibration investigation are given in Appendix G.

After mounting the mold on the spintable truss, the mold was leveled on three legs until a minimum dial indicator reading was obtained on the paraboloidal surface when manually rotating the mold.

Upon visual inspection of the sixth coat surface through the plexiglass cover, severe orange peel was observed within a 10-inch radius, faint flow lines and less severe orange peel up to a 4-foot diameter. Severe orange peel was noticed within 1/2 in. of the outer mold diameter. A fair quantity of dimples was intermittently dispersed throughout the mold surface, and air bubble clusters formed at the extreme periphery of the mold.

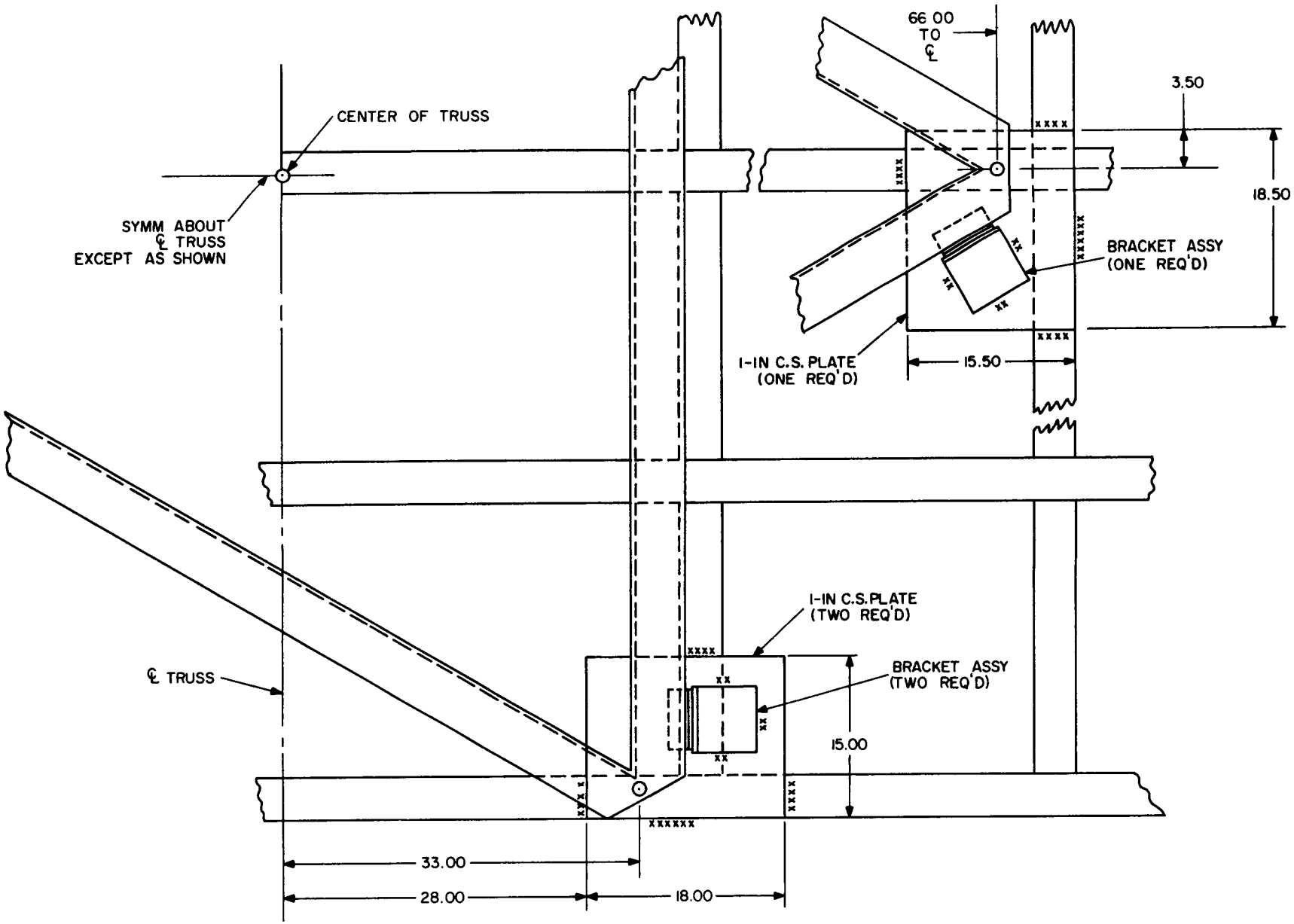

Figure 5.2-12. Attachment of 10-ft-diameter Spincast Mold to GE Space Simulator Support Truss Structure

Several full-scale resin-flow tests were dynamically performed on the mold surface prior to Pour No. 6 after which the mold surface was washed with Genesol "D", toluene, and trichlorethylene. It was proposed that the surface imperfections of the sixth pour might have resulted from residual solvent which leached from the substrate and reacted with the epoxy constituents of the sixth pour. The sixth pour was considered essentially as a dust binder and therefore preparations were made for a seventh pour.

5.2.7 SPINCAST POUR NO. 7

Pour No. 7 was made with the same spincast formulation as Pour No. 6. Ambient temperature was maintained between 70 to 75°F throughout the pour cycle. The 100cc mixing head was set at 1000 rpm for pours 7, 8, 9 and 10. During Pour No. 7, 1,000 strokes were dispensed at 344 grams per 100 strokes, approximately a total of 9 gallons.

Foreign material which looked like dark cellophane seemed to flow from the mixing head through the plastic dispensing tube. After completion of the seventh coat, large chunks of a foreign material were apparent in the spincasting. This material was subsequently diagnosed to be pre-cured resin. The seventh coat was, therefore, eliminated and the surface imperfections removed by hand grinding. The entire contents of the spincasting system were dumped, and the system thoroughly cleaned.

An examination of the entire mixing system was made to determine the source of this foreign material. At first it was suggested that the dispensing tube or the mixing head chamber had a residual quantity of catalyzed resin from previous pours. This was discounted because:

a. There were very large quantities of this stringy material coming from the mixing head.

b. The mixing head had been disassembled as were the dispensing tubes, and both were solvent-cleaned each time a pour was completed.

c. A dark material such as this would have been visually observed either in the mixing head or the translucent pouring tube prior to spincasting.

The following checks were made without finding any traces of this foreign material:

a. The resin reservoir lid was removed and several gallons of resin were poured through fine cheesecloth.

b. The hardener reservoir was examined; the liquid was clear and transparent.

c. The hardener and resin lines were disconnected, inspected and cleaned.

d. The resin and hardener pumps were completely disassembled. Examination of the piston packings indicated no traces of wear.

e. The water jacket on the mixing head was checked with red dye under pressure. There were no signs of water jacket leaks into the mixing chamber.

The hypothesis was developed that one of the ingredients in the Claremont black paste dye reacted with the spincast hardener system to form a quickly cured stringy material. As a result of this hypothesis, use of the Claremont paste was discontinued.

5.3 COAT NO. 8

5.3.1 SPINCAST POUR NO. 8

Based upon tests which indicated superior resistance to electroform solutions and also upon the need to eliminate the foreign material which caused an abort of pour No. 7, a slightly revised spincasting formulation was used.

Ambient temperature was maintained between 65 and 73°F throughout the pour and cure cycle; 1100 strokes were dispensed (116 strokes = 1 gallon). The resulting cured surface appeared to be of good quality. Therefore, the decision was made to optically inspect the mold, postcure at 120°F, optically re-inspect and scribe. Results of these optical inspections are tabulated in Section 5.5.3.

5.3.2 THERMAL CURE OF 8th SPINCAST COAT

The spincast female master was thermally cured in the following manner. The room was heated by regularly installed steam heat supplemented by kerosene-fired

portable "salamander" heaters. This brought the temperature to slightly above 100°F. A polyethelene test was then erected enclosing the spintable and the spincasting. Four 1500-watt electrical heaters were placed inside the tent. Since this did not prove sufficient, a "salamander" was placed in the access tunnel to the spincast table support bearing at approximately 8 feet below floor level and at a distance sufficient to prevent local hot spots on the spincast drive assembly. The temperature in the tent was raised to 120°F and maintained there for four hours. The last-named "salamander" and the heaters inside the tent were then shut off, but the room temperature outside the tent was maintained above 100°F. When the ambient temperatures inside and outside the tent were equal, the tent was removed. The room temperature was then lowered to ambient at the rate of 10°F per day. During optical inspection the ambient temperature remained between 80 and 90°F; during subsequent scribing it dropped as low as 74°F. A copy of the log kept during the thermal cure is reproduced on page L-1 (Appendix L).

Prior to thermal curing, thermocouples were placed in the epoxy and on the master support structure in various locations (Figure 5.3-1). Recorded temperatures from two of these thermocouples are shown in Figure 5.3-2. The thermocouples plotted represent the low and high values of temperatures which existed during the cure cycle. As can be seen from the Figure, a maximum difference of less than ten degrees existed between a point on the structure (No. 6) and a point in the epoxy (No. 5). The No. 6 thermocouple was located on the underside of the structure near the outside of the dish.

The No. 4 and No. 5 thermocouples were located in holes drilled radially into the side of the epoxy from its periphery. Three thermocouples were placed near the center of the master, imbedded into the epoxy at depths of 1/2 in., 13/16 in., and 1-5/8 in., respectively, below the surface (Figure 5.3-1). The readings of these thermocouples were within five degrees of No. 5 and are therefore not shown in Figure 5.3-2. Table L-1, Appendix L is a partial copy of the thermocouple records kept during the significant part of the thermal-cure cycle.

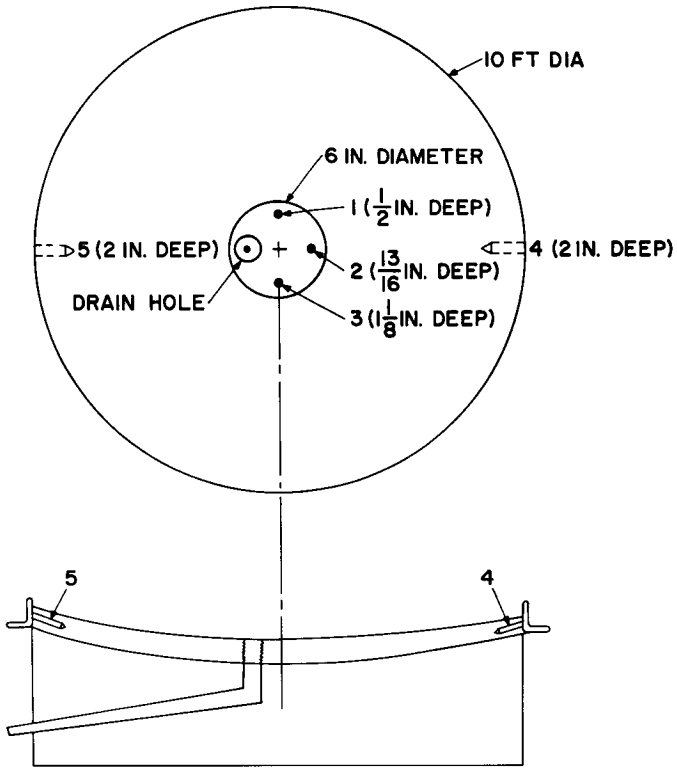

Figure 5.3-1. Location of Thermocouples After Pour No. 8

5.3.3 CRACKING OF THE MOLD

During the heating phase of the thermal cure cycle, two sharp cracking noises were heard. Visual inspection immediately after each of these noises did not disclose any damage. During the scribing operation (Appendix D) which was performed subsequent to the second optical inspection, the scribing tool did not continuously cut into the surface, but missed it over part of a full revolution. During the final stages of scribing and three days after it had been cooled to room temperature the spincast mold cracked as shown on the pattern in Figure 5.3-3. A close-up of the cracked area is shown in Figure 5.3-4. The area between the two cracks, approximately one-quarter of the total mold area, lifted up from the aluminum support structure a distance of approximately 5/16 of an inch (Figure 5.3-5). A portion of the cracked spincasting after removal from the aluminum dish is shown in Figure 5.3-6.

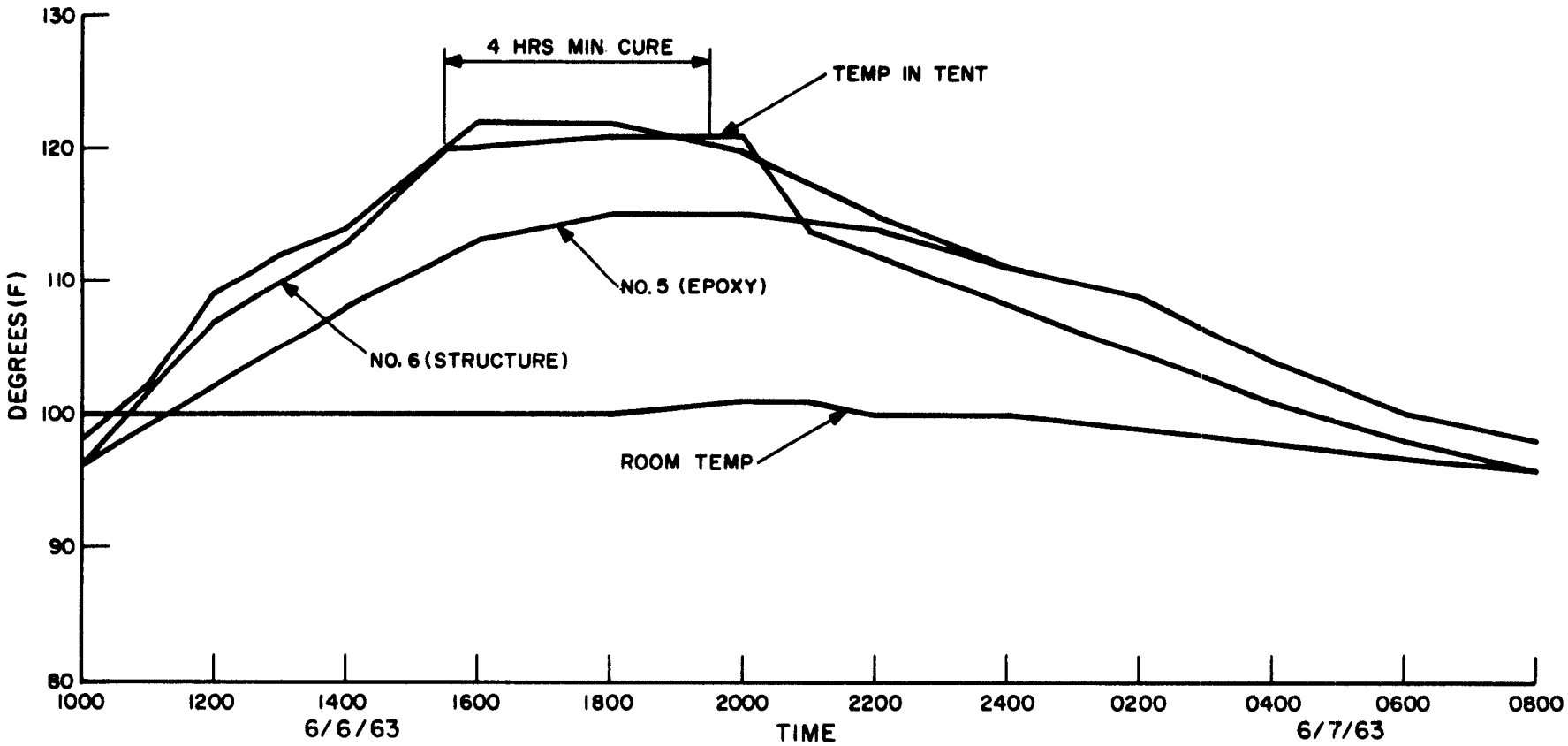

Figure 5.3-2. Temperature Recorded During Thermal Cure of Pour No. 8

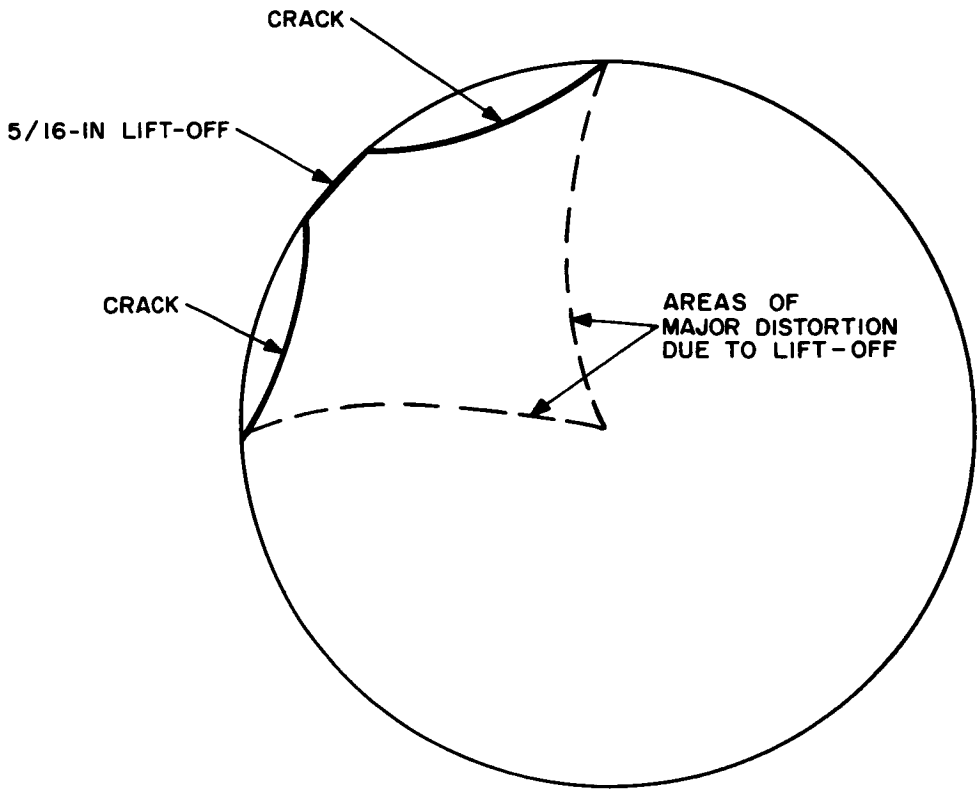

Figure 5.3-3. Pattern of Cracked Mold

It is believed that the thermal cure cycle caused shear stresses between this exceptionally thick spincast epoxy mold and its aluminum back-up structure which exceeded the bond strength between the two materials. The above-mentioned cracks heard during the cure probably indicated the occurrence of shear separation. The mold, however, continued to be held down to its support structure by the bending strength of the plastic which bridged the separated areas. The drop in temperature to as low as $74^{o}F$ and the mechanical shock caused by intermittent scribing were instrumental in triggering the cracking of the mold, but were not the actual causes of it.

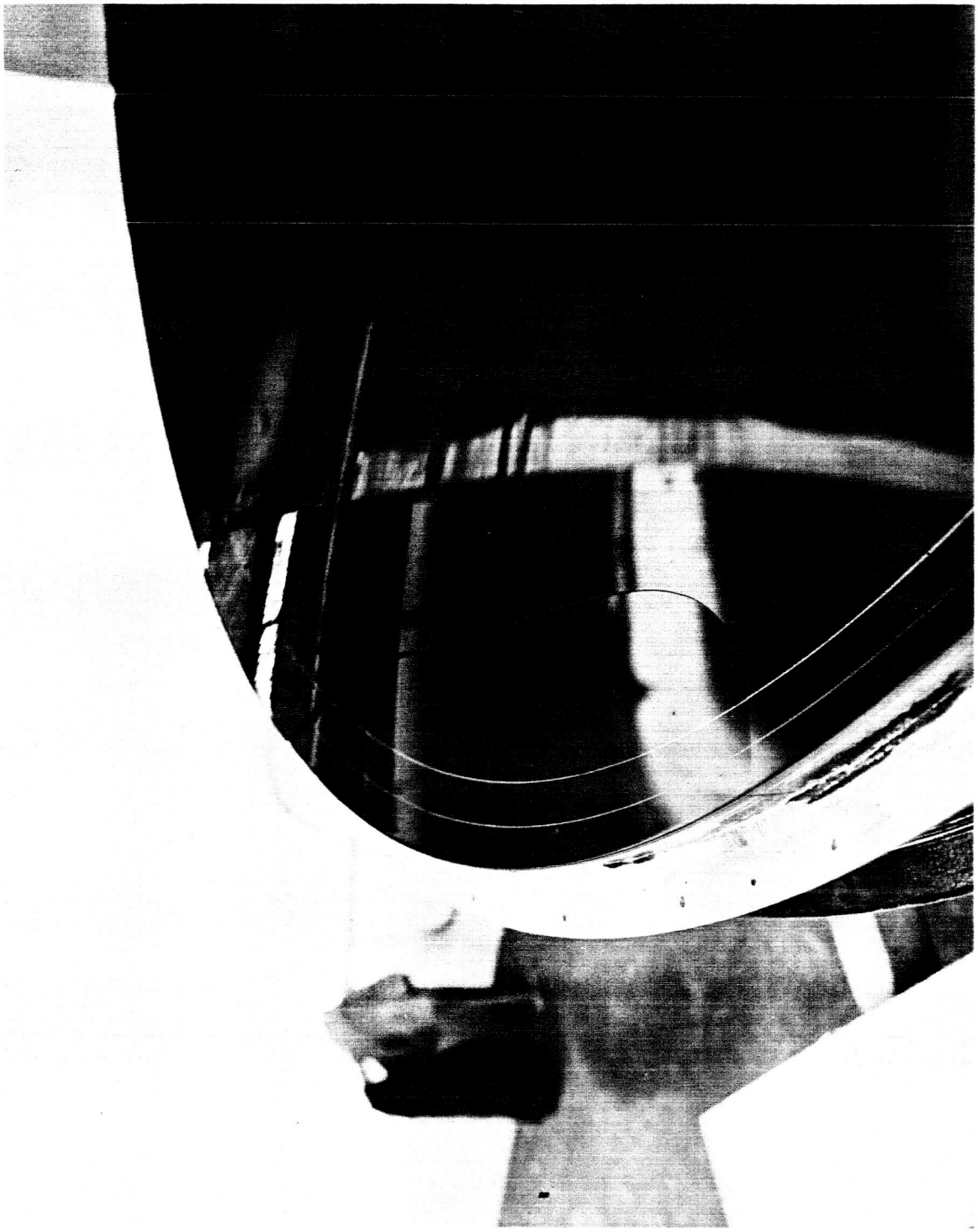

Figure 5.3-4, Close-up of Cracked Mold

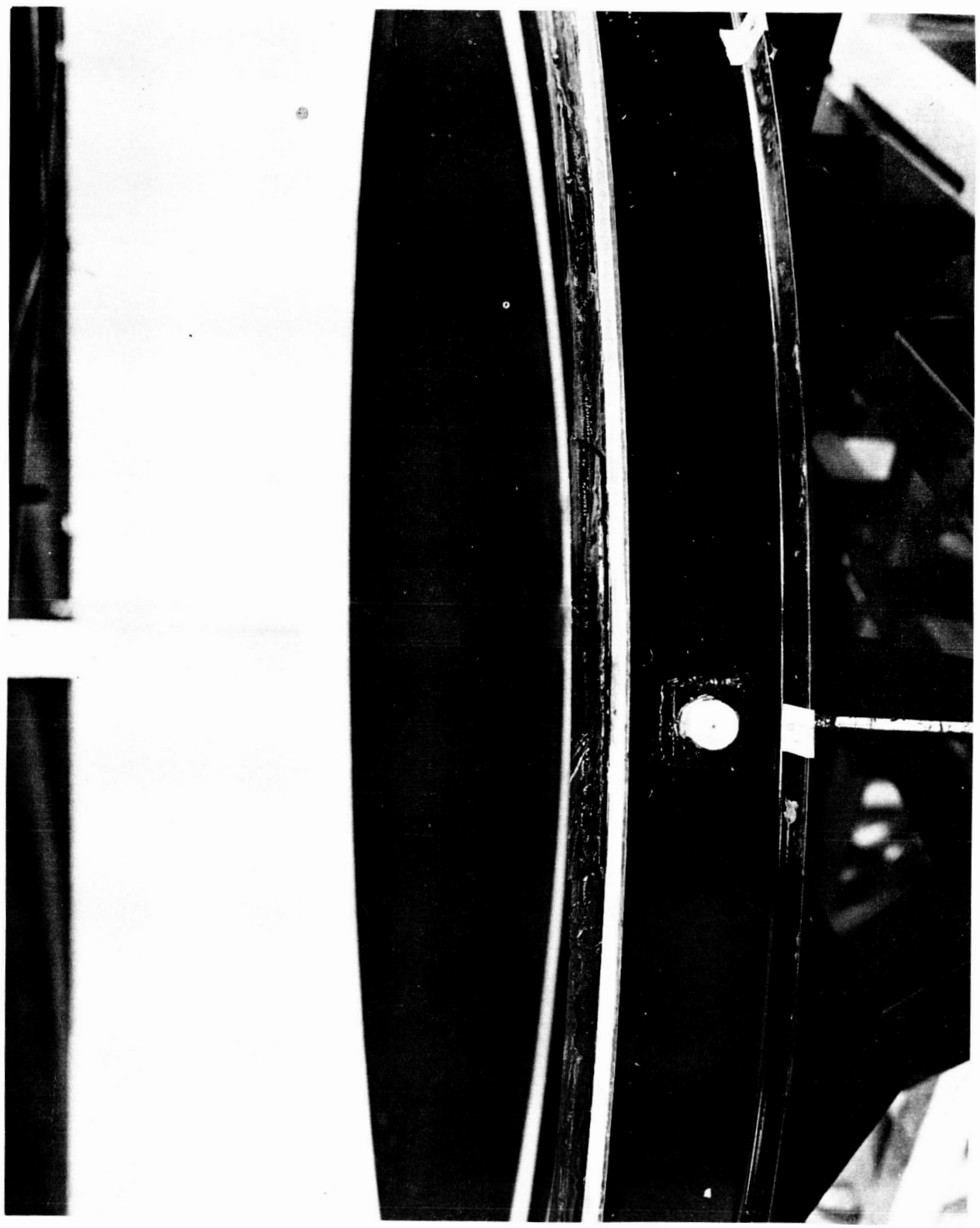

Figure 5.3-5. Side View of Cracked Mold

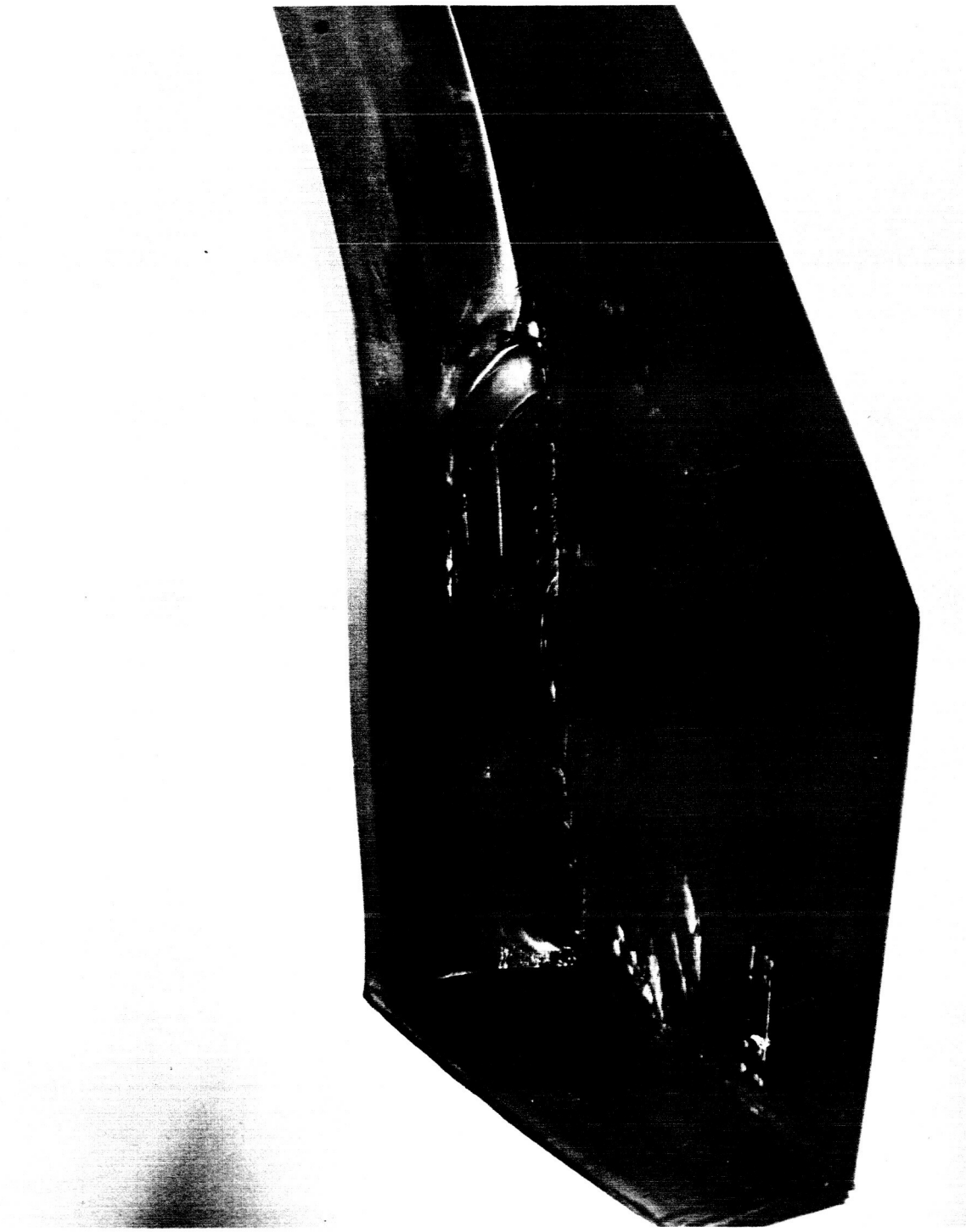

Figure 5.3-6. Cross Section of Cracked Mold; The Eight Pours are Clearly Visible

It must also be realized that a total of eight spincast pours had been made on this mold which produced a total epoxy thickness of 1-5/8 inches. This compares to the normally planned two or three pours with an aggregate thickness of 5/8 inch. Every time an additional layer of spincasting was added, it was realized that the possibility of mold separation due to relative thermal expansion was increased. The accompanying calculated risks were taken after due consideration of the probability of failure, schedule and cost. Separation of mold and back-up structure had never occurred in previous spincastings, but no spincastings of 1-5/8-inch thickness had ever been produced by General Electric. The unusual thickness must definitely be considered a major contributory cause to the separation of the mold.

5.4 FINAL SPINCASTING COATS

5.4.1 PREPARATION

In order to save the aliminum support structure, all the epoxy was removed from the mold dish by thermal shocking with dry ice, using crow bars, and sanding (see Appendix B). In order to avoid mold separation the following additional precautionary steps were taken:

a. Reduce the total thickness of the spincasting by pouring fewer layers.

b. Increase the metal-to-plastic bond by applying a hand-brush coat of flexibilized epoxy to the aluminum dish prior to pouring.

c. Maintain mold at 90°F after thermal curing to minimize thermal stresses and embrittlement of the epoxy.

When the "cracked" eight-layered casting was removed from the metal substructure (with the aid of dry ice), the adhesive bond between the epoxy casting and the metal surface appeared spotty in places, non-existent in others. To prevent a reoccurrence, treatment with a flexible resin overcoat was performed. The surface preparation consisted of two stages, metal treatment and coating, and is described in detail in Appendix B. Plugs of cured resin were pried loose from the metal mold near the periphery and the center of the first spincast coat to check the quality of

adhesion of the flexible resin primer coat. The adhesive bond was found to be stronger than the cast resin itself.

5.4.2 SPINCAST POUR NO. 9

The spincast formulation used for Pour Nos. 9 and 10 was identical to that used for Pour No. 8.

After pouring the base spincast coat on the reworked mold substructure, a fuse blew in the input power line to the spintable motor causing the entire system to shut down. Fortunately monitoring personnel acted quickly to correct the source of trouble, and a good surface quality base coat was attained in spite of the forced shutdown. Since flow, curing, and surface quality of a spincast epoxy system are closely tied in with the time sequencing of events, the unusual events occurring during the ninth pour are considered sufficiently important to warrant detailed documentation (see page L-3, Appendix L).

Observation of the mold surface through the plexiglass cover indicated a very good surface with no readily apparent visual imperfections. The forced shutdown presented an unusual opportunity to observe, in large scale, the effects of the cast epoxy which continued to flow to a position of equilibrium for more than 8 hours after casting was initiated.

5.4.3 SPINCAST POUR NO. 10

Having poured a successful base coat (No. 9), the final coat (No. 10) was poured by the same method. The pouring log is reproduced on page L-4, Appendix L. Monitor data sheets are shown on pages L-6 through L-14. Similar logs and monitor sheets were, of course, kept for each of the 10 pours.

The spintable was stopped after 38 hours, when a control sample poured on the small spintable (Figure 5.2-5) and statically poured samples exhibited sufficient hardness. Inspection through the plexiglass cover disclosed no defects, and the

cover was removed. The final spincasting surface had very faint, almost indistinguishable (and considered negligible) orange peel and very faint circumferential flow lines. The flow lines did not appear this time to coincide with any structural parts of the cover. There was a total absence of alligatoring near the center.

Severe alligatoring near the center was observed on other spincastings during this program. It is interesting to note that those that had alligatoring likewise had it for up to 20 minutes after pouring and while the resin was still fluid, while those that had no alligatoring had none during pouring or anytime thereafter.

5.4.4 THERMAL CURE OF 10th SPINCAST COAT

Following the 10th pour, the tent was again set up over the spintable and the master was cured at a temperature of 120°F for a period of four hours. The procedures and set-up were identical to the previous cure as described in Section 5.3.2. As an added precaution, the temperature of the mold was never allowed to go below 90°F after the curing cycle.

5.5 OPTICAL INSPECTION

5.5.1 METHOD OF INSPECTION

A. Inspection Grid

If a light source is placed at the focal point of a perfect paraboloidal surface which is concave to the incident light, the light reflected from that surface will be collimated as paraxial rays (Figure 5.5-1). If the reflecting surface deviates from a true paraboloid or has zonal errors (ripples, hollows, etc.) light will be reflected out of collimation (Figure 5.5-2). Thus, the magnitude of the surface errors can be obtained by measuring the angles between the optical axis and the reflected rays.

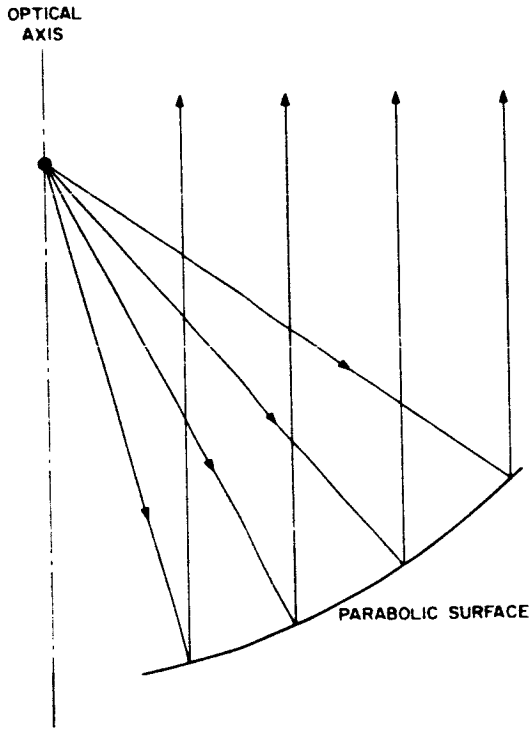

Figure 5.5-1. Paraxial Reflection from a Perfect Parabolic Surface

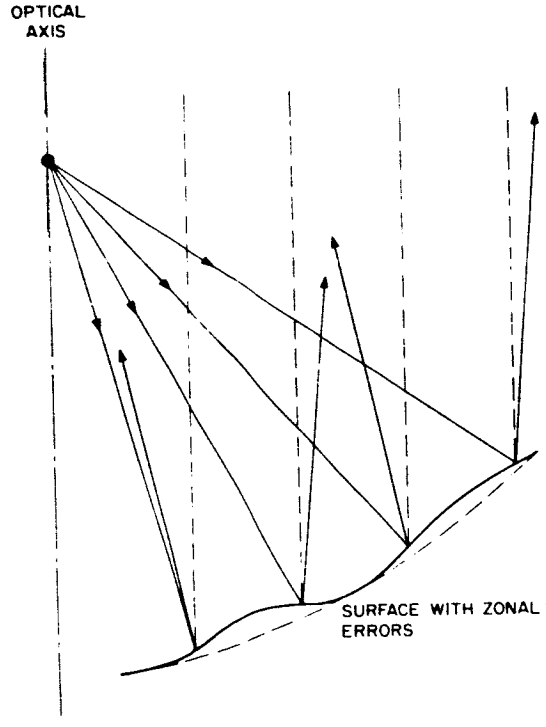

Figure 5.5-2. Uncollimated Reflections Due to Zonal Errors

In order to measure the mirror geometry adequately by a limited number of measurements taken at discrete points, each measured point should be representative of an area not exceeding one square foot. It was therefore decided to take error angle readings at 8 radial and 12 circumferential locations. Thus a total of 96 error readings would be taken which corresponds to one reading for every 0.74 square foot. The mirror was divided into 96 zones (Figure 5.5-3) of equal areas whose centers lie on 8 radial and 12 circumferential lines as shown in Figure 5.5-4. By making surface measurements at these 96 points, a uniform coverage of the mirror surface was obtained which was sufficiently accurate to predict the mirror geometry, yet did not require an excessive quantity of measurements.

The test setup used for the optical inspection of the epoxy mirror master consisted of a light source placed at the focal point and eight telescopes aligned with their optical axes vertical. Throughout the optical inspection, the epoxy master was never removed from the spintable. Since the master had to be rotated during testing, this arrangement guaranteed the axis of rotation to be coincident with the optical axis of the paraboloid, because the spincast surface had been generated by rotation about this same axis.

B. Preliminary Arrangement

The general arrangement for optical inspection is shown schematically in Figure 5.5-5. The light source used was a 100-watt, 20-volt lamp operated at 6 to 8 volts. It consisted of a spherical, clear-glass bulb containing a tungsten filament which measured approximately 5mm across the coils. The lamp and lamp holder were mounted approximately at the focal point in a device which allowed for movement in any direction.

The objectives of the eight telescopes were simple plane-convex lenses. These lenses had a clear aperture of 62mm and a focal length of 2019mm. They were mounted in a wooden 2 x 4 with the plane of the lenses normal to the spin axis (Figure 5.5-6). As explained below, no special care was necessary to mount the lenses accurately or parallel.

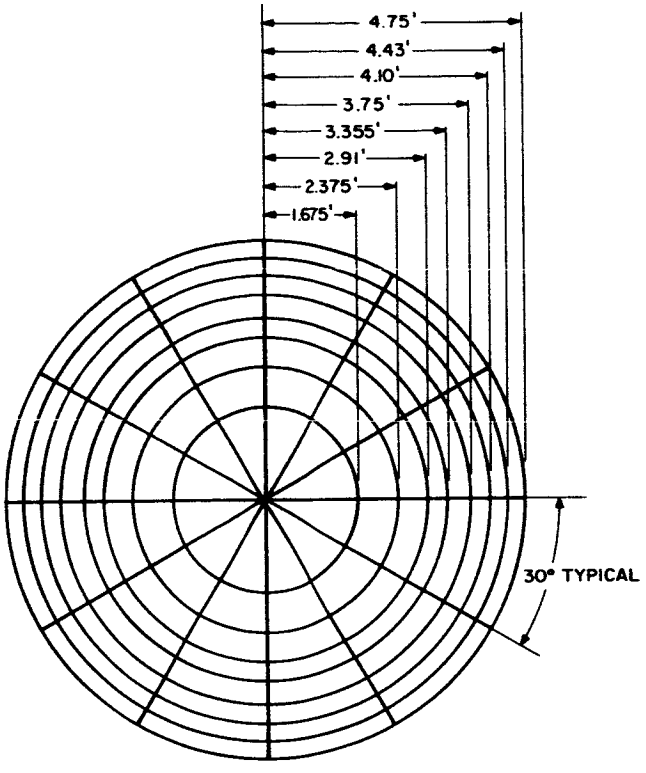

Figure 5.5-3. Subdivision of Mirror Surface Into 96 Equal Areas

The eyepieces of the test telescopes were of the Ramsden type and had an effective focal length of 1 inch. A 10mm crossed reticle with 100 divisions each in the X and Y axes was located at the focal plane of each eyepiece (see insert in Figure 5.5-5) such that the X axes were along a radial line. The eyepiece and reticles were mounted in simple draw-tube adapters (Figure 5.5-7) and arranged in a line on another wooden 2 x 4. Adjustment of the adapters in any direction was made possible by a simple clamping arrangement. The mounted eyepieces were then located at the infinity focus of each of the eight objective lenses.

C. Alignment of Test Telescopes

A vital aspect of the test setup was the alignment of the optical axis of each telescope parallel to the axis of the paraboloid. Since the production of the master surface by rotation ensured a perfectly vertical optical axis, it was only necessary

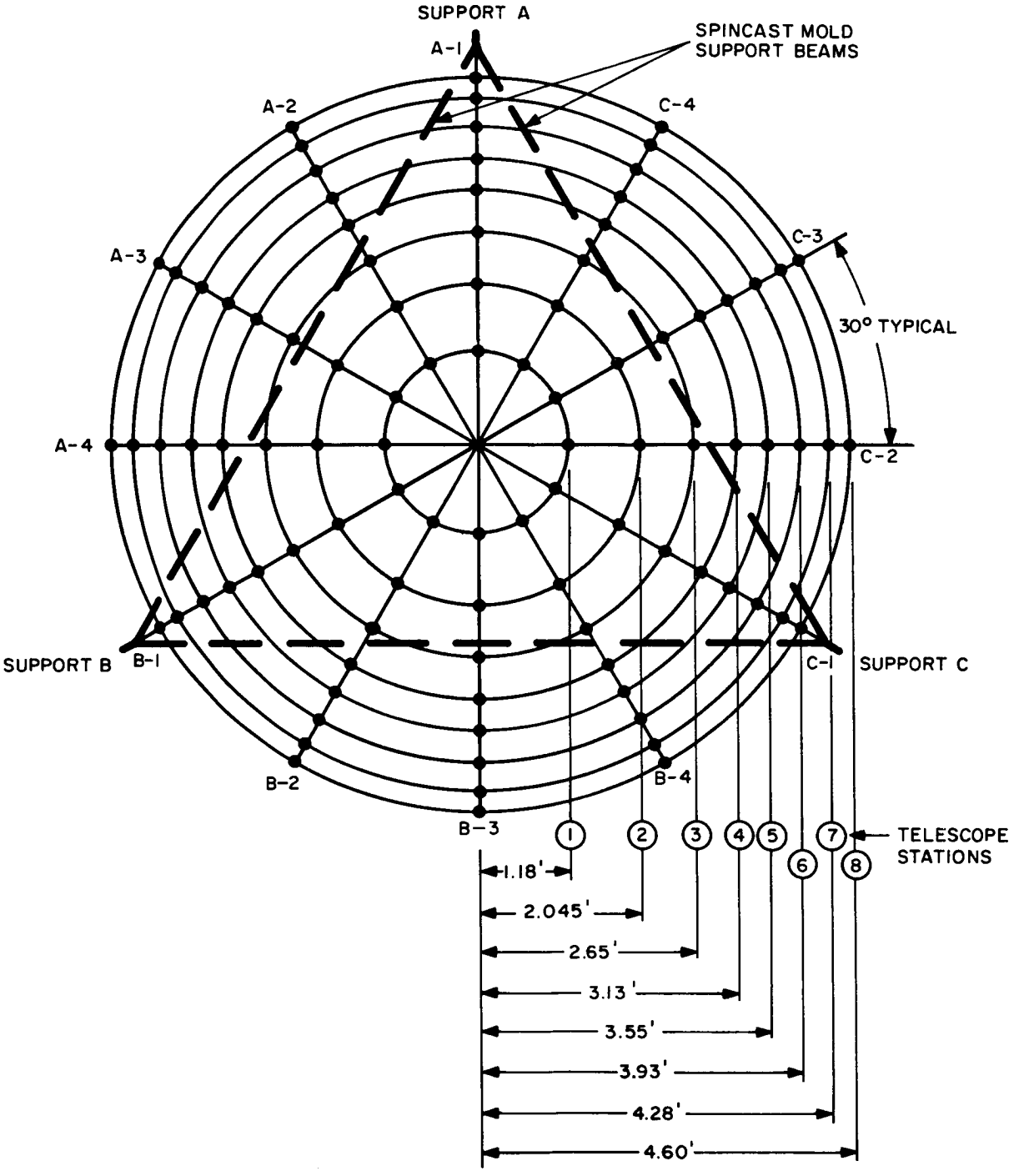

Figure 5.5-4. Location of 96 Optical Inspection Points Relative to Spincast Mold Support Structure

87

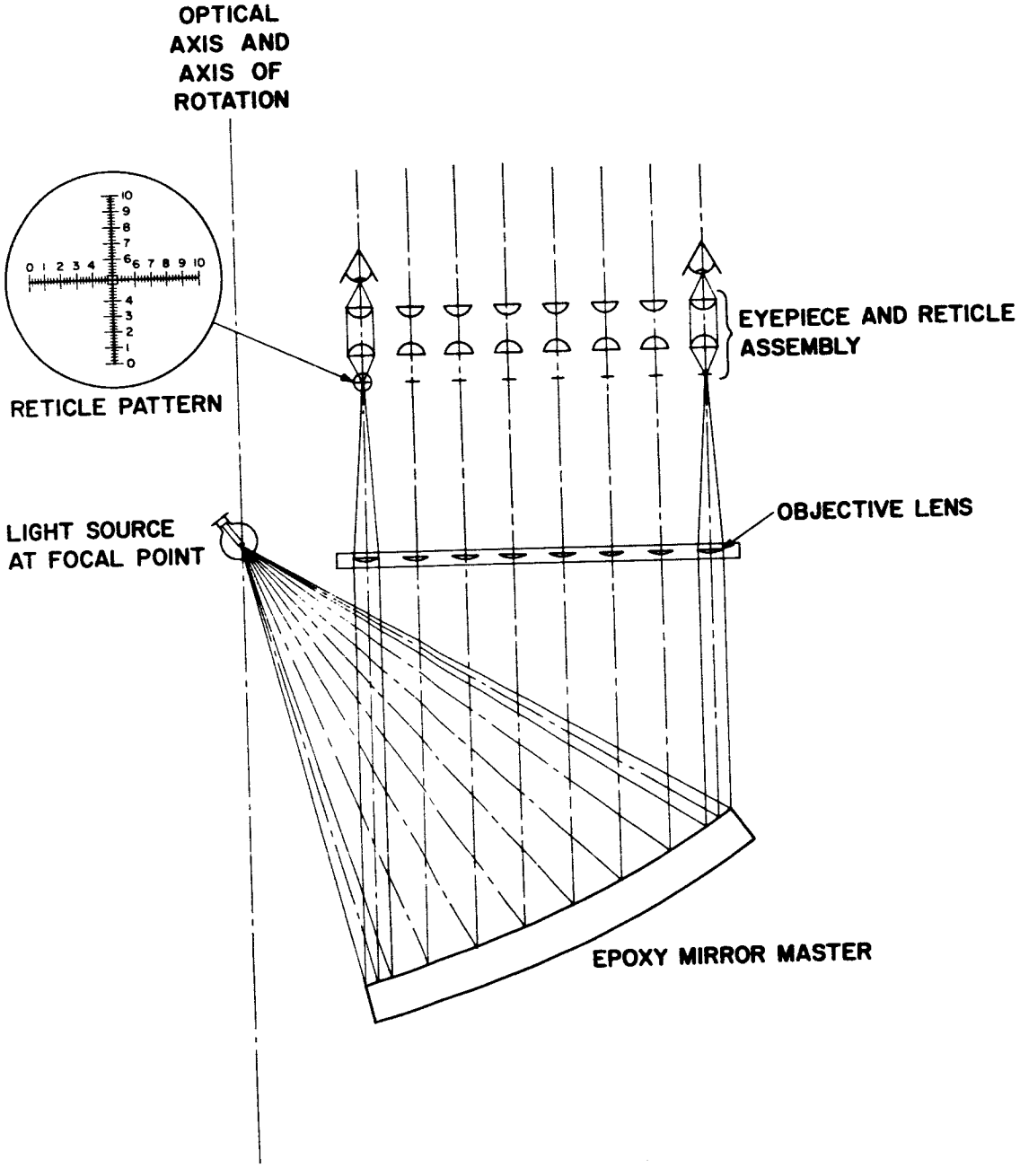

Figure 5.5-5. General Arrangement of Test Elements

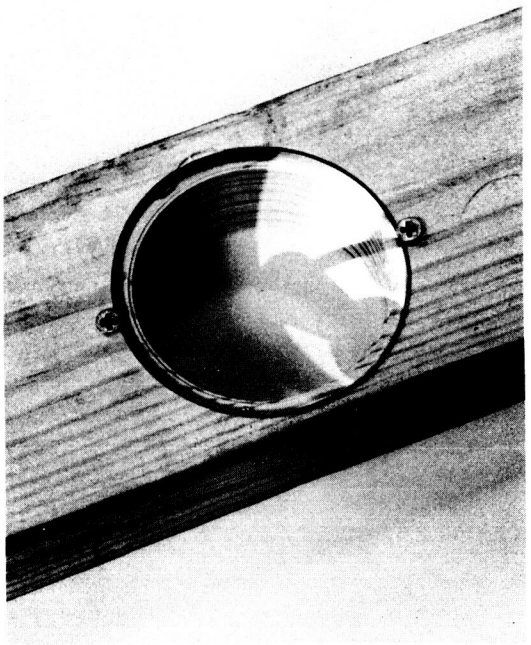

Figure 5.5-6. Mounted Telescope Objectives

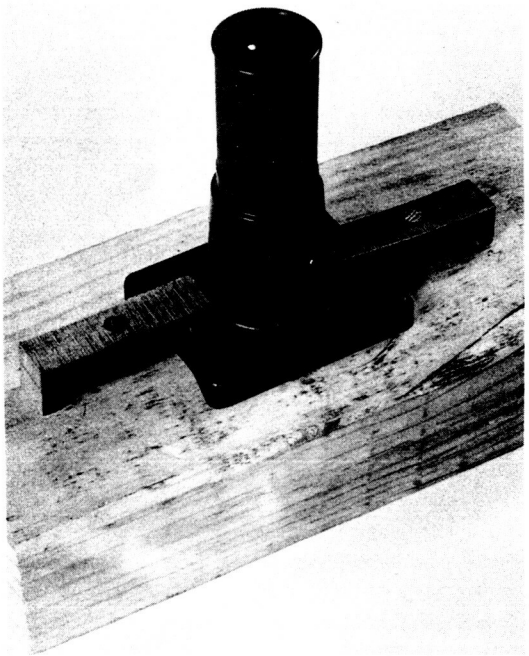

Figure 5.5-7. Mounted Eyepiece and Reticle Adapter

to align the axis of each telescope system vertically. A collimating theodolite was used in aligning the eight inspection telescopes. The theodolite, which was adjusted to project a cross-hair reticle at infinity, was located exactly under one of the telescope objectives by use of a plumb line and was aligned vertically by use of the adjustments on the instrument.

The image of the theodolite reticle was then viewed through the eyepiece of the telescope being aligned. When the optical axis of the theodolite is coincident with the axis of the test telescope, the intersection of the theodolite cross hairs will be seen at the center of the reticle in the test telescope. The eyepiece adaptor was adjusted until the two reticles were superimposed. This alignment procedure was repeated for each of the eight test telescopes.

D. Location of Focal Point

The final preparatory step was the location of the test lamp filament at the exact focal point of the paraboloid. If the test telescopes are properly aligned and the mirror is a perfect paraboloid and the test lamp is located precisely at the focal point of the mirror, each telescope will produce a sharp image of the lamp filament at the exact center of the telescope reticle. If the test lamp is placed in a position other than at the focal point of the mirror, the filament image will be displaced from the center of the field. The direction and amount of image displacement is an indication of the correction required in lamp position.

If the light source is located on the axis of the parabola beyond the focal point of the mirror, the reflected light will converge and the images in the telescopes will be displaced toward the optical axis of the parabola. If the light source is placed inside the focal point of the mirror, the reflected light will be diverging and the images will be displaced away from the mirror optical axis. When the light source is moved to the right of the optical axis, all eight images move to the left and vice versa. It becomes obvious, therefore, that by simply manipulating the position of

the light source until the filament image is centered in each telescope, it is possible to precisely locate the light source at the focal point of the paraboloid. For example, a 1/16-in. shift in lamp position can cause an average change of 50 to 60 seconds in the reflected light beam with a resulting image shift of 5 to 6 divisions on the telescope reticle.

Location for perfect alignment on all telescopes is prevented by local slope errors on the paraboloid. Therefore, the lamp was adjusted until a "best fit" condition was achieved; that is, the light source was manipulated until the filament image was as close to the center of the reticle of all the test telescopes as possible. This procedure located the mean focal distance of the paraboloid to within one-quarter of an inch. A refined method of locating the focal points within the focal plane is discussed in Section 5.5.1(F).

E. Slope Error Measurement

Since the displacement errors have a considerably smaller effect on mirror efficiency than the slope errors, it is common practice to assign the entire surface error to slope error. This practice was followed in this report.

With the source located at the mean focal point of the mirror, any deviation of the filament image from the center of field of the eight test telescopes is due to geometric errors of the mirror surface. Thus, the local slope error at any point on the eight arcs under the telescopes can be obtained directly by reading the displacement of the filament image from the center of the telescope reticle.

The first step was to calibrate the telescope reticles. This is a simple trigonometric process, and the calculation used for the epoxy mirror test arrangement is shown below. The calculation was checked by theodolite measurements and found to be satisfactory.

1. Theoretical Calibration:

Telescope Data:	
Focal length of telescope objective	2019 mm
Size of reticle scale	10mm over 100 divisions
Field of view	Angle the sine of which equals 10/2019 = 0.00495
Angle the sine of which equals 0.00495	0.291^{o} or 17.5 minutes
Calibration in seconds of arc per division	17.5 x 60/100 = 10.5

2. Calibration Check by Theodolite:

Immediately following the test telescope alignment as described in Section 5.5.1(C), the theodolite was depressed 7.5 minutes from the vertical by a vernier adjustment of the elevation. The image of the theodolite reticle was observed to shift 45 divisions on the test telescope reticle. It follows then that:

$$\text{Full scale} = \frac{100}{45} \times 7.5 = 16.7 \text{ min.} = 1000 \text{ seconds, or } 10 \text{ sec,}$$

$$\text{thus each division} = \frac{1000}{100} = 10 \text{ seconds of arc.}$$

Since the slope deviation of the light entering the telescope is twice the slope error on the paraboloidal surface, the actual surface slope error can be read directly on the telescope by considering each division as 5 seconds of surface slope error.

The accuracy of the reticle readings on the spincasting master was ±1 division which equals ±5 seconds of slope in the radial and circumferential directions each. The total slope error of the master is therefore, accurate to within approximately ±7 seconds.

F. Adjustment of Measured Data for Errors in Lateral Focal Point Location

As described in the preceding sections, all telescope eyepiece and reticle assemblies are accurately aligned vertically by means of a collimating theodolite. The focal point of the paraboloid, however, is obtained by a trial and error "best fit" of the reflected image in all the reticles. The accuracy of the slope error measurements depends on the location of the inspection lamp filament at this approximate focal point.

The vertical location of the focal point (along the axis of revolution of the paraboloid) can be determined quite accurately, because no sharp image is obtained in the telescopes if the filament is not located in the focal plane. The lateral location within the focal plane, however, is not equally well defined. Therefore, an error in filament location will be read as an apparent slope error of the surface. This is indicated in Figure 5.5-8 by the dashed lines. If the error in focal point location is denoted by e, the apparent slope error $d\beta = \Delta/L$ is measured. This angle is given by the following expression:

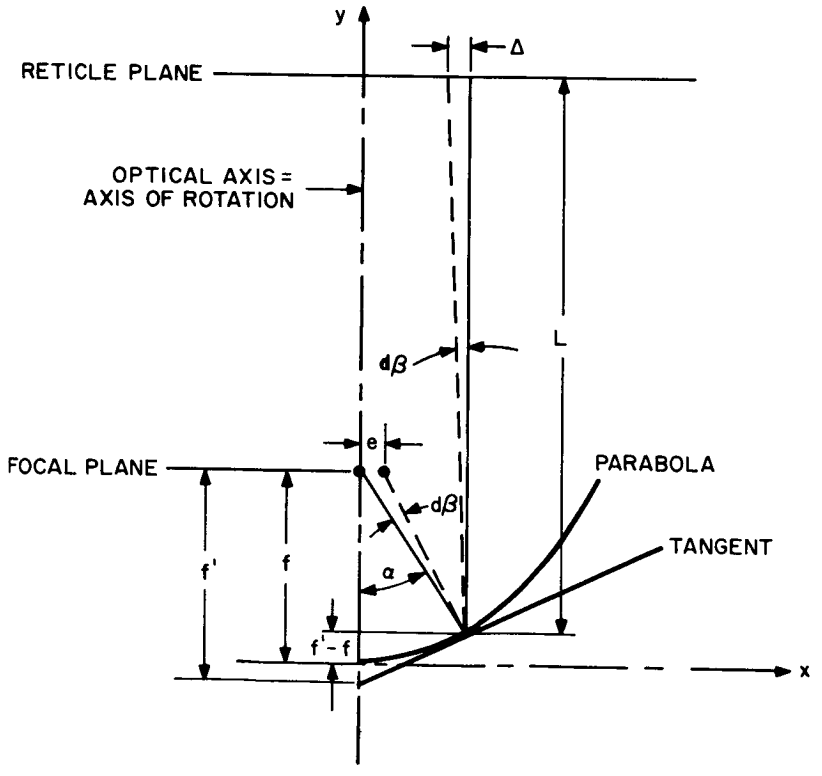

Figure 5.5-8. Slope Error Due to an Error in Focal-Point Location

98

$$d\beta = \frac{\Delta}{L} = \frac{e \cos^2 \alpha}{f - (f' - f)} . \quad (1)$$

By the use of the equation of a parabola,

$$x^2 = 2 py, \quad (2)$$

where,

$$f = p/2 . \quad (3)$$

The demoninator of Equation (1) becomes equal to (p/2 - y). Substituting the value for (cos α) from the large triangle in Figure 5.5-8 allows Equation (1) to be brought into the form

$$d\beta = \frac{\Delta}{L} = \frac{e}{f} \frac{1 - (y/f)}{1 + (y/f)} , \quad (4)$$

$$d\beta = \frac{\Delta}{L} \cong \frac{e}{f} . \quad (5)$$

If the simplified expression (5) is used for the apparent slope error $d\beta$ due to an error e in the focal point location, this error can be calculated from the inspection data by obtaining the average radial and average circumferential deviations of all the reticle readings. If both of these averages are equal to zero, the best fit (least square error) focal point location has been obtained.

If they are not equal to zero, the "raw" readings can be adjusted by subtracting the average radial deviation from each radial deviation reading and the average circumferential deviation from each circumferential reading. Vector addition of these two adjusted readings at each point yields the adjusted slope error. This value corresponds to the actual measured slope error if the filament had originally been located at the exact focal point.

The maximum error introduced by using the approximate expression Equation (5) rather than the more accurate Equation (4) for the 9.5-foot diameter master and mirror is 28% for points along the outer rim. Since this expression is only used for a least-square error adjustment, it was deemed sufficiently accurate. All the adjusted slope errors shown in this report were obtained by the use of the approximate Equation (5).

5.5.2 INSPECTION RESULTS FOR THIRD SPINCAST COAT

A. Focal Length

The third coat of the spincast master was inspected by the method described in Section 5.5.1. The focal length was determined to be 68-3/4 inches. This compares with a design focal length of 68.8 inches.

B. Slope Errors

The X and Y deviations read in the 8 telescope reticles at 12 circumferential locations are shown in Appendix H, Table H-1. Using the conversion data of 5 seconds per division, derived in Section 5.5.1(E), and realizing that a reading of (50, 50) corresponds to the center of the reticle cross hairs (See insert Figure 5.5-5), the slope error is obtained by the formula

$$s = \left[(X - 5)^2 + (Y - 5)^2\right] \times 5. \qquad (6)$$

here,

s = slope error,

X, Y = reticle readings.

Table H-2, Appendix H shows the result of this calculation for the 96 points inspected. Visual inspection of the surface disclosed the presence of two annular areas having approximate diameters of 2 feet and 4 feet, respectively. Each of these areas was 1 to 3 inches in width and had a small radial outcropping connecting

it to a point below the exterior corner of the pouring chute (Figure 5.2-8). These annular areas covered 3 to 4% of the mirror area and had a relatively rough surface. Table H-2 shows that, with the exception of these areas, the maximum measured slope error of the spincast surface was 65 seconds of arc. The median slope error was 35 seconds.

Since the maximum slope error was 65 seconds over 96 to 97% of the area, it was approximately equivalent to the self-imposed goal of 2 minutes (120 seconds) over 98% of the area.

5.5.3 INSPECTION RESULTS FOR EIGHTH SPINCAST COAT

A. Inspection Before Thermal Cure

1. Focal Length

The focal length was determined by the method described in Section 5.5.1 (D) and found to be 68-3/4 inches. This compares with a design focal length of 68.8 inches.

2. Slope Errors

The reticle readings determined by the method of Section 5.5.1 (C) are given in Table H-3 (Appendix H). The corresponding slope errors calculated from Equation (6), are tabulated in Table H-4 (Appendix H) from which the maximum slope error is shown to be 80 seconds, and the median slope error 35 seconds.

B. Inspection After Thermal Cure

1. Focal Length

The focal length was measured to be 68-3/4 inches, compared to the design value of 68.8 inches.

2. Slope Errors

The reticle readings are shown in Table H-5 (Appendix H) and the slope errors in Table H-6 (Appendix H). The maximum measured slope error was 140 seconds and the median slope error 66. Over 95% of the area, the error did not exceed 2 minutes (120 seconds). The self-imposed design goal was 2 minutes over 98% of the area.

If the readings given in Table H-5 are adjusted as explained in Section 5.5.1 (F) to eliminate the error in the lateral location of the focal point, the resulting adjusted slope errors are tabulated in Table H-7 (Appendix H). The maximum slope error was 86 seconds, and 100% of the area (compared to 98% according to the self-imposed design goal) was within 2 minutes of the theoretical slope.

3. Comparison of Inspections Before and After Thermal Cure

The eighth spincasting coat was inspected both before and after thermal curing in order to determine whether the cure cycle caused any significant changes in geometry. The focal length did not change measurably. The maximum measured slope error increased from 80 seconds before curing to 86 seconds after curing. The mean measured slope error remained unchanged at 35 seconds.

If it is considered that the two inspections were performed independently, with independently established focal-point locations and angular positions which may have varied 5 to 10 degrees between inspections "before" and "after", it can be stated that thermal curing did not affect the quality of the surface.

5.5.4 INSPECTION RESULTS FOR FINAL SPINCAST COAT

A. Procedure

Since the optical inspections of the eighth spincast coat described in Section 5.5.3, had shown that thermal curing causes no permanent geometrical distortions of the surface, the final spincast surface was inspected after thermal cure only. In order

to be absolutely sure of the results of the optical inspection, however, two entirely independent inspections were performed. This means that, after the telescopes had been aligned, the focal point located, and all slope error readings taken, the optical equipment was removed. The eight telescopes were then individually re-aligned, the focal point re-established, and a complete, new set of slope error readings taken.

B. Focal Length

The focal length of the final spincast surface was measured and found to be 69 inches for both inspections. The design focal length of the mirror was 68.8 inches.

C. Slope Errors

The reticle readings of the first optical inspection are shown in Table J-1 (Appendix J). The raw slope errors were calculated according to Equation (6), Section 5.5.2(B). The results are given in Table J-2 (Appendix J). Adjusting these slope errors for an error in lateral focal point location as described in Section 5.5.1(F) yielded the adjusted slope errors shown in Table J-3 (Appendix J).

The reticle readings and adjusted slope errors for the second optical inspection are given in Tables J-4 and J-5 (Appendix J), respectively.

A graphical comparison of the results of the first and second optical inspections is shown in Figure 5.5-9. That graph demonstrates that the two independent inspections are equivalent and equally valid. Considering the data of both inspections as a single group is, therefore, permissible.

All of the adjusted slope errors for both inspections (a total of 192 data points) were plotted in Figure 5.5-10. The mean slope error at each telescope is also indicated in that plot. Only 7 points exceeded the 2 minute value; all of them occurred at telescope No. 1.

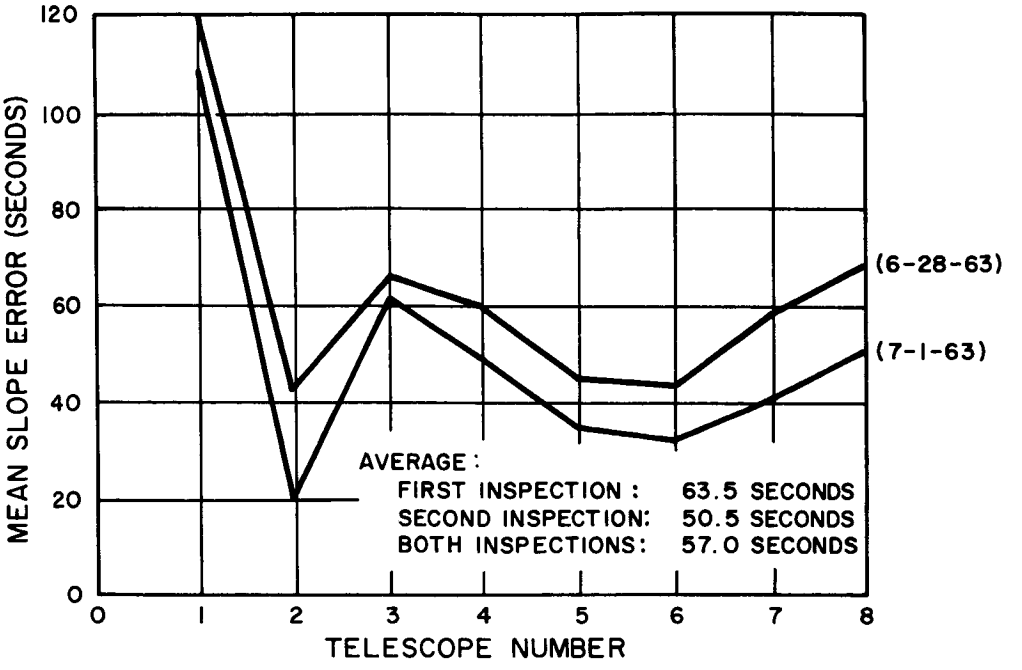

Figure 5.5-9. Optical Inspection of Final Spincast Coat; Mean Adjusted Slope Errors vs. Radial Location for Two Inspections

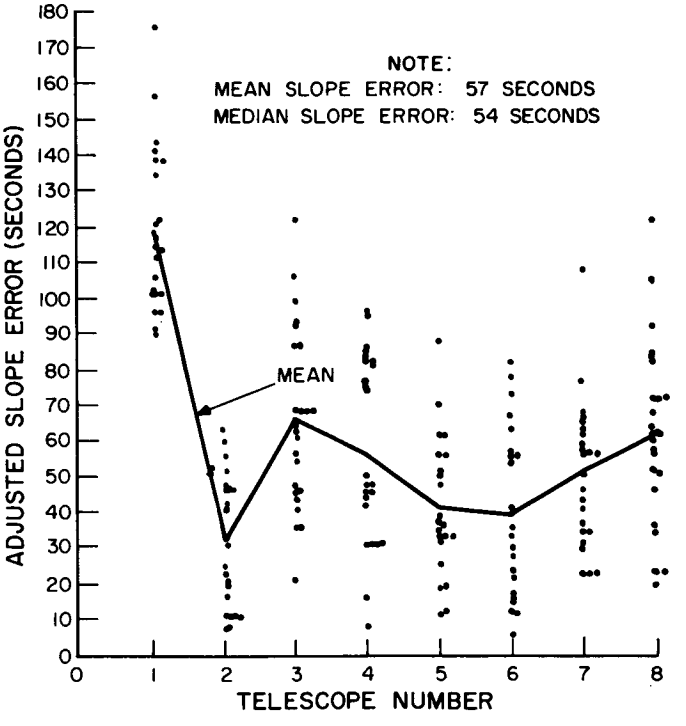

Figure 5.5-10. Optical Inspection of Final Spincast Coat; Adjusted Slope Errors

D. Conclusions

Combining the results of the two optical inspections of the final spincast surface from Tables J-3 and J-4 in Figure 5.5-10 it can be concluded that:

1. The measured focal length is 69 inches compared to the desired 68.8 inches.
2. The median slope error is 54 seconds of arc; the mean slope error is 57 seconds of arc.
3. The maximum measured slope error anywhere on the spincast surface is less than 3 minutes of arc.
4. Seven slope error readings out of a total of 192 (i.e., 3-1/2%) exceeded 2 minutes of arc. All of them occurred near the center of the spincast master.
5. The maximum slope error, therefore, is 2 minutes of arc over 96.5% of the area.
6. The 3-1/2% of area exceeding the 2-minute slope error is located in the center 3-foot diameter of the master; some of this area was omitted from the final mirror, thus decreasing the effect of the largest slope errors on the mirror geometry.

Since a mirror made from this spincasting would have an insignificantly reduced efficiency compared to a mirror made from a spincast mold having a maximum slope error of 2 minutes over 98% of the area, as planned, the spincast master was considered satisfactory.

5.5.5 SUMMARY

Table 5.5-1 summarizes the results of all the optical inspections performed on the various spincastings. The table shows that the accuracy of the master surfaces is consistent. The results achieved on the final surface were somewhat below the self-imposed design goal. The difference, however, was not enough to affect mirror efficiency to a significant degree.

TABLE 5.5-1. SUMMARY OF OPTICAL INSPECTIONS OF SPINCAST SURFACES

Spincasting Coat	Pour No.				Design Goal
	3	8		10 (Final)	
Before or After Thermal Cure	Before	Before	After	After	After
Number of Points Inspected	96	96	96	192	96
Focal Length (Inch)	68-3/4	68-3/4	68-3/4	69	68.8
Median Slope Error (seconds of arc)	35	35	35	54	**
Maximum Slope Error (seconds of arc)	*	80	86	174	**
Slope Error not exceed over 98% of area (seconds of arc)	*	72	82	137	120
Area not exceeding 2 minutes of slope error (percent)	96-97	100	100	96.5	98

Notes: * not determined
** not specified

6. FABRICATING THE NICKEL MASTER

6.1 PREPARATION FOR ELECTROFORMING

6.1.1 PRELIMINARY EVALUATION

A. Materials Compatibility

Representative epoxy specimens from each spincast pouring were evaluated in the laboratory under conditions simulating the required electroforming sequence. Pours failing to pass these static screening tests, listed below, were rejected.

a. 1-hour soak in 5cc/l. detergent solution

b. 1-hour soak in cleaning solution (20g/l. Na_2CO_3, 10g/l. Na_2HPO_4, 2ml/l. Triton X-100)

c. 30 minutes in sensitizing solution (8g/l. $SnCl_2$ + 3cc/l. HCl)

d. 1 hour silvering solution

e. Nickel sulfamate (electroforming) bath.

Over 40 epoxy specimens representing different formulations and cure cycles were screened in the laboratory. Eighteen further samples, representing pours which passed the static screening, were later tested for the full sequence at the vendor's site under plant conditions. This rigid evaluation of the spincast materials was believed necessary for the success of electroforming on our relatively unstable epoxy formulation.

B. Vendor's Facility

The electroforming vendor was evaluated early in the program, along with other potential vendors. The rigid process control maintained by this vendor for the production of high-quality record masters was impressive. In addition to their usual controls, in tooling up for the master electroforming, GE installed a temperature controller and a recorder for the 13,000-gallon electroforming bath. Thermocouples

placed at the anode, the cathodes, and near the wall of the tank in trial runs indicated that the temperature difference at the various locations within the bath was less than $1^{o}F$. The bath temperature could be controlled to within $5^{o}F$ in the 90 - $125^{o}F$ range.

The ambient temperature of the plating room was monitored concurrently to determine whether a 90 ± $2^{o}F$ ambient temperature could be maintained, as proved to be the case.

C. Electrolyte

A representative sample of the vendor's nickel sulfamate bath was evaluated by GE-MSD. Using GE's proprietary "Schmidt" stress cell, the stresses corresponding to a number of process parameters were charted with high accuracy and resolution. The vendor's solution was retested after reconditioning (purification and additions), and just prior to the start of the male-master electroforming; the previously established results were re-confirmed. Accordingly, the operating conditions were established as follows:

Composition: Metallic Ni-6.9oz/gal
Ni Sulfamate-29.6oz/gal
Chloride-1.2oz/gal
Boric Acid-4.0oz/gal
pH: - 4.5 - 4.6
Surface tension - 32.5 - 33.5 dynes/cm
Agitation: vigorous, (by impinging)
Filtration, purification: continuous
Cathodic CD: 15asf (later changed to 20asf)
Temperature: 120 ± $.5^{o}F$

Daily analysis (nickel, pH, surface tension) was to be performed during the entire process.

6.1.2 PREPARATION OF THE SPINCAST MOLD

Prior to shipping the spincast mold to the Columbia Records' electroforming facility, the aluminum substructure was masked with epoxy coating and with

Microstop stopoff-compound (see Appendix A for detailed description). To prevent thermal shock, heaters accompanied the crated spincasting, and the electroforming area was kept at 90 ± 2°F. After uncrating, the mold was prepared for the electroforming sequence. This included attaching filter hose, legs, applying further stopoff masking, etc.

To start the electroforming sequence, the spincasting was washed with warm water and treebark detergent, then thoroughly rinsed. After treatment with a sensitizing solution (8g/l. $SnCl_2$, 3cc/l. HCl), the surface was silvered by sprayed ammoniacal silver solution. Despite highly successful trial runs on small samples, the result was poor; the silver was brown, powdery, and had to be removed by washing the surface alternately with 10% chromic acid and 20% sodium thiosulphate solution. A pitting of the mold surface resulted, causing a reduction in specular reflectivity. (Other processes for silver removal were also tried on small samples but the results were no better.)

When trying to find the reason why some 14 small samples successfully went through this same silvering sequence, while the identically composed mold failed, the investigation revealed that the surface temperature of the small epoxy samples was rapidly lowered to 80°F by spraying them with cleaning and sensitizing solutions at room temperature, but the sizable mass of the spincasting maintained the surface temperature near 90°F. This temperature difference of 10°F was critical in silvering this epoxy. Next, the surface temperature of the mold was lowered to 80°F by carefully controlled cool-water spraying, and the silvering proceeded smoothly. Though it is realized that even 80°F is considerably higher than commonly practiced silvering temperature, it was thought necessary to avoid thermal cycling of the mold and to silver as closely as possible to the 120°F electroforming temperature

6.2 ELECTROFORMING THE NICKEL MASTER

After the silvered spincast mold was lowered into the electroforming tank, the temperature of the nickel sulfamate solution (90°F) was increased very slowly to the

deposition temperature (120°F) to prevent thermal shocking of the spincasting. Approximately 50 amps total current flow was provided from 5 auxiliary anodes, while the anode rings and anodes were positioned over the tank. The current was slowly increased during the next 20 hours with the temperature until a level of 15 asf was reached at 120°F. The current was again increased to its maximum average value of 20 asf during the next 24 hours. Deposition was terminated after 19 days since a sufficient thickness had been reached.

6.2.1 ELECTROFORMING CONDITIONS

An operating temperature of 120°F ± .5°F was maintained in the electroforming bath. Acceptable current density levels were established using a GE proprietary method (Schmidt-cell) for the determination of stresses as a function of current density. Initially, the master was electroformed at 15 asf. After several days operation, the current density was raised to 20 asf for the remainder of the deposition time due to a shift in the minimum stress conditions.

Daily chemical analysis of the nickel sulfamate solution indicated that the composition was maintained constant. The typical analysis is presented in paragraph 6.1.1 (A). Except for periodic additions of wetting agent, Duponol (manufactured by DuPont) to adjust the surface tension level, no additions were required during the run, indicating satisfactory anode corrosion.

6.2.2 ANODE CONFIGURATION

Two-hundred bagged cast-nickel anodes of varying lengths were suspended vertically and positioned so that the contour of the cathode (spincast mold) was followed. The anodes were supported in the bath by four rings made from 1 1/2-inch diameter solid copper rods. The rings in turn were supported by an I-beam framework. The framework and the rings are shown in Figure 6.2-1. Also shown are three legs which were used to support the spincast structure in the electroforming tank. The length of the legs was chosen so as to properly position the spincasting in relation to the anode assembly since the anode assembly was in a fixed position.

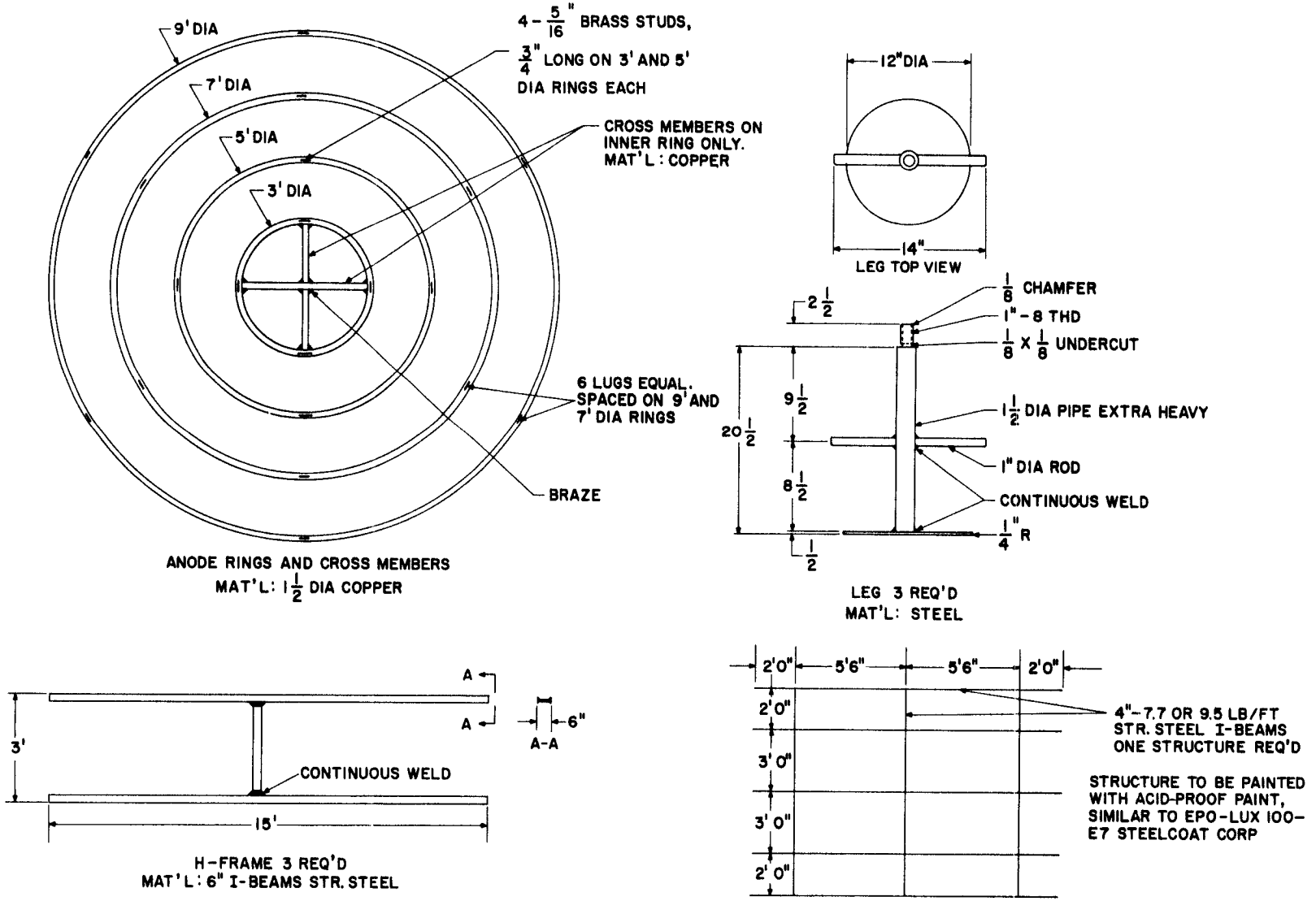

Figure 6.2-1. Anode Rings and Support Structures for Electroforming Male Master

The I-beam structure rested on the sides of the electroforming tank. It was designed to minimize stresses of the copper rings when all of the anodes were placed on the rings. The stress analysis of these rings is shown in Appendix F.

6.2.3 INSTRUMENTATION

The plating bath temperature was maintained at 120°F ± 1/2°F by a specially modified controller-recorder. A copper-constantan thermocouple, located in the center of the tank, was connected to the controller-recorder. Three other thermocouples were placed in the electroforming bath and connected to a GE multipoint recorder, providing additional checks of the bath temperature and making available alternate control thermocouples, if needed. Ambient room temperature was also monitored on this recorder.

Deposition current was monitored and charted on a GE recording ammeter. Also, current and voltage were read directly from meters and recorded. Permanent records of these operating conditions were kept on file.

6.2.4 PRELIMINARY SEPARATION FROM THE SPINCAST MOLD

Upon completion of the electroforming operation, the plating tank was drained of solution. The spincast mold and male master were removed from the tank, placed on the floor, and the bath residue was rinsed off. A few large-size growths were removed from the nickel electroform prior to actual separation.

6.3 CORRECTED DIFFICULTIES DURING ELECTROFORMING

A number of mishaps occurred during the electroforming of the male master. These difficulties are not inherent to the electroforming process, but were due to inappropriate action (causative and remedial) on the part of the vendor. Close around-the-clock surveillance of the project by GE in-plant surveillance later in the electroforming operation averted several potential disasters.

6.3.1 CURRENT INTERRUPTIONS

A municipal power failure kicked out the relays at the electroforming facility and interrupted deposition after one day of operation. This occurred Sunday morning at 1 A.M. and, after six hours without power, the vendor's workmen resumed deposition at full current density immediately and without prior anodic activation.

After two weeks deposition time, current was again interrupted when maintenance personnel lowered the solution level below the anodes while removing nickel "trees" (described more fully in Section 6.3.2). This improper procedure was immediately corrected by in-plant surveillance.

While these interruptions did not seriously damage the electroformed master, they could have turned out disastrously.

6.3.2 SHORTING

Electrical shorting occurred periodically between individual nickel anodes and nickel growths on the cathode bus bars, which connect to the spincast mold within the bath.

Shorting occurred three times during the 19-day deposition period, as indicated by a drop in cell voltage and a slight increase in the bath temperature. The shorting was caused by a breakdown of the cathode bus-bar insulation. Nickel "trees" grew from these bare spots toward the anodes on each occasion. Since these growths were not detrimental to the male master and removal of the spincasting to repair the insulation would have created new problems, it was decided to remove these growths periodically by hand. The solution level was sufficiently lowered and a very low current density was maintained to keep the nickel master cathodic during this cleaning operation.

No damage to the male master resulted from the shorting since close surveillance of the operation did not permit a bath temperature increase to go uncorrected. Downtime for growth removal was considered in determining total deposition time.

6.3.3 TEMPERATURE DEVIATIONS

The temperature controller efficiently maintained the temperature at $120^{o}F \pm .5^{o}F$. However, the heat generated each time shorting occurred increased the bath temperature because the cooling capacity for the tank was inadequate for this condition. Close surveillance ensured immediate corrective action, and at no time did the bath temperature exceed $122^{o}F$.

The bath temperature decreased to about $115^{o}F$ during the removal of the "tree-like" growths and was brought back to $120^{o}F$ before the full current density was resumed. In one instance, the bath temperature dropped to $110^{o}F$ when the growth removal operation took 8 hours.

Some difficulties were experienced with the stainless-steel thermocouple wells initially used, when they became cathodic due to stray currents and were replaced with glass thermocouple wells.

6.4 SUPPORT STRUCTURE

6.4.1 DESIGN

It was the purpose of this structure to maintain the paraboloidal shape of the 3/8-in. nickel master during separation, overturning, electroforming of the female mirror, and final shipment to the customer. Two designs were considered, one was a stainless-steel structure essentially similar to the spincast support structure except that the face contour was convex instead of concave; the other consisted of a reinforced plastic structure. In either design the nickel master was uniformly supported over its entire surface. Based on price, delivery, weight, and the fact that no stop-off was required, the reinforced plastic structure was chosen.

The back-up structure was built as a fiberglass-reinforced plastic layup having top and bottom sheets which were separated by an egg-crate structure. It is shown in Figure 6.4-1. All members of the structure were bonded together so

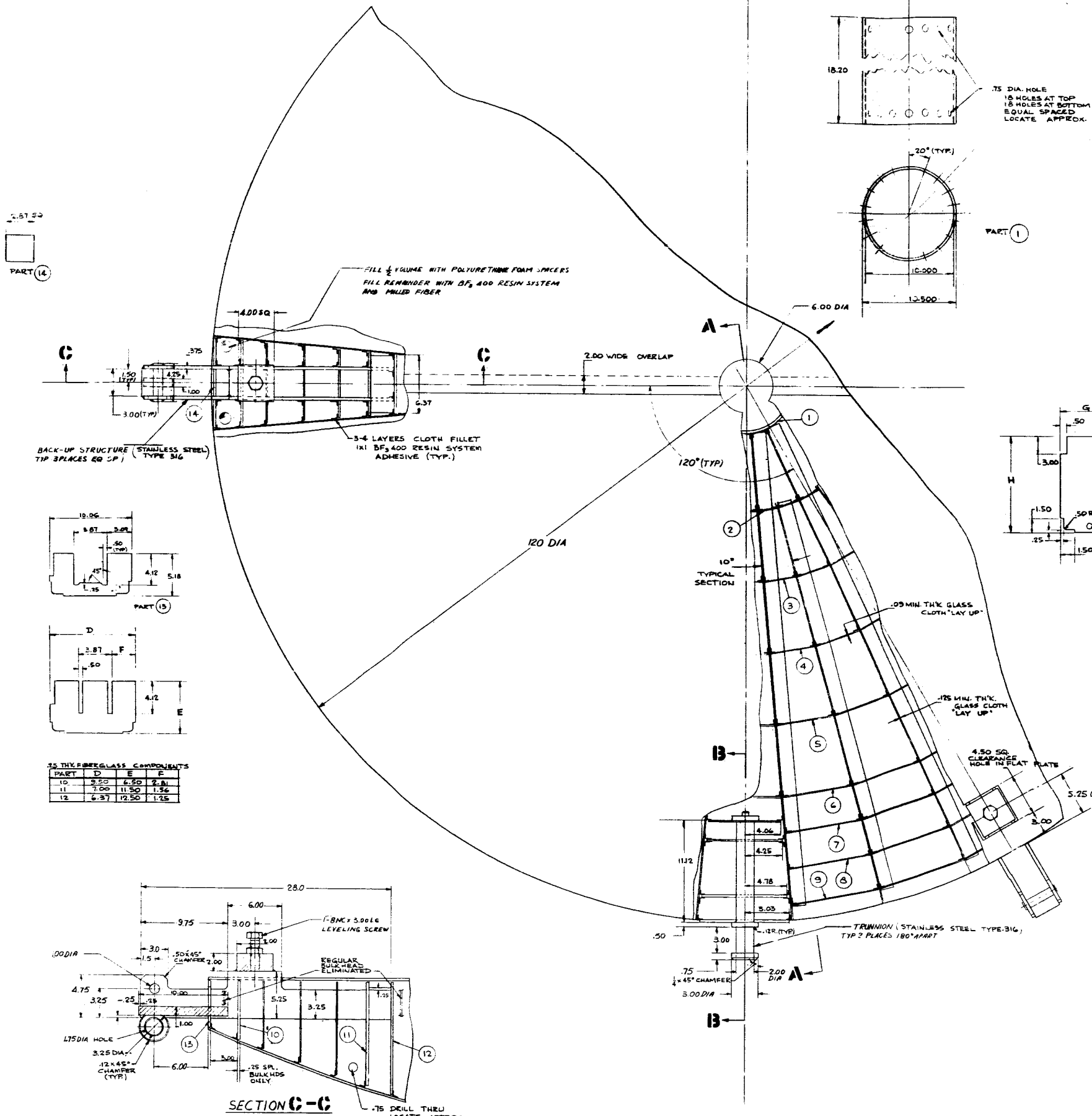

FIBERGLASS COMPONENTS

PART	G ALLOWING CLEARANCE EACH SIDE .125	H ALLOWS NO CLEARANCE ON TOP OF .25 +.15 -.15
2	2.09	17.33
3	3.48	16.48
4	4.86	14.86
5	6.27	12.97
6	7.66	10.52
7	8.36	3.13
8	9.05	7.60
9	9.75	5.97

.75 THK FIBERGLASS COMPONENTS

PART	D	E	F
10	2.50	6.50	2.81
11	7.00	11.50	1.56
12	6.37	12.50	1.25

Y	X
0	0
2.390	.021
4.783	.084
7.179	.188
9.579	.335
11.984	.524
14.396	.757
16.818	1.032
19.251	1.353
21.695	1.718
24.154	2.129
26.627	2.588
29.118	3.095
31.627	3.651
34.157	4.259
36.708	4.919
39.283	5.633
41.886	6.403
44.516	7.233
47.176	8.123
49.869	9.076
52.595	10.096
55.360	11.185
58.163	12.346
59.913	13.100
59.960	13.121
60.008	13.142

SECTION C-C

SECTION B-B

SECTION A-A

Figure 6.4-1. Male Master Support Structure

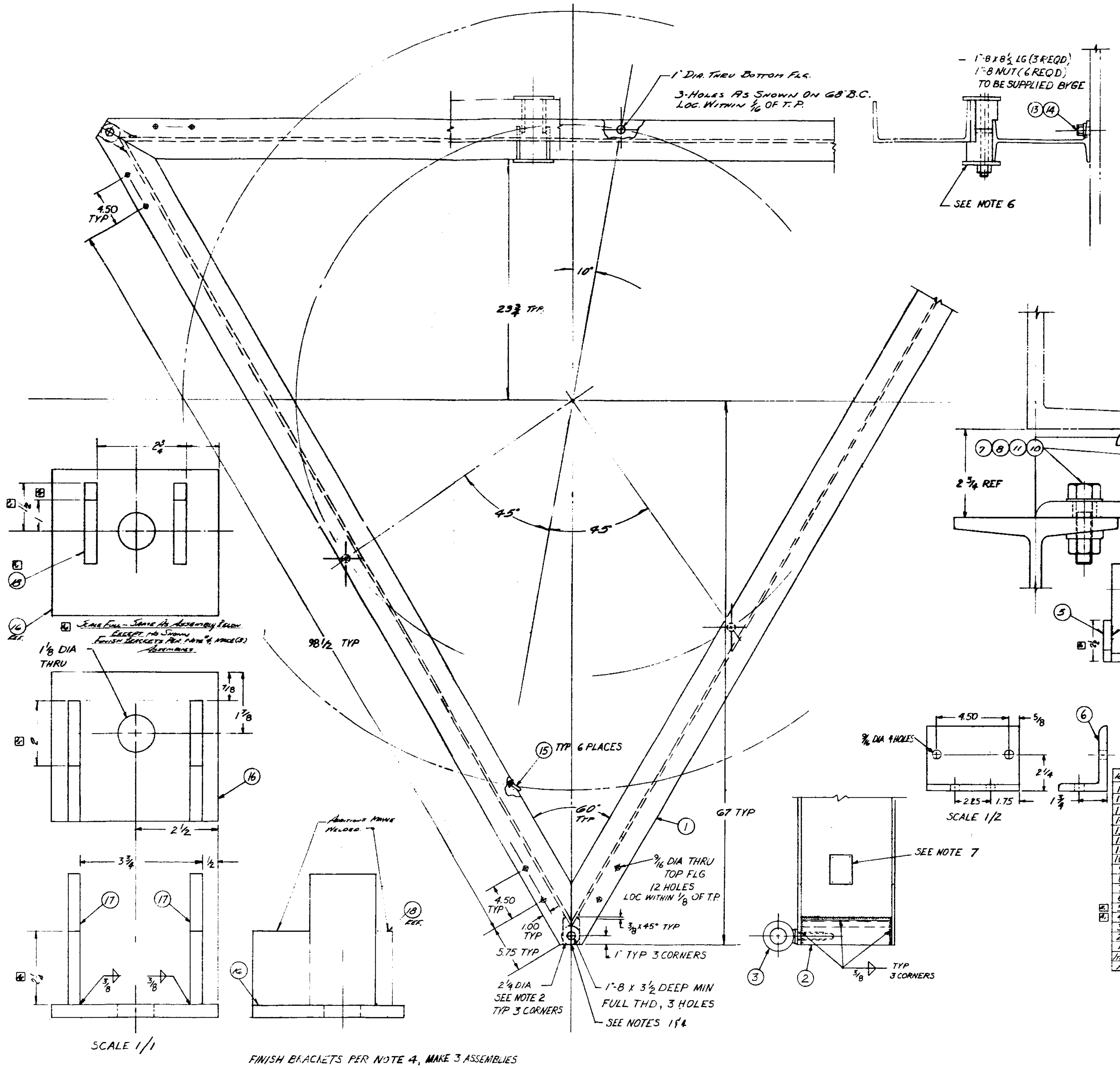

NOTES

1. ITEM 1 TO BE CONTINUOUSLY WELDED WITH FULL PENETRATION TO ITSELF AT THE 3 CORNERS.

ZONE A9 2. GRIND WELD FLUSH TO TOP OF FLANGE IN AREA INDICATED BY PHANTOM LINE CIRCLE.

4. FINISH ITEM 1, I BEAM FABRICATION, ITEM 5&6, ANGLE & GUSSET FABRICATION, AND ITEM 4, ANGLE, WITH ONE (1) COAT OF METALIC PRIMER AND (1) FINISH COAT, COLOR GREY.

5. NUTS, BOLTS, & WASHERS TO BE MEDIUM CARBON STEEL OR EQUIVALANT.

ZONE L5 6. INSTALL "T" SECTION CLAMPS IN EACH CORNER TO HOLD MOLD AND MOLD SUPPORT IN PLACE UNTIL THEY ARE PERMANENTLY SECURED. REMOVE AFTER FINAL ASSEMBLY.

7. ATTACH METAL PLATE STAMP-MOLD SUPPORT NO. SKS-0147 GROSS WEIGHT OF STRUCTURE______

8. PROVIDE PLYWOOD BOX WITH COMPARTMENTS FOR STORAGE OF ALL SMALL PARTS. ATTACH METAL TAGS INSIDE AND OUTSIDE OF BOX. IDENTIFY AS SKS-0147.

FINISHED SIZE BILL OF MATERIAL

ITEM	REQ	MAT'L	FINISHED SIZE	DESCRIPTION
18	6	H.R.S.	3/8 x 2 1/2 x 4	SUPPORT PLATE
17	6	CARB STL	3/8 x 3 1/4 x 4	SUPPORT PLATE
16	6	CARB STL	3/8 x 4 1/8 x 5 1/8	BASE PLATE
15	6	NO.44 3" OPENING HARGRAVE CLAMP, MADDOCK & CO INC.		"C" CLAMP
14	3		3/4-10 (RYERSON STEEL OR EQUIV)	BEVELED WASHER
13	3		3/4-10 X 2 1/2 LG	HEX HD BOLT
12		NOT	USED	
11	36		1/2-13 (RYERSON STEEL OR EQUIV)	BEVELED WASHER
10	54		1/2-13	HEX NUT
9	18		1/2-13	LOCKWASHER
8	54		1/2-13	FLAT WASHER
7	54		1/2-13 X 2 LG	HEX HD BOLT
6	6	CARB STL	1/2 X 4 X 3 X 5 3/4 LG	ANGLE OR EQUIV
5	6	CARB STL	1/2 X 2 1/2 X 6	GUSSET
4	6	CARB STL	1/2 X 6 X 6 X 6 3/8 LG	ANGLE OR EQUIV
3	3	COMM STL	1"-8 X 3" LG (RYERSON STEEL OR EQUIV) SHOULDER	EYE BOLT
2	3	H.R STL	2 X 2 3/8 X 11 1/4	BLOCK
1	3	CARB STL	12" X 31.8#/FT X 121" LG (APPROX)	I BEAM

Figure 5.1-2. Spincasting Mold Support

37-A B

that effectively a honeycomb structure resulted which had one flat and one curved face. Tests were conducted in electroforming solutions to determine the effect of the solution on the plastic and the effect of the plastic on the solution for various epoxy-resin formulations. The formulation chosen was completely unaffected by the bath, and had no effect on the bath composition. The hardener used with the epoxy resin was BF3-400.

In order to give added strength to the bottom (flat) skin of the structure, a series of stainless-steel screws was used to connect it to the egg-crate webs. These screws are not shown in Figure 6.4-1. To permit the electroform solution to flow easily in and out of the structure, vent holes and slots were placed in the webs near the top and bottom skins.

The three-point support system used on the female master support structure was also used for the male master support structure. The lifting hook locations were kept in the same position so that the same special lift sling, described in Section 8.1, could be used. Two additional handling points were added, however. Two trunnions were imbedded in the structure to be used for rotating the assembly on a turnover stand. All handling fittings were made of stainless steel to eliminate the necessity of "stopping off" any part of this structure.

To uniformly support the nickel master over its entire surface and to accommodate any relative radial motion between the nickel electroform and the support structure, a flexible bonding medium was used. Various possibilities were investigated such as epoxy resin loaded with a high glass or fiber content to decrease its thermal expansivity, self-bonding urethane foam, epoxy-bonded neoprene rubber, and elastomeric (silicone) foam. All of these materials were chemically tested for their resistance to the electroforming solution. The self-bonding urethane foam was chosen because of its superior resistance to the electroforming solution, ample strength, relative ease with which it could be applied, and General Electric's past favorable experience in using this material for similar applications.

6.4.2 ATTACHMENT TO MALE MASTER

Following preliminary steps of separation, ice and hot water treatment; preparations were made to bond the support structure to the nickel electroform prior to complete separation. To ensure good adhesion of the foam to the nickel electroform and the plastic support structure, both parts were thoroughly cleaned, and a coat of American Latex Stabond C-136 was applied to their surfaces.

When the primers were dry, the support structure was positioned with an overhead crane so that it was approximately centered and a gap of approximately one inch existed between the support structure surface and the electroform. Clamps were fastened along the periphery to prevent any relative movement between master and structure due to foaming pressure.

The center hole in the support structure was sealed off, and a pipe mounted in the center. The foam dispenser was connected to this pipe. A given quantity of foam was then injected through this pipe and allowed to expand radially outward until all expansion had stopped. Foam was then injected around the periphery toward the boundary where expansion from the center injection had stopped. It was estimated that a foam density of approximately 15 pounds per cubic foot resulted.

Following a cure period of three days, the excess foam was cut along the periphery, and preparations for separation were made.

After shipment of the attached master to GE's "D" Street facility, peripheral nickel bridges (left for conduction) were cut through, and a 6-inch diameter hole was opened in the center of the electroform. For separation from the mold, the electroform was covered with crushed ice and thoroughly cooled, followed by a hot-water thermal shock. This produced audible cracking and visible separation along the outer periphery, but no separation at the center.

6.5 SEPARATION AND VISUAL INSPECTION

Final separation was effected by thermal shocking of the aluminum spincast support structure with liquid nitrogen (Figure 6.5-1).

The general appearance of the electroform was adjudged good, (Figure 6.5-2), but two significant indentations were caused by the vendor's personnel accidentally dropping an 18-pound, sharp-edged nickel anode on the spincasting during the early stages of electroforming. The anode was pulled free only after about 6 days. (See Figure 6.5-3). All this occurred without GE's knowledge. Since only a small percent of the total area was affected, this will detract more from the aesthetic value than from the overall efficiency of the final mirror.

The current leakage through the breaks in the bus-bar insulation caused the thickness of the electroform to be somewhat less than the intended 3/8 inch, particularly in sections adjacent to the bus-bar connections.

The surface texture had a slight "orange peel" appearance, resulting from replication of the mating epoxy surface, which was affected by the removal of the first faulty silvered layer described in Section 6.1.2. An attempt was made to eliminate this effect by wiping with a special French cotton (Figure 6.5-4). This procedure was only partially successful.

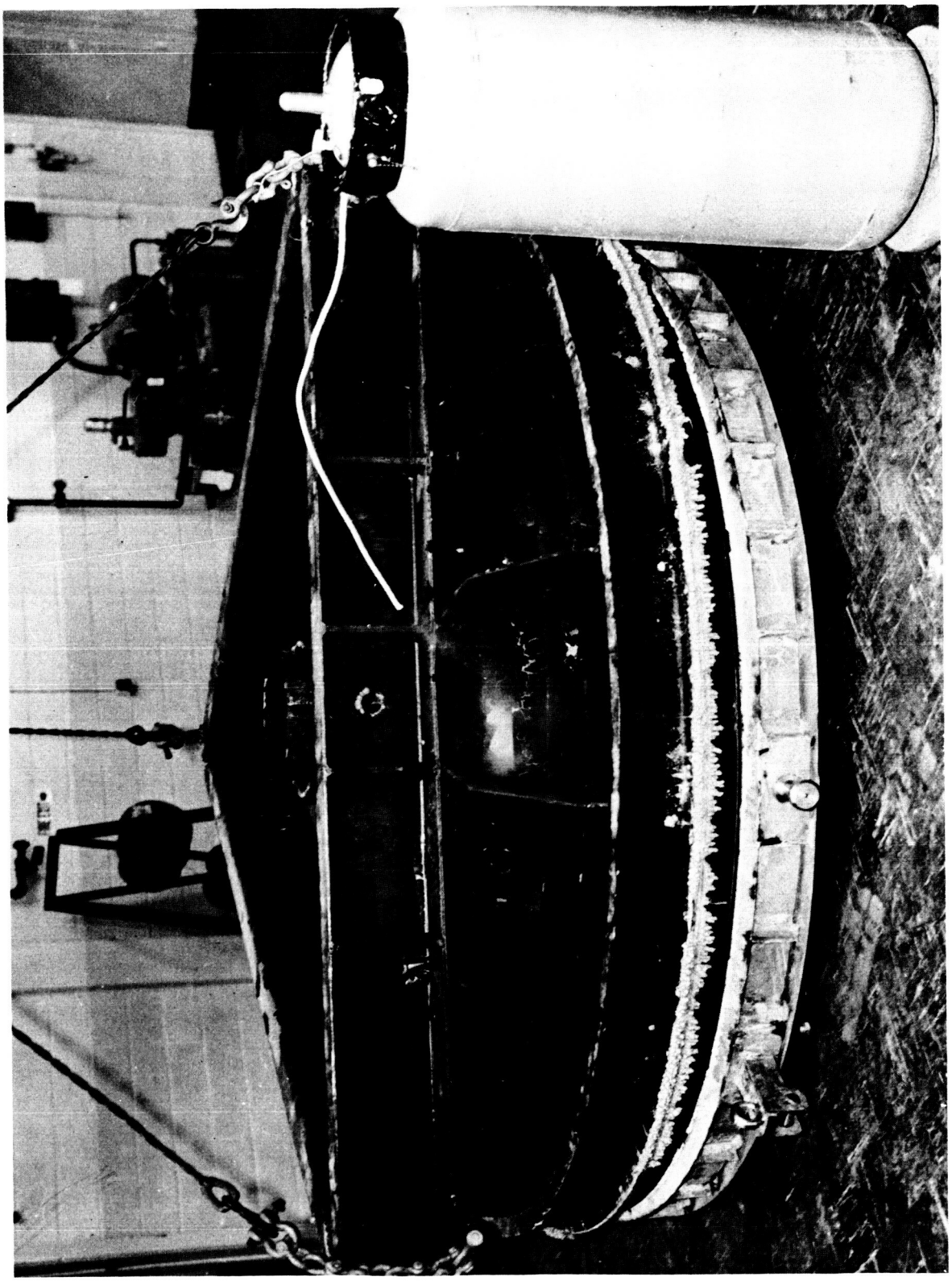

Figure 6.5-1. Separation of Male Master from Spincasting. Liquid Nitrogen is Being Sprayed over the Spincast Back-up Structure.

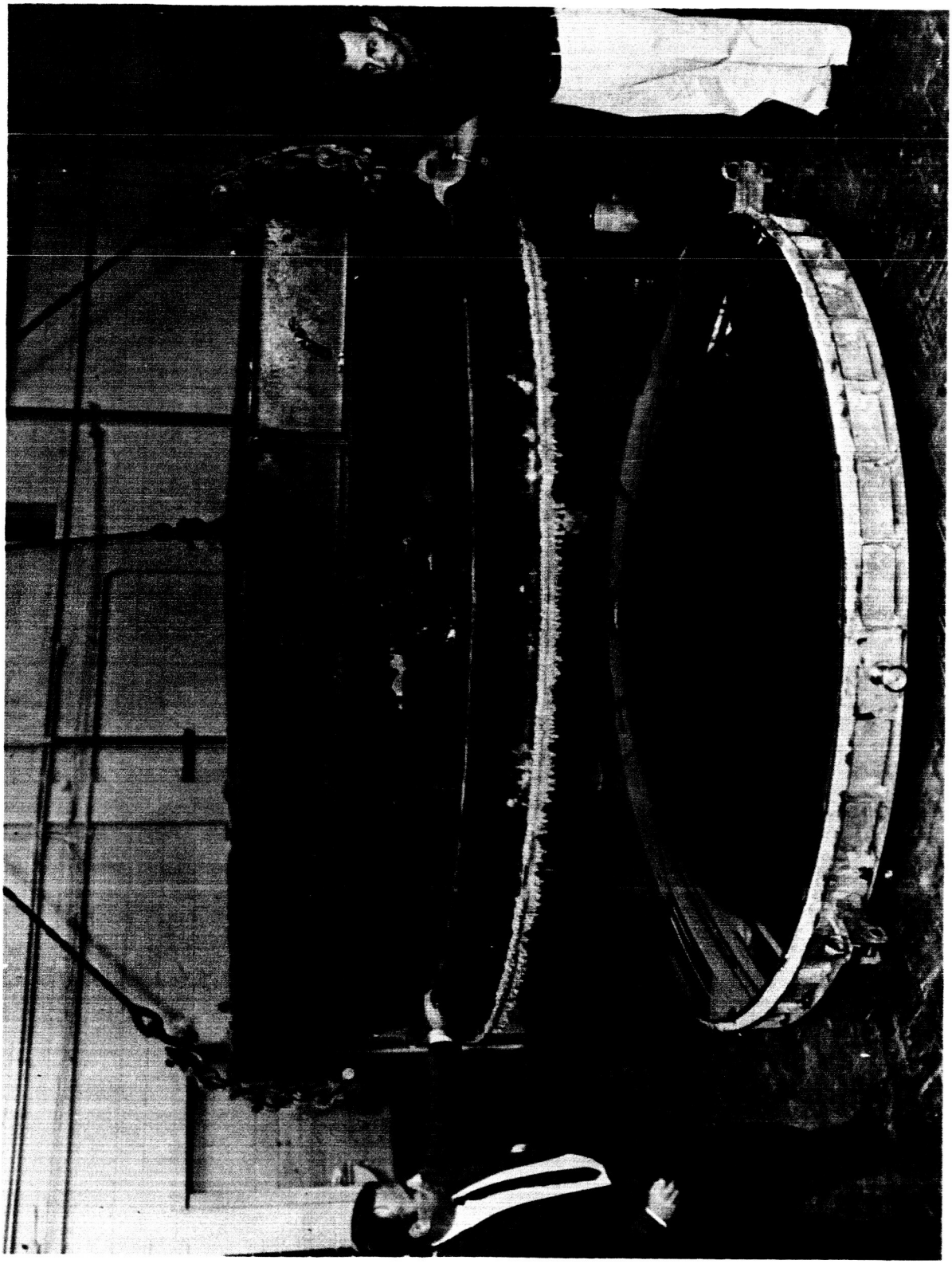

Figure 6.5-2, Removal of Spincast Structure from Nickel Male Master

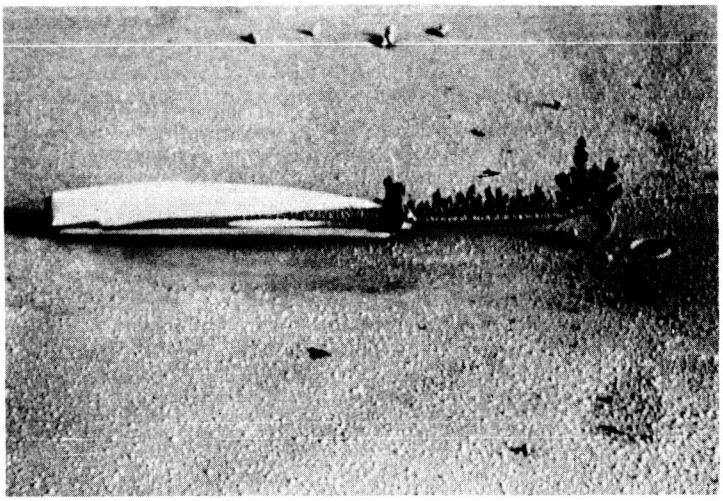

Figure 6.5-3. Anode Dropped on Master. Nickel Trees Indicate Current Robbing from Underlying Area

6.6 CONCLUSIONS

The success of the electroforming process has been demonstrated with the fabrication of a low-stress male nickel-master, which faithfully reproduced the geometry and surface characteristics of the mold. GE's proprietary stress cell, which enabled daily process control for low stress conditions, must be given the major share of credit. Close surveillance by GE personnel averted, on numerous occasions, potential disasters caused by vendor lapses in process control. The thin mirror to be electroformed is particularly vulnerable to any mishap. Therefore, after some deliberation, it was decided to electroform the mirror at Bart Manufacturing Co. in Belleville, New Jersey, to increase the probability of success of the program.

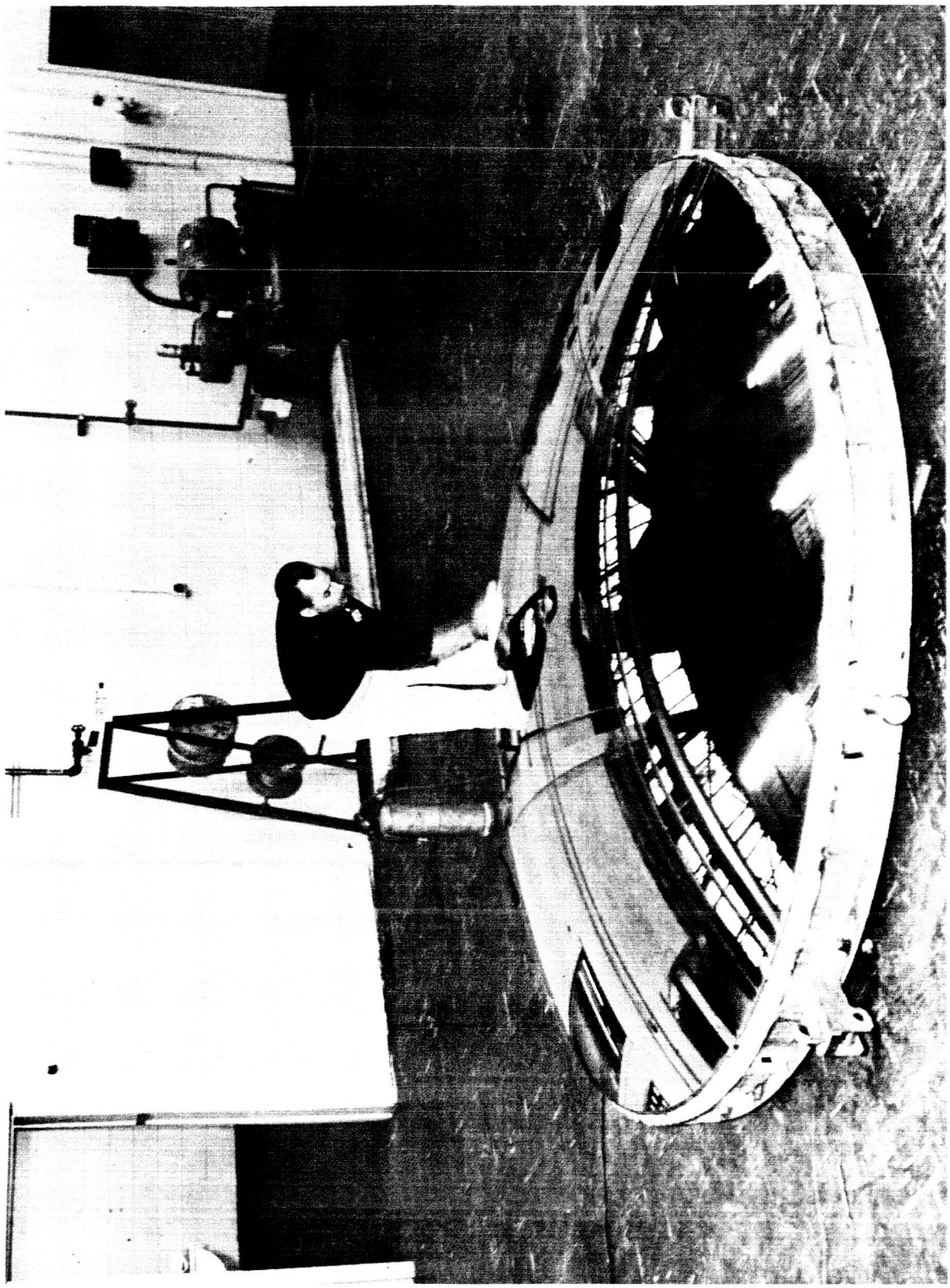

Figure 6.5-4. Wiping of Male Master

7. MIRROR

7.1 PREPARING FOR ELECTROFORMING

7.1.1 PRELIMINARY EVALUATION

A. Vendor's Facility

The ambient temperature, so important for the epoxy spincast, is of minor concern with the nickel male master. Bart Manufacturing Company completely enclosed the electroforming room, separating it from the general work area and excluding personnel not involved on the project from the area. This was part of the vendor's effort to maintain cleanliness in the electroforming area.

B. Plating Bath Characteristics

A quantity of the vendor's nickel sulfamate solution was supplied to GE for evaluation. The stress levels of this electroforming bath were determined for a number of process parameters. Based on these results, the operating conditions for deposition start-up were established; specifically, bath temperature 120^{o}F at a current density of 19 asf.

7.1.2 PREPARATION OF MALE NICKEL MASTER

The depressions and hole in the male nickel master were covered with a high temperature plater's wax to ensure easy separation of the electroformed mirror (see Figure 7.1-1). A hot "trowel" was fabricated by brazing a small brass plate to a soldering iron. With this, wax patches were applied to the damaged areas. The wax application process was initially evaluated in the laboratory under surface treatment conditions, simulating those required for electroforming.

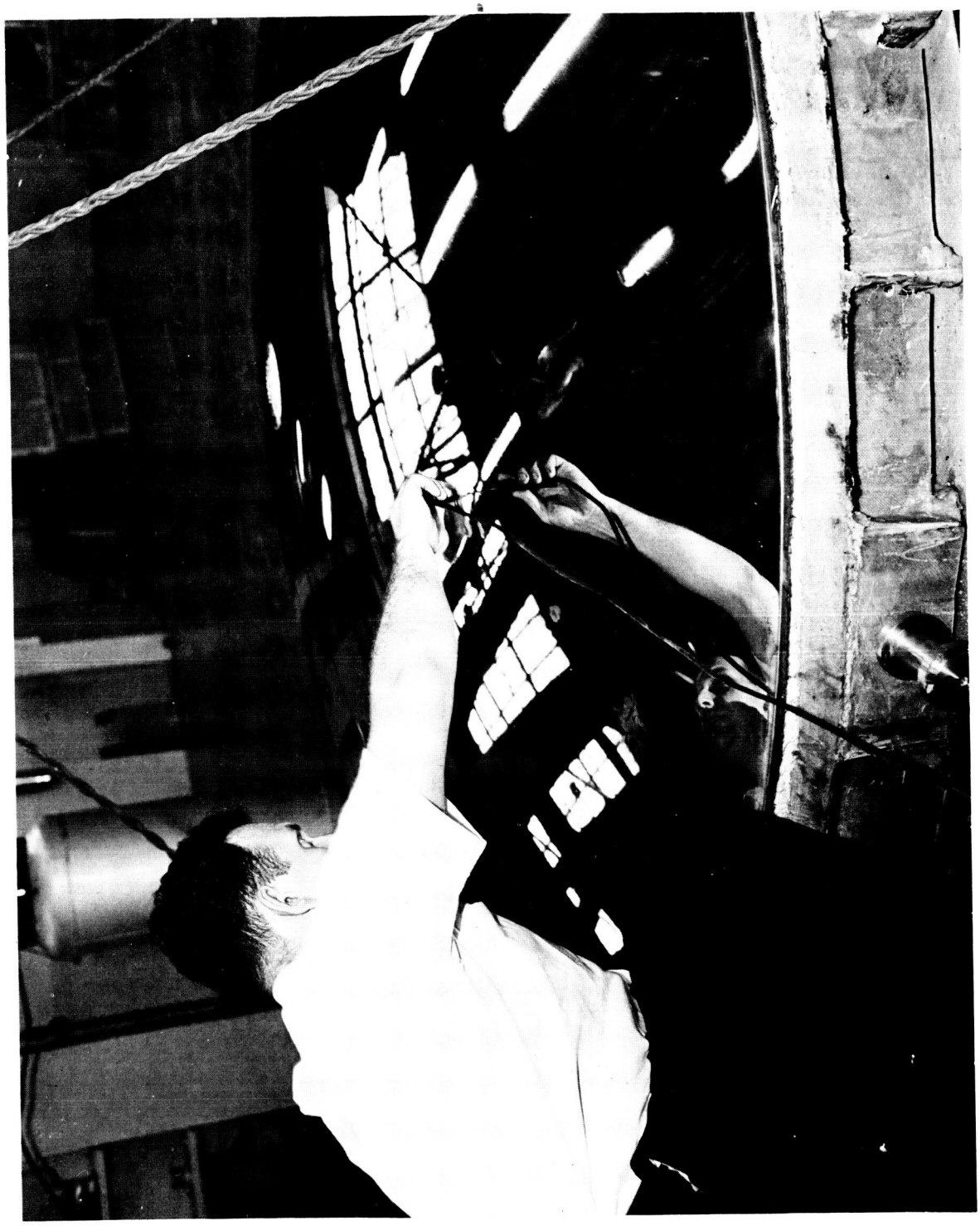

Figure 7.1-1. Filling of Depressions in Male Master with Wax

The nickel master was shipped to the vendor's facility. It was uncrated and placed on a specially constructed stand within the closed electroforming area. The male master was cleaned with detergent, cleaning solution, and thoroughly rinsed to obtain a break-free surface; a very thin deposit of chemically reduced silver was applied to effect easy separation of the electroformed mirror.

7.1.3 GUTTER

A quarter round skin on the periphery of the mirror was to be formed for torus attachment by electroforming against a copper gutter. This gutter was formed from a copper pipe which was first rolled into a ring, welded, and then machined as required. Location and details of this gutter are shown on Figure 7.1.2.

Two methods of fabricating this gutter were considered. They are shown in Figure 7.1-3. Method A had the advantage of easy machining on a horizontal boring mill because the ring could be machined without additional back-up under the tool other than the table bed. To obtain a similar back-up for design B would have required a second rolled tube which would have to be placed under the gutter. The greatest disadvantage of Method A was that it was impossible to obtain a continuous contour at the joint of the gutter and the male master; method B was therefore chosen.

To eliminate the need for the tube back-up, the gutter was machined to a point where the thickness of the knife edge was approximately 1/32 inch. A knife edge was then formed by grinding with a hand grinder. The fit of the gutter to the male master was very good and required only local forming of the knife edge in a few places to produce a good fit without gap between gutter and master. The gutter was held against the mold by special C-clamps spaced approximately 14 inches apart.

7.2 ELECTROFORMING THE NICKEL MASTER

The silvered male master was lowered into the electroforming tank (see Figure 7.2-1). A low current density was maintained initially while the conforming anode

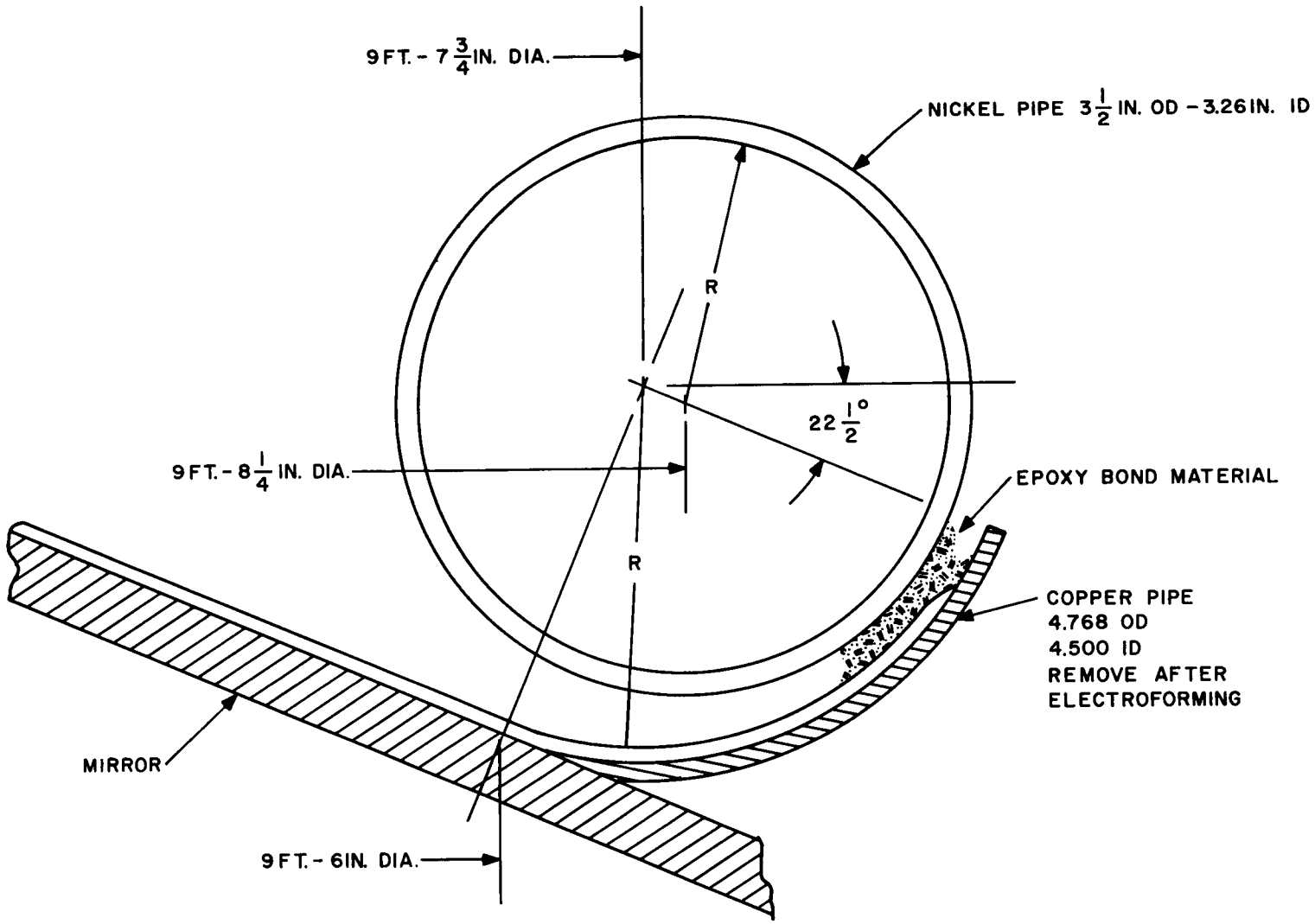

Figure 7. 1-2. Torus and Gutter Detail

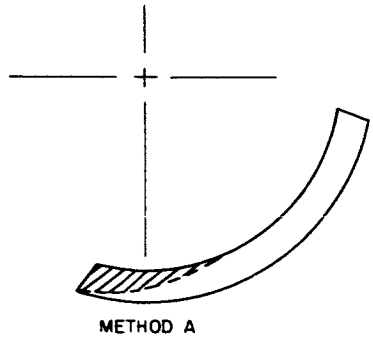

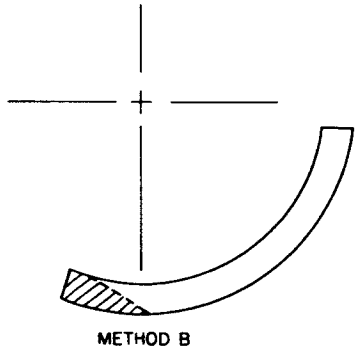

Figure 7.1-3. Methods of Machining Copper Gutter

(described in Section 7.2.2) was installed and the bath temperature increased to 120°F. Electroforming at a current density of 19-20 asf, the run proceeded for 70 hours.

7.2.1 ELECTROFORMING CONDITIONS

An operating temperature of 120°F ± .5°F was maintained in the electroforming bath. Acceptable current density levels were established daily, using the GE proprietary stress cell.

Daily chemical analysis of the nickel sulfamate solution indicated that the bath composition remained constant. Except for periodic additions of wetting agent to adjust the surface tension level, no additions were required during the run.

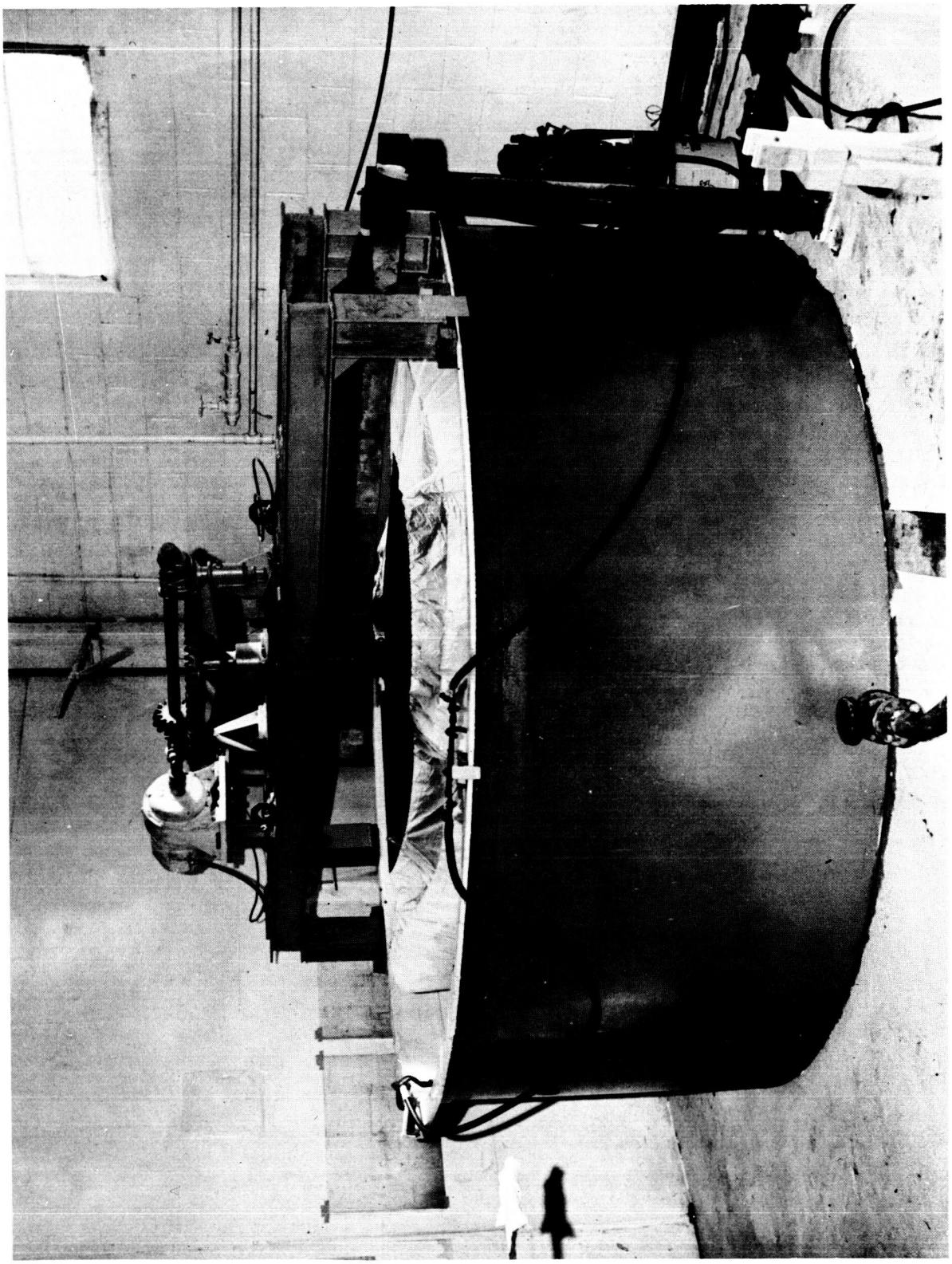

Figure 7.2-1. Male Master in Electroforming Tank

7.2.2 ANODE CONFIGURATIONS

A rotating conforming anode, illustrated in Figure 7.2-2, was designed for this project. The anode was constructed of titanium to which were attached the consumable cast nickel ingots. The entire immersed part of the assembly was bagged (see Figure 7.2-3). The rotational speed of the anode (about 10 rpm) provided bath agitation. Several vertical hanging anodes, placed along the tank wall, were utilized initially during the low-current density start-up phase, while the conforming anode was brought into position.

7.2.3 INSTRUMENTATION

The plating bath temperature was maintained at $120^{o}F \pm .5^{o}F$ by a specially modified controller-recorder. A copper-constantan thermocouple, in a glass thermocouple well, was placed in the bath along the wall and connected to the controller-recorder. Three other thermocouples were similarly placed in the bath and connected to a GE multipoint recorder. This provided additional checks of the bath temperature, and provided alternate control thermocouples, if needed. Ambient room temperature was also monitored on this recorder.

Deposition current and voltage were monitored and tabulated around-the-clock by operators.

7.3 SEPARATION OF THE MIRROR

7.3.1 PREPARATIONS

Upon completion of the electroforming operation, the plating tank was drained of solution. The male master and electroformed mirror were removed from the tank, and the solution residue was washed off. The masking compound was removed from the mirror periphery to simplify separation. (See Figure 7.3-1.)

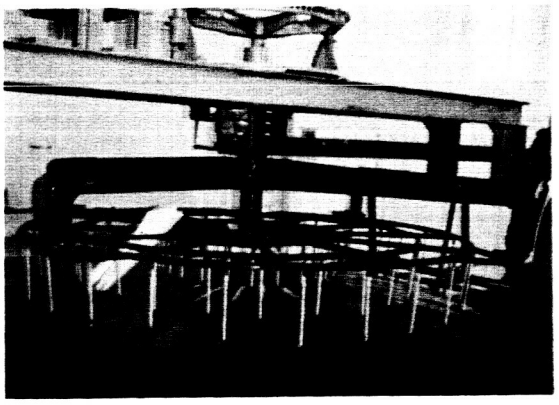

Figure 7.2-2. Rotating Anode Configuration

Figure 7.2-3. Bagged Rotating Anode

7.3.2 SUPPORT TORUS

A. Design

Several types of mirror support systems were considered: single torus, double torus with connecting ribs, ribs bonded to the mirror skin, and ribs riveted to the mirror skin. The double torus with connecting ribs has the disadvantage of possible distortion due to thermal growth differences between the support structure and the mirror skin, while the bonded and riveted rib designs have additional problems of local distortion at the points of attachment. The single torus on the outer edge of the mirror appeared to present the least probability of serious distortion and was therefore chosen for the support design. As requested by the customer, three points of support were used.

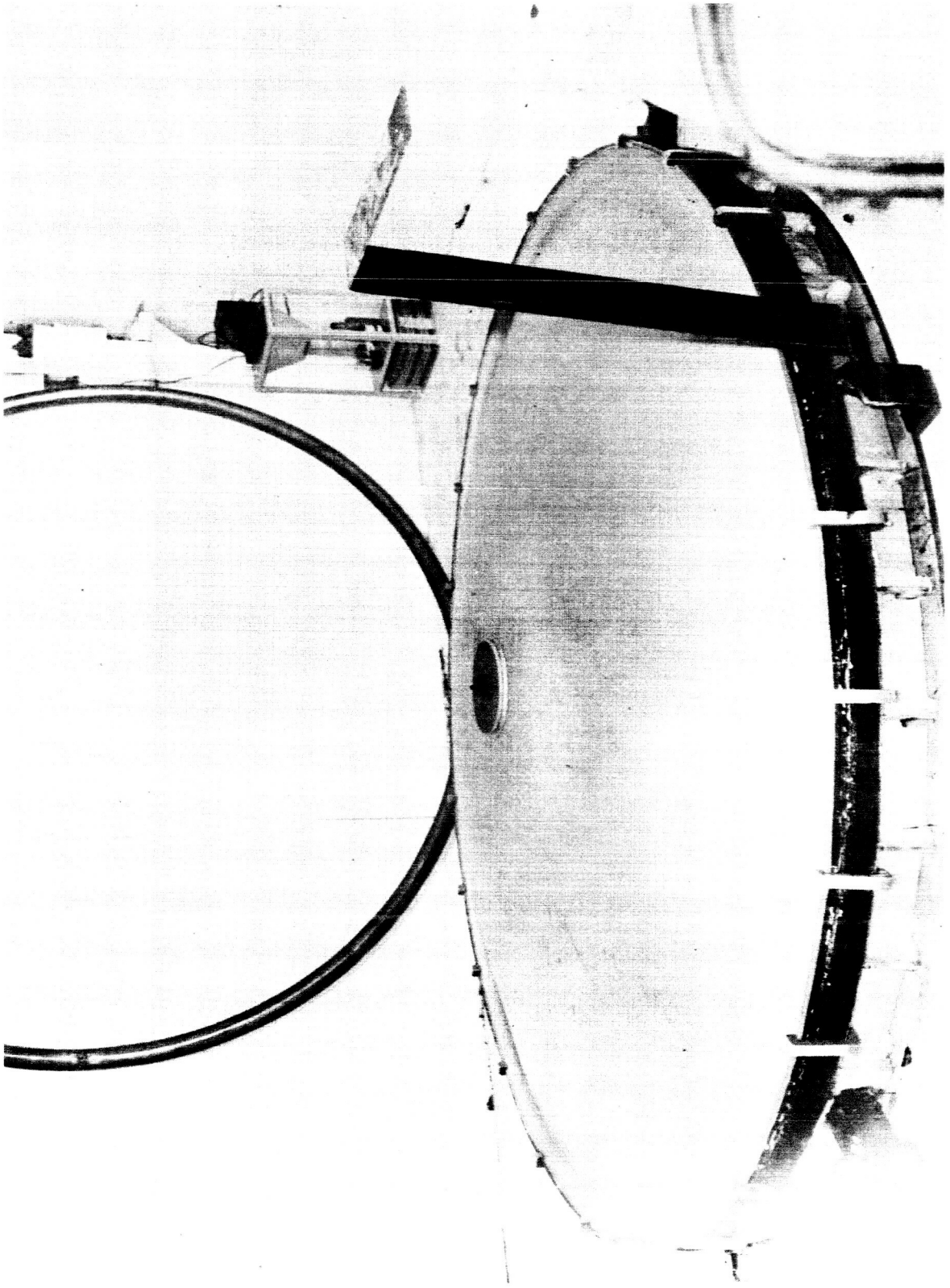

Figure 7.3-1. Male Master and Mirror after Removal from Tank; the Torus is Leaning against Wall in the Background

Because the mirror was not to be flight-weight, the torus was fabricated from a 3-1/2-inch OD nickel pipe having a wall thickness of 1/8 inch. This standard pipe size was readily available. The pipe was rolled in the conventional manner and welded to form the torus (Figure 7.3-2).

To form the three hard points required for mounting, three one-inch diameter nickel rods were inserted in the torus at three equal distances around the circumference. These rods were drilled and tapped for 3/8-inch-16 thread. These holes are located on the back side of the mirror and are parallel to its axis. The diameter of the torus centerline is 9 feet, 8-1/2 inches.

To attach the torus to the mirror skin, an extension of the mirror was electroformed in the shape of a quarter-round, and the torus was epoxy bonded to this quarter-round at the outer end as shown in Figure 7.1-2. By bonding at the outer edge of this extension, any mirror distortion caused by shrinkage or thermal growth differences of the epoxy bond are largely eliminated before they reach the mirror surface proper. A nominal gap of 1/4 inch was allowed between the torus and the quarter-round to allow for manufacturing tolerances.

B. Attachment

Prior to attaching the torus, both the torus and the back of the nickel electroform were thoroughly cleaned. The torus was lowered into position by hand, and shims were placed between the torus and the skin to properly set the clearance. Shims were also placed between the quarter-round and the torus to make the gap as uniform as possible prior to bonding. This gap was then filled with Bondmaster M-688 epoxy using CH-8 hardener, obtained from the R&A Rubber and Asbestos Corp., Bloomfield, N. J. This epoxy formulation has a pot life of approximately 45 minutes so that it had to be mixed and applied in small batches. Because the formulation is almost 100% solids, there is essentially zero shrinkage during

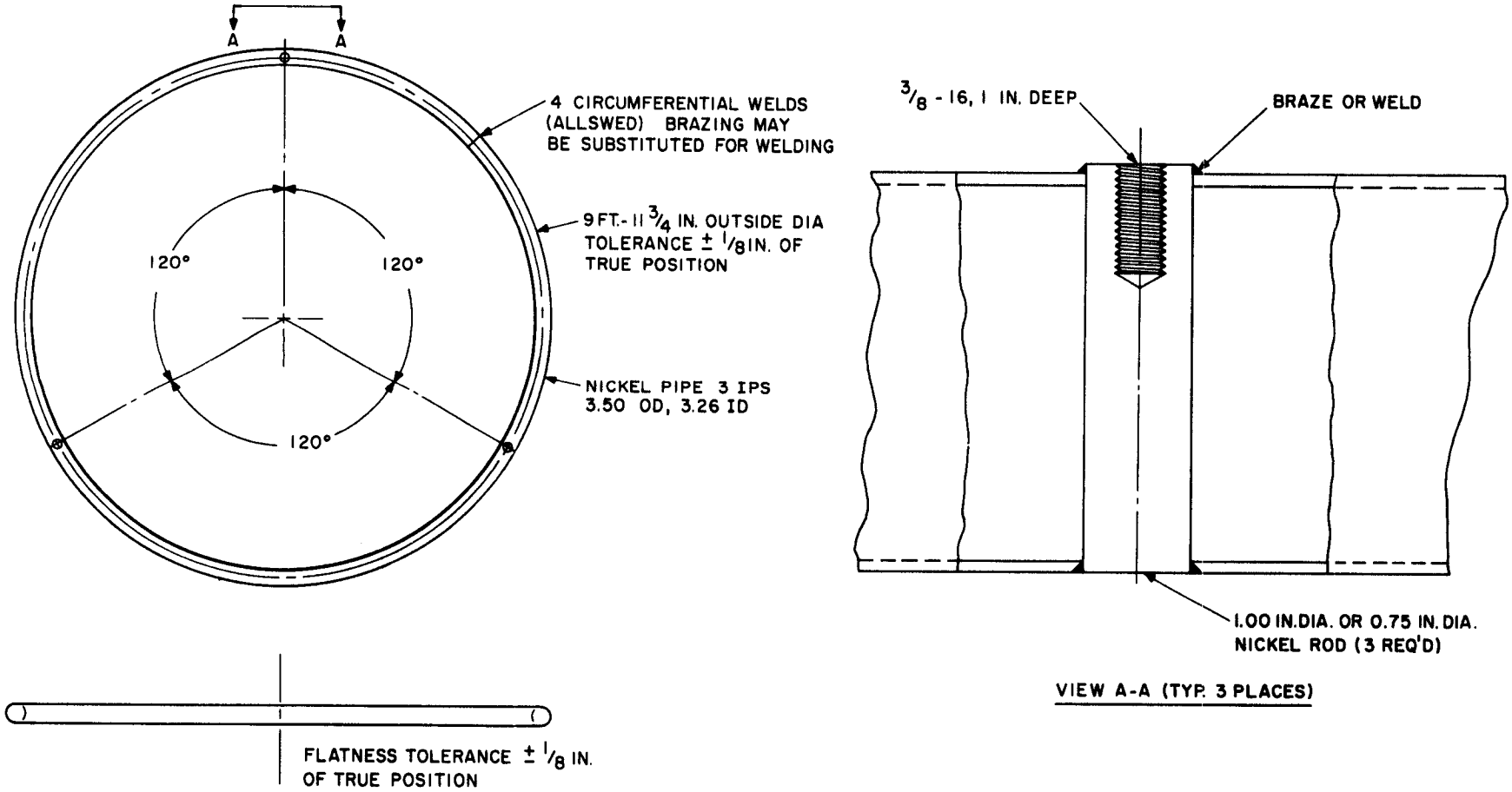

Figure 7.3-2. Mirror Support Torus

hardening which makes it ideal for this type of application. Because this formulation is thick and does not run, it was unnecessary to stop off the area under the torus which was not to be bonded. As a precautionary matter, twenty-four hours elapsed before the mirror was handled through the torus, although the cure time of the Bondmaster is only a few hours.

7.3.3 THERMAL SHOCKING

After the support ring was firmly attached, Figures 7.3-3, 7.3-4, the electroform surface was chilled thoroughly with dry ice. The ice was removed and hot water ($190^{o}F$) was poured over the back of the mirror deposit. The resulting thermal shock produced audible cracking and visible separation from the male master. The mirror was then hand-lifted away.

7.3.4 VISUAL INSPECTION

Inspection of the mirror's rear surface prior to separation indicated a smooth, non-nodular, defect-free surface, Figure 7.3-5. After separation, the optical surface appeared excellent at the vendor's location.

7.4 OPTICAL INSPECTION

7.4.1 METHOD

The mirror was optically inspected by the method described in Section 5.5.1 with the following exceptions. Due to the reduced specularity, the center of the filament image could be located in the reticle to the nearest ten divisions only. The resultant slope error readings are therefore accurate to the nearest minute only.

The light used was a model No. 54 Aristo-craft 16-volt bulb having a smaller filament than the bulb used for the inspection of the female master. This concentrated the resultant image but reduced the total brightness.

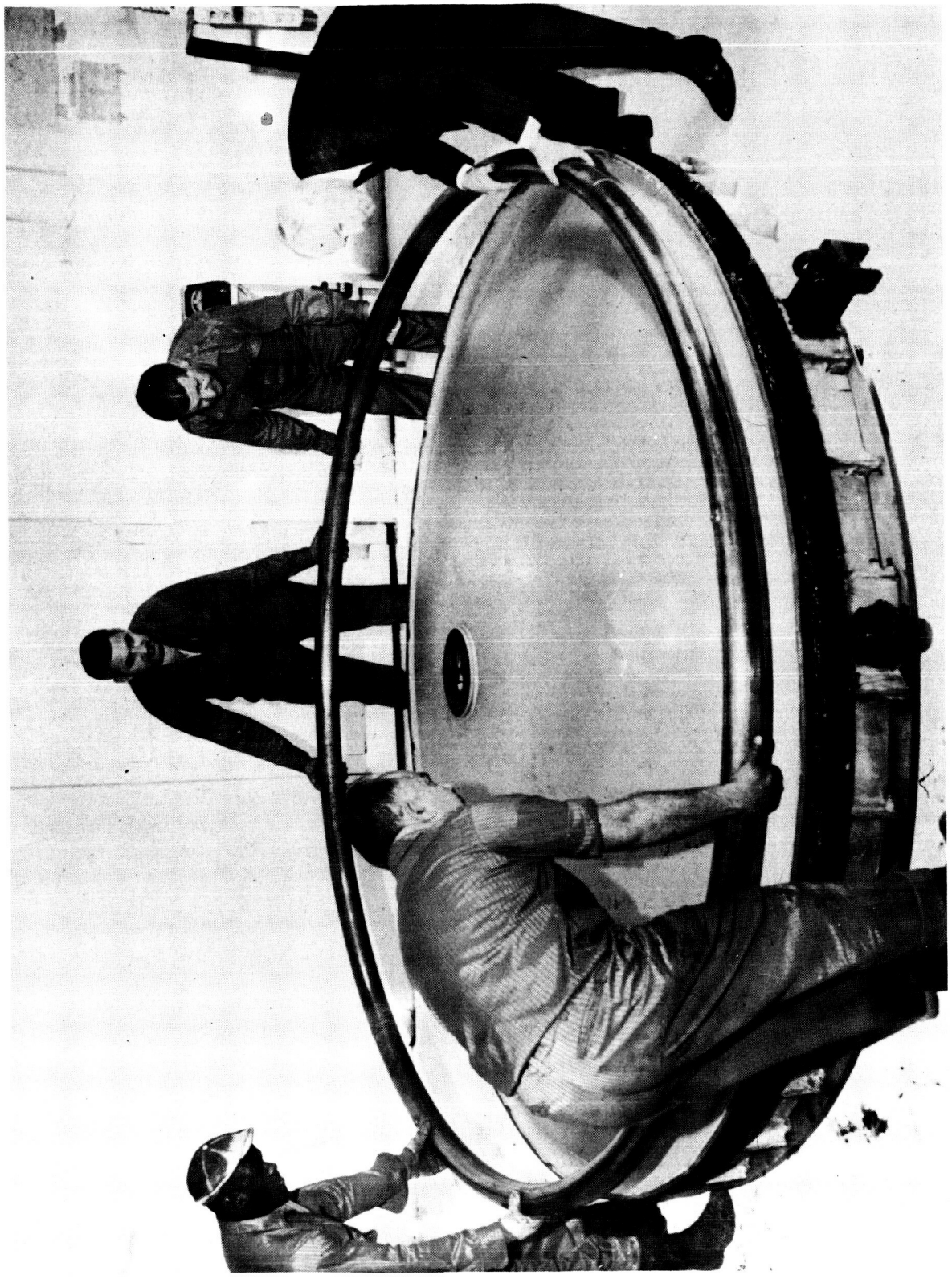

Figure 7.3-3. Fitting of Nickel Pipe Torus to Mirror

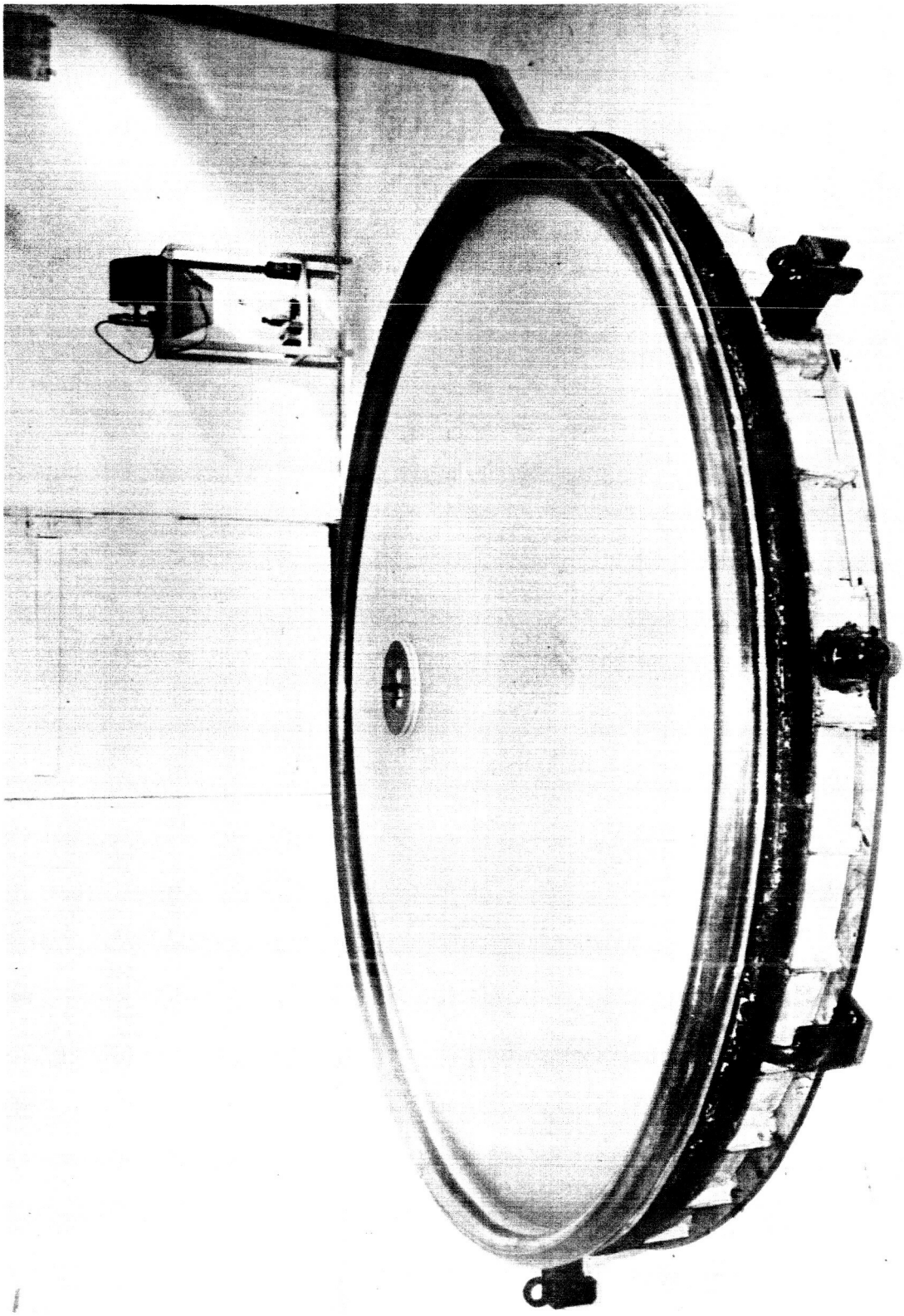

Figure 7.3-4. Handling Torus in Place, Ready for Separation of Mirror from Master

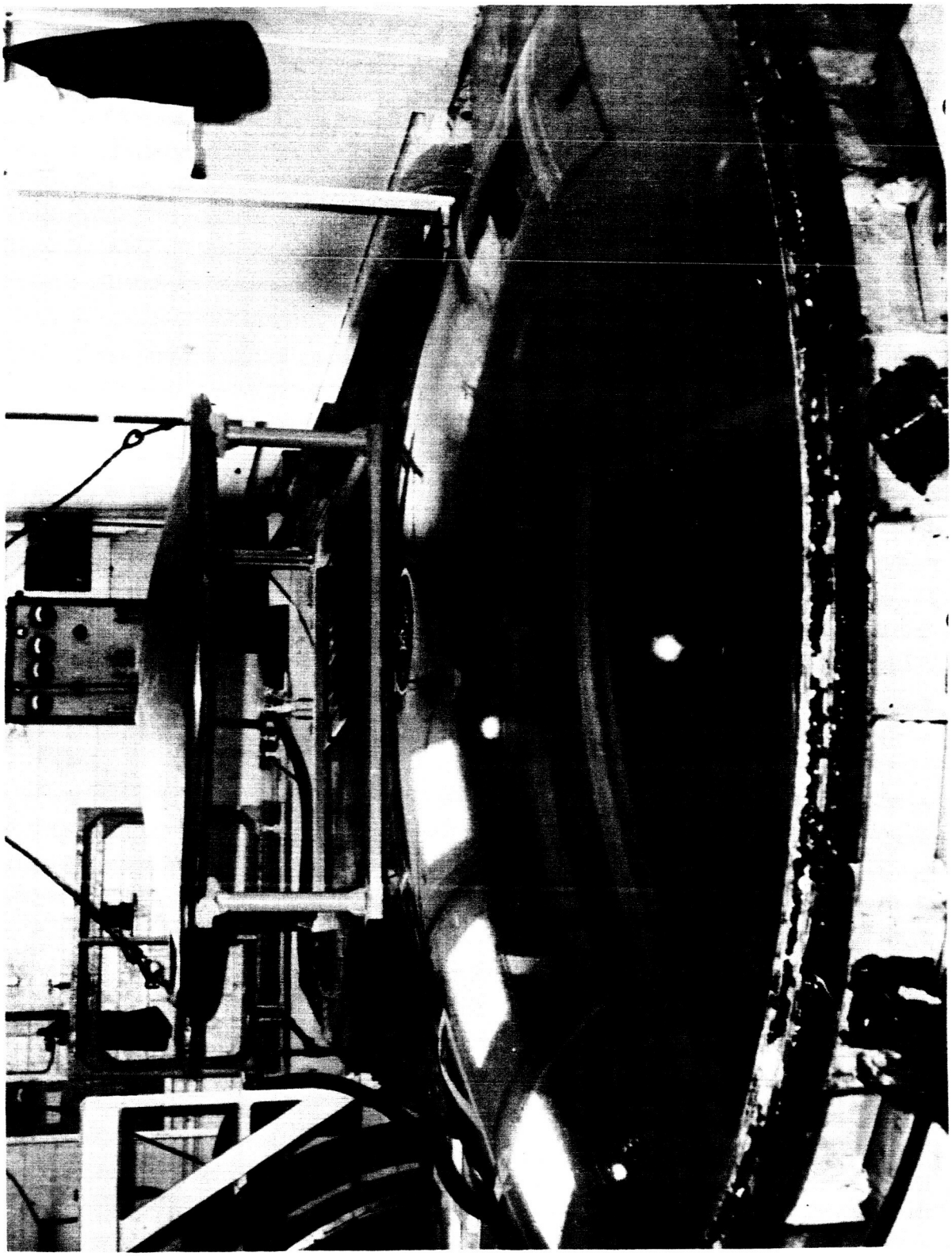

Figure 7.3-5. Male Master (Foreground) and Mirror (Background) Immediately After Separation

The mirror was centered and leveled, and the focal point was located by placing a matte glass plate in the approximate focal plane shining flashlights through eyepieces 1 to 6, and rotating the mirror on the turntable. Since errors in the mirror lateral and angular locations cannot be separated by simple optical methods, successive trial and error changes in these locations had to be made in order to position the mirror properly on the spintable. After this was done, the "best fit" focal-point location was determined and the focal length measured to the nearest 1/16 inch. The glass plate was then replaced by the above-described bulb, and slope error readings were taken.

In order to obtain values for the slope error for those points at which the reflection of the lamp filament lay outside the eyepiece field of vision, and which therefore could not be determined in the usual manner, a theodolite was set up in the optical tower at a distance of 3-1/2 inches (measured circumferentially) from each successive telescope location. The image of the lamp filament was then brought to the center of the theodolite cross hairs by inclining the axis of the theodolite from the vertical. The angle of inclination of the theodolite was read; it is equal to twice the slope error.

7.4.2 RESULTS

A. Focal Length

The focal length of the mirror, obtained by the method described in Section 5.5.1(D), was determined to be 69 inches. This compares with the design focal length of 68.8 inches.

B. SLOPE ERRORS

The reticle readings obtained by the methods described in Section 5.5.1 (E) are shown in Table K-1 (Appendix K). Where a dash appears in the table, the center of the filament image appeared to lie outside the field of the telescope eyepiece, and

no meaningful readings could be taken. These readings were adjusted for errors in the lateral location of the lamp filament (see Section 5.5.1 (F)). The resultant slope errors are shown in Table K-2 (Appendix K). Those points for which no reticle readings could be obtained at the regular angular stations are indicated by a dash in Tables K-1 and K-2.

An attempt was made to take reticle readings in the outer quarter of the mirror, at the telescope stations 7 and 8. These data (in units of ten reticle divisions) and the resultant raw (not adjusted by the method of Section 5.5.1(E)) slope errors are shown in Table K-3 (Appendix K). The special angular stations are linearly interpolated between the regular angular stations used for all other mirror and master inspections and shown in Figure 5.5-4. Thus station A-2.8 is located between stations A-2 and A-3, at four times the distance from A-2 which it is from A-3.

The mirror areas lying outside the reticle inspection limits are indicated by blank spaces in Figure 7.4-1. This Figure gives a graphical interpretation of the location of mirror areas with slope errors in excess of approximately 6 minutes.

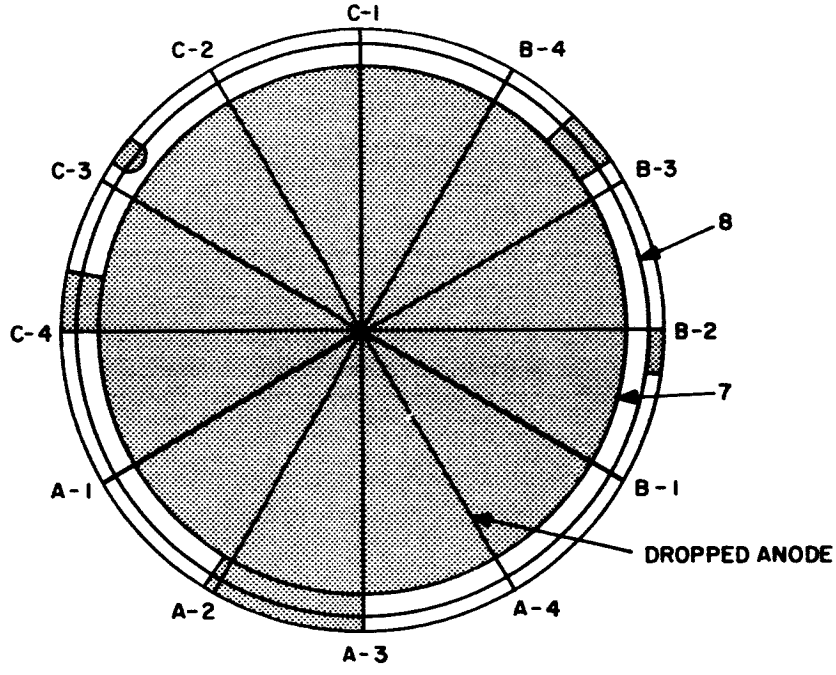

Figure 7.4-1. Mirror Regions Where Reticle Readings Could not be Obtained (Non-Shaded Areas)

Because the data in Table K-3 occur at irregular angular intervals and, therefore, afford an inferior statistical representation of mirror accuracy, slope errors at the regular angular stations were determined with a theodolite at the points marked with a dash in Table K-1. The procedures used are described in Section 7.4.1. The theodolite readings are given in Table K-4 (Appendix K). The true slope error is equal to one-half of these readings. Also shown in Table K-4 is the theodolite azimuth, i.e., the approximate direction in which the theodolite had to be inclined at each point in order to center the filament image at the cross hairs. For these angles, 0^{o} denotes a radially inward inclination of the theodolite, thus a radially outward slope error. No adjustment for error in lateral location of the focal point (see Section 5.5.1 (E)) was made for the slope error readings obtained by theodolite.

7.4.3 SUMMARY

Table K-5 (Appendix K) combines the slope error data from Tables K-2 and K-4. The readings taken with the theodolite were not adjusted for a lateral error in focal-point location because that adjustment would, at most, reduce these errors by 50 seconds. This would have been the total correction in the radial direction; there was none in the circumferential direction.

The maximum measured slope error was 21.7 minutes; the median error was 2.7 minutes. This value reduces to 1.8 minutes if the outermost quarter of the mirror is not included. A slope error of 6 minutes was not exceeded over 78% of the area. The self-imposed design goal was a maximum slope error of 6 minutes over 98% of the area.

Visual inspection of the mirror showed that the outer quarter (corresponding to telescope numbers 7 and 8) exhibited a strong orange peel in addition to regularly spaced indentations which can be compared to ball-peen hammer marks. If this area of the mirror is excluded from consideration, only a single point (at the

location where an anode was dropped on the female master during the electroforming process) had a slope error exceeding the design goal of 6 minutes.

Figure 7.4-2 summarizes and compares the slope properties of the female spincast master and the mirror. Correlation over the inner half of the area appears excellent. The outer half of the mirror is disturbed by the above-mentioned orange peel area along the perimeter. The Figure indicates that excellent replication by two electroformings can be achieved, if the causes for the orange peel can be removed.

7.5 THICKNESS AND SURFACE ROUGHNESS

7.5.1 THICKNESS TEST METHOD

The thickness of the mirror was determined ultrasonically. The equipment used was a Vidigage Thickness Tester Model 14-IC, No. OE-0001. The ultrasonic resonance method utilizes continuous, compressional, ultrasonic waves transmitted

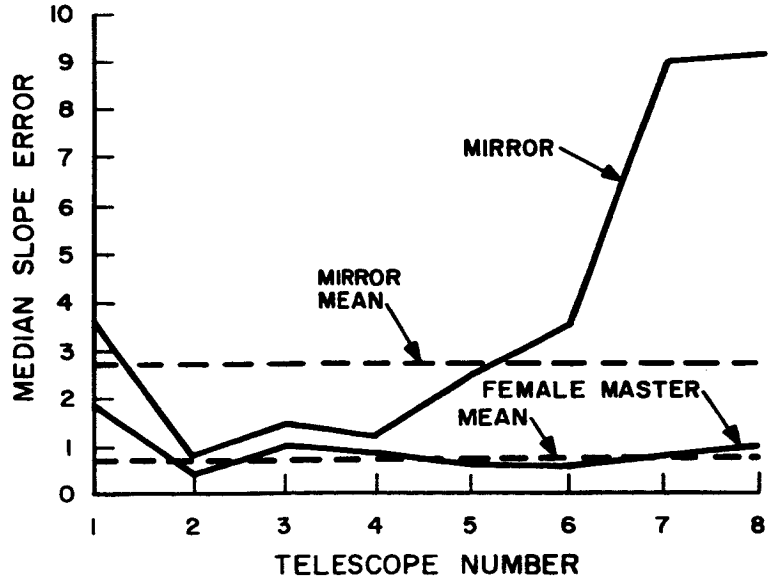

Figure 7.4-2. Mirror and Master Slope Error versus Radial Location

into plate material from one surface. The frequency (and therefore the wavelength) of these waves is set so that a wave is twice reflected and leaves the first material surface in phase with another incoming wave. Standing waves are then set up within the plate, causing it to resonate or vibrate at a larger amplitude. When the thickness is one-half of the wavelength, the plate will resonate. Resonance is indicated by its loading effect upon the ultrasonic transducer coupled with the test specimen. Similar conditions occur at multiples or harmonics of this frequency. In each case a standing wave is set up and the plate resonates.

The fundamental resonant frequency in the thickness direction of a plate is:

$$F = \frac{V}{\lambda} = \frac{V}{2T} + \frac{K}{T}$$

where: F = fundamental frequency, mc;

V = sound velocity, million in./sec;

T = thickness, in.;

K = constant, million in./sec;

λ = sound wavelength, in.

The thickness (T) of a plate can therefore be measured from one side by determining the fundamental resonant frequencies (F) from

$$T = \frac{K}{F}. \qquad (1)$$

The constant K for nickel is $0.113 - 0.115 \times 10^6$ in./sec.

The interval between any two adjoining frequencies equals the fundamental frequency. The difference between any two adjoining frequencies can therefore be substituted for F in equation (1), and the thickness can then be computed from harmonic frequencies as:

$$T = \frac{K}{3F - 2F} = \frac{K}{nF - (n-1)F} = \frac{K}{F}.$$

It is not necessary to know the harmonic number n in order to measure the thickness.

The accuracy of ultrasonic resonance measurements is not appreciably affected by such variables as ambient temperature, shape of part, magnetic properties, small differences in alloy composition, heat treatment, or deposits on the reflecting surface. Accuracy is limited by the resolution of the instrument, slight variations in the value of K, variations in contact between transducer and part, and calibration of the instrument.

7.5.2 CALIBRATION

Given the thickness of the solar mirror as .070 inches the scale selected covers .020 to .125 inches with overlaps of 10 harmonics. Resolution of any harmonic line is at least .0005 inch. Calibration blocks were prepared from various samples of nickel in thicknesses from .020 to .080 inches. A set of calibration blocks from the same electroformed material as the mirror was prepared. Slight variations in the material, K, could then be demonstrated with the separate nickels.

For this scale an oscillator variable from 4 to 8mc was selected and a 9mc transducer used for all measurements. A 9mc transducer is normally used with the 4 - 8mc tuning range because, while this is close enough to the transducer natural frequency for best sensitivity, the indication of the 9mc transducer resonance will not obscure indications from the test sample within the tuning range.

Final calibration of the scale was done by utilizing the electroformed nickel standard blocks and adjusting the oscillator frequency so that the resonance indications matched the scale markings. This standardizing method was shown to be repeatable and accurate to $\pm$ .002 inch.

There is very little drift in the instrument. Any drift effects were eliminated as an accuracy factor, however, by checking the instrument against the calibration blocks at the conclusion of the test. There was no change in scale reading during measurement of the mirror.

7.5.3 THICKNESS MEASUREMENT PROCEDURES AND RESULTS

A. Test Procedure

The mirror was measured as follows: the transducer was applied to the mirror surface by hand and coupled for the transmission of the sonic wave with a thin layer of glycerine. The coupling can be considered to be uniform because of the excellent finish on the mirror surface and because of the care taken in positioning the transducer by hand. Periodic re-checks of the readings obtained substantiated this uniformity. The mirror was probed radially at six-inch intervals from the edge of the center circular hole to the rim of the mirror. Eight such radii were measured at approximately 45° spacings (see Figure 7.5-1).

B. Results

The results of the thickness measurements are given in Table 7.5-1.

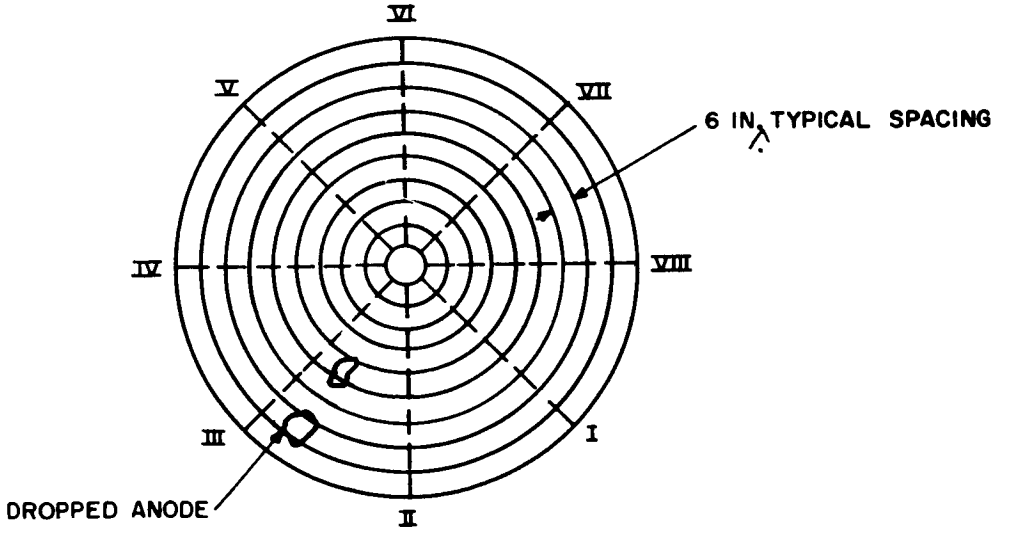

Figure 7.5-1. Thickness Measurement Locations

TABLE 7.5-1. MIRROR THICKNESS, 10^{-3} INCHES

Angular Station	Center ←							→ Rim
I	81	79	80	77	74	67	62	64
II	78	75	78	77	74	71	79*	67
III	81	75	77	76	74	70	64	64
IV	84	76	76	76	73	69	71	67
V	80	77	77	75	73	68	69	67
VI	84	78	78	76	73	67	66	66
VII	83	79	79	77	74	69	71	69
VIII	82	79	80	79	76	68	64	69
AVG.	81	77	78	77	74	69	68	66

* This reading is questionable

The design goal was a mirror thickness of .070/.075 inch. The average measured mirror thickness was .074 inch with a maximum of .084 at the center and a minimum of .064 at the rim. If the single questionable reading (marked (*) in Table 7.5-1) is disregarded, the circumferential variation in thickness was .004 inch on the average with a maximum of .007 and a minimum of .003 inch.

The quarter-round along the outside perimeter was measured by micrometer before the torus was attached to it. Its thickness varied from .035 to .065 inch. This is due to the fact that the conforming anodes stopped short of this quarter-round.

In summary it can be said that the mirror demonstrates the reliability of the GE electroforming method in which the deposition rate is closely controlled.

7.5.4 SURFACE ROUGHNESS

Profilometer readings were taken in the region between the two discrepant areas (anodes dropped on female master) using a model 21-IC No. MN-1755 profilometer.

The sensor of the profilometer was traversed across a fifteen-inch run. The readings over approximately 85% of the run showed an average of five micro-inches RMS. The maximum reading during this run was 7 micro-inches. The same region on the master had been checked, and the same value of surface roughness, i.e., 5 micro-inches had been obtained.

For comparison purposes, another run was taken on a good portion of the mirror. The average reading in this case was three micro-inches with a peak reading of five micro-inches.

8. HANDLING AND SHIPPING

8.1 SPECIAL SLING

To prevent radial loads from being exerted on the spincast and nickel masters during handling, a special sling was designed and fabricated. Because of an unusual crane arrangement at the electroforming vendor's plant, the sling was designed to fit the vendor's lifting cranes as well as a standard three-cable choke for use by GE and by the shipper.

The vendor's lifting facility consisted of a traveling portal frame which supported four chain hoists. Because of the three support points on the spincast structure, it was necessary to have the sling capable of lifting the structure at three points while the sling itself was supported at four points. When the sling was used with a three-cable choke for a single crane hook, one large I-beam was removed, leaving only a triangular piece.

8.2 SPINCAST MASTER

To ship the epoxy spincasting from the GE spincast facility to the electroforming vendor, a special plywood shipping container was prepared which completely enclosed the structure. Electric heaters were installed inside the container and powered by a motor-generator set carried on the truck. The temperature of the master was maintained at $90^{o}F$ during transport to prevent thermal stresses.

Because of the stiffness of the spincast support structure, it was impractical to fabricate a container which would rigidly support the structure. Therefore, the container was actually supported by the structure at the three support points. All lifting and supporting of the female master was accomplished by attaching directly to its structure through access holes in the container.

Thick rubber pads were used between the three female master support points and two heavy timbers placed crosswise on the truck bed. A maximum speed of 25 mph was allowed during the shipment. Upon arrival at the electroforming vendor's plant, the container was placed inside the building and the doors were closed before the female master was removed from the container.

8.3 SHIPPING OF MALE AND FEMALE MASTER ASSEMBLY

After electroforming of the male master, the female and male master assembly was returned from the electroforming vendor to the GE Philadelphia "D" Street plant by truck. No shipping container was used because protection from thermal shock was no longer necessary. Rubber pads, however, were again used between the three spincasting support structure load points and the timbers placed on the truck in order to minimize mechanical shock effects.

8.4 MALE MASTER

The trunnions on the male master support structure could not be located at the center of gravity, and the stable position of the assembly is the one with the face of the master down. Precautions should therefore be taken when rotating the master on the trunnions. These trunnions were intentionally located off-center to simplify the structural configuration and to keep the trunnions away from the face of the master thus avoiding interference with the electroforming of the mirror.

When properly supported at the three support points, the male master may be shipped or otherwise handled either horizontally or vertically without damage to the electroform. The two trunnion supports should not be used for shipping supports or other rough handling. They are only to be used for turning the master over.

8.5 MIRROR

When the mirror is to be handled with a crane, a specially provided lift sling should be used. This sling consists of three angle irons joined to form a triangle. At each joint is a hole into which a hook from a three-cable choke may be inserted, and three chains hanging downward which attach to three U's. These U's, which are fabricated from channel, are bolted to the three lift points on the torus. The U's prevent any twisting moment from being transmitted to the torus, and prevent the chain from bearing on the bonded edge of the quarter-round.

A special container was designed and fabricated for use in shipping the mirror. This special container was considered necessary because of the many handlings to which the mirror would be exposed and because the natural frequency of the mirror is in the ten cps range.

The container was constructed of wood and had a horizontal truss-stiffened base. Stiffness of the bottom portion of the container was attained from the truss structure, a plywood base mounted to this structure, and reinforced plywood sides permanently attached to the base. A removable reinforced plywood top was used. Attached to the base were three hat-shaped aluminum legs fabricated from 1/8-in. material. The three support points on the torus were bolted to these legs. Rubber pads were placed between the support points and the legs.

To prevent distortion due to vibration, eight conforming radial supports on both the top and bottom of the container were used. These supports were fabricated from styrene foam and had a one-inch thick pad of foam rubber bonded to them. The mirror was nested between the foam rubber supports. The two sets of radial supports were bonded to the top and bottom of the container, respectively, and care had to be taken when the top was removed so as not to damage the foam supports.

9. OPTICAL COATING

A proprietary coating was applied by Liberty Mirror, a Division of Libbey-Owens-Ford Glass Company, in their Research Laboratory at Toledo, Ohio. The coating is a vacuum-deposited coating of aluminum and has suitable undercoats and overcoats. The following specifications are guaranteed by the vendor for this coating.

9.1 LIBERTY MIRROR SPECIFICATION NO. 1054

9.1.1 REFLECTIVITY

The mirror shall have not less than 87% total reflectivity for light in the visible region as measured with a Weston photronic cell with a Viscor filter and a tungsten lamp supplying light at an angle of incidence of 22.5^{o}.

9.1.2 ADHERENCE

No visible part of the mirror coating shall be removed by the cellulose tape test described here:

A. Test

The tacky surface of cellulose tape shall be carefully placed in contact with a portion of the mirror surface and firmly rubbed against that surface. It shall then be quickly removed with a snap action which exerts the greatest possible stripping action on the mirror film.

9.1.3 HARDNESS

No evidence of film removal or film abrasion shall be visible to the eye when the following test is applied:

A. Test

A pad of clean dry cheese cloth (previously laundered) 3/8 inch in diameter, 1/2 inch thick, bearing with a force of one pound on the coating shall be rubbed across the coated element in any direction 200 times.

NOTE

During the above test, care should be exercised to prevent contaminating abrasives contacting the coated surface causing slight sleeks.

9.1.4 CORROSION RESISTANCE

There shall be no noticeable deterioration of the finished mirror when given the salt atmosphere test described here:

A. Test

The mirror shall be placed in a thermostatically controlled cabinet with a salt atmosphere for 24 continuous hours at a temperature of 95°F. The salt atmosphere shall be obtained by allowing a stream of air to bubble through a salt solution containing 1-1/2 pounds of sodium chloride per cubic foot of water.

9.1.5 EFFECT OF TEMPERATURE

The coating shall function satisfactorily and shall not be damaged to exposure to an ambient temperature of minus 60°F. and plus 500°F.

141

APPENDIX A
STOP-OFF OF ALUMINUM SPINCAST STRUCTURE AGAINST ELECTRO-CHEMICAL ATTACK

APPENDIX A

STOP-OFF OF ALUMINUM SPINCAST STRUCTURE AGAINST ELECTRO-CHEMICAL ATTACK

A. 1 PROTECTION OF THE SPINCAST STRUCTURE AGAINST ELECTRO-CHEMICAL ATTACK

All exposed aluminum surfaces were protected by "stop-off" against chemical attack by the electrolyte. The following procedure was used.

A. 1. 1 SURFACE PREPARATION

1. Remove all rough areas from cut ends and edges of channel supports and bracing structure. Removal may be accomplished by filing or by grinding with power equipment.
2. Wire brush all weld areas to remove all loose weld scale, oxide, and weld splatter.
3. Chemically clean all sub-structure surface per MSI 24417 sections 6. 1 through 6. 8 which are abstracted below. Solution concentrations are listed in the main body of the MSI.

MSI 24417

6.1 Activate the water supply and heaters on the steam generator about 45 minutes prior to use of the equipment.

6.3 Wearing rubber gloves, a rubber apron and safety glasses, clean the structure by wiping with acetone. Follow with an ethyl alcohol wipe.

6.4 Using the Pantex Hydro Steam-Jet Cleaner and the Hurriclean gun, alkaline clean the structure by spraying Detrex AL onto the surface for 2 minutes for each 15 square feet of surface area.

6.4.1 All solutions are syphoned from the storage containers to the secondary (solution) valve on the Hurriclean gun through a ¼" diameter hose. The steam valves on the generator and the gun are opened to permit full pressure (150 psig) when applying Detrex AL. The solution valve on the gun is open full to permit rapid flow of the Detrex solution.

6.5 Thoroughly water rinse the structure until all Detrex is removed. If water breaks are present after rinsing repeat Step 6.3, 6.4 and 6.5.

6.5.1 High pressure rinsing can be achieved by closing the steam valve on the generator and the solution valve on the gun. Then open the water and rinse valves on the steam generator.

6.6 Deoxidize the surface by steam spraying Deoxidine 624 onto the surface for 5 minutes. Allow the Deoxidine to remain on the surface for 5 to 6 minutes prior to rinsing.

6.6.1 The steam valves on the steam generator and the gun are opened to one-half the full pressure when applying Deoxidine 624. The solution valve on the gun is open full to permit rapid flow of the Deoxidine.

6.7 Thoroughly water rinse the surface for 2 to 3 minutes. High pressure rinsing should be employed (see paragraph 6.4.1)

6.8 Blast the aluminum surface with steam (full pressure) until the smut, dark grey color, is removed.

4. Blow all condensed water from the structure, and allow to air dry a minimum of 8 hours prior to coating application.

A. 1. 2 APPLICATION OF EPOXY FILLET COMPOUND 178A-10-3

1. All fillet gaps between tack-welded structure should be filled with epoxy calking compound 178A-10-3 by means of a calking gun. Areas inaccessible to a calking gun may be filled by means of trowels or spatules.
2. Allow the epoxy to cure at ambient for a minimum of four hours.

A. 1. 3 APPLICATION OF EPOXY SPRAY COATING V-7106B-SP

1. Spray apply a uniform continuous coating of apoxy (Table A-1) to all metallic surfaces. Considerable care must be exercised to ensure that all crevices and shielded areas are completely spray coated.
2. Air dry at ambient temperature for a minimum of six hours, or preferably, over-cure at 140^{o}F for 1-1/2 hours.

3. Spray apply two additional coats of epoxy as outlined in 1 and 2 above. Total dry film thickness after cure should be 8-10 mils (0.008 - 0.010 inch). Film thickness may be checked by means of a Gardner Scratch Gauge for each coat.

A. 1. 4 APPLICATION OF "MICROSTOP" LACQUER

1. Thin "Microstop" for spray application by addition of "Microstop" Reducer. Reduction is approximately 1/3 by volume.
2. Spray apply a total of ten uniform, continuous spray coats of lacquer, allowing a minimum of two hours air-dry period at ambient temperature between each spray coat, and a minimum of four hours air dry after application of the final coat.
3. Should minor damage occur to the lacquer coating during handling, a minimum of four brush coats may be applied to the damaged area, allowing a minimum air-dry period of four hours between coats.

NOTE: The lacquer must be handled as an enamel; i.e., the coating is flowed on from a full brush, smoothed lightly, and allowed to dry. The coating must not be brushed out in the same manner as house paint.

A. 1. 5 MATERIALS REQUIRED

1. Detrex AL Cleaner, Detrex Chemical Industries, Inc., Detroit, Michigan.
2. Deoxidine 624, American Chemical Paint Co., Ambler, Pa.
3. Epoxy Fillet Compound 178A-10-3, Chemistry Research, Space Sciences Laboratory, G. E. Valley Forge.
4. Araldite Solution #571KX-75%, Ciba Products Inc., Rt. 208, Fairlawn, New Jersey.
5. Pentamide #815 - Same Source as for item 4.
6. Toluol (Toluene) - Any source.
7. Cellosolve - Any source.
8. Methyl Isobutyl Ketove (MIBK) - Any source.
9. "Microstop" Lacquer and Reducer - Michigan Chrome and Chemical Co., Local Distributor - W. A. Reynolds Corp., 2213 W. Glenwood Ave., Phila., Pa.

TABLE A-1. FORMULATION OF EPOXY SPRAY COATING V-7106B-SP

Part A	
Resin Solution #571KX-75%	16
	40.0
Part B	
Pentamide #815	35.0
Toluol	21.0
Cellosolve	2.5

Final Blend Mixing (blend small quantities as needed)

Part A 65% by vol.
Part B 35% by vol.

Thin to spray viscosity, 15-25 sec No. 4 Ford Cup, with the following solvent blend:

Toluol	50 parts by weight
MIBK	45 parts by weight
Cellosolve	5 parts by weight

APPENDIX B

PREPARATION OF ALUMINUM MOLD SUBSTRATE WITH MATERIAL COMPATIBLE WITH SPINCAST RESIN

APPENDIX B

PREPARATION OF ALUMINUM MOLD SUBSTRATE WITH MATERIAL COMPATIBLE WITH SPINCAST RESIN

After the eighth coat was cast, the epoxy thickness ranged from 1-5/16 to 1-11/16 inches as measured around the outer periphery of the ten-foot mold. Subsequent to post-curing the mold at 120°F and several days later, when the room temperature reached a low of 74°F, the mold cracked. This occurred when scribing of the outer diameter was nearing completion. The cause of cracking has been attributed primarily to excessive thickness of the epoxy and the resulting effects of thermal differential expansion. All of the epoxy was removed from the aluminum substructure by laying numerous blocks of dry ice over the epoxy and prying in these areas with cold chisels and crowbars wherever audible sounds of cracking were noticed. Liquid nitrogen was not used since there was some concern that weld cracking might occur in the aluminum substrate as a result of severe local thermal shock. Thin spots of epoxy residue adhering tenaciously in numerous areas were removed with a disc grinder. The entire surface of the aluminum mold substrate was cleaned by washing and wiping with TURCO #1 (phosphoric acid cleaner, one part to three parts of water) for ten minutes followed by thoroughly washing with tap water and drying. The aluminum surface was then brush coated with a thin layer of epoxy consisting of:

571KX - 65% by volume

PENTAMID 815 - 35% by volume

This mixture was diluted to brush consistency by adding ethyl cellosolve (Ethylene Glycol Monoethyl Ether). Thin layers of the brush coating were observed to harden fairly well in 24 hours at room temperature, while thicker areas took considerably longer. In future applications, it is recommended that a slightly elevated temperature cure be given to similar base coats.

The flexible epoxy overcoat was applied to the aluminum dish to promote additional adhesion for the thick epoxy layers during 120°F heat cure and treat cycles. Tests have not been made to date to determine an optimum treating process for the resin-metal interface.

The circumferential aluminum angle was spatula coated with a thin layer of RTV-60 (catalyzed with 1/2% by weight of T-12 and thoroughly mixed) which served as a mold release agent between the outer peripheral angle and the spincast epoxy.

APPENDIX C
SPINTABLE DRIVE AND CONTROL SYSTEM CHECKOUT

APPENDIX C

SPINTABLE DRIVE AND CONTROL SYSTEM CHECKOUT

C.1 PRELIMINARY CHECKOUT PREPARATIONS

a. Reference: 1 - Hewlett Packard Amplifier Model 450A I.G. #AH-0236

2 - Hewlett Packard Electronic Counter Model 522B, I.C. #AH-1087

Deliver to Valley Forge Lab for calibration.

b. Refer to PIR 635-117, page 5, Electronic Counter and Amplifier, are to be set per above PIR.

c. It is requested that all traces of rust be removed from the spincast machine mounting base and that the machine be repainted if this is found necessary.

d. Remove the rubber pads along with their restraining brackets. These are located at four sides of the machine at floor level.

e. Turn off all control panel switches and set potentiometer to zero.

f. Align paraflex coupling with formsprag clutch; check location of keys in drive shaft, then tighten flange to formsprag clutch.

g. Check table bearing pre-load adjustment nut for pre-load taper rolling bearing.

h. Tighten bolts holding the cast top of spintable to the drive shaft.

i. Align table shaft in a vertical plane within ± .001 inch by adjusting the height of the Korfund Vibro-Isolators supporting the table legs in the spin pit.

j. Fill table bearing housing to capacity marked on sight level indicators. SAE No. 20 motor oil may be used.

k. Complete electrical hookup of Hewlett Packard Tachometer Head (photocell light source).

l. Blacken rim of table, apply a piece of reflective white tape to table rim and sharply focus the light source on the tape. Rotate table by hand and check light trip mechanism by observing the electronic counter.

m. Mount and pre-set four 5-in. diameter dial deflection indicators, .0001 increments between the table and the floor at positions 90° apart.

C.2 CHECKOUT OF SPINTABLE DRIVE AND CONTROLS

After preliminary preparations are complete, the following porcedures are to be employed.

a. Turn on the photoelectric light speed sensor at the outer rim of the table, The Hewlett Packard counter, and the counter amplifier. Give the counter and amplifier a one-hour minimum warmup period. Check counter and amplifier settings per PIR 635-117, page 5.

b. Set 40 psi pressure to the table brakes and actuate brakes several times. Disengage brakes and slip a .020 to .040 shim between the surface of the brake shoe and the rim of the table to confirm clearance. Turn off the brake switch at the control panel as a precautionary measure to prevent engagement of brakes while table is spinning.

c. Clear spintable and railed area of all tools and equipment, and alert all personnel to stay outside safety railing.

d. Turn off all power to the table drive system and set potentiometer control to the zero position.

e. While one man rotates the table, check to ensure that speed counter starts and stops each time a pulse is generated by the light reflected from the taped edge of the table.

f. Check both tachometer generator drive belts in the spin pit. Check oil level of the table drive shaft bearings, check operation of exhaust vents in the spin pit. Bring table to rest.

g. Check operation of table level monitoring dial indicators. Adjust eight table rim support rollers to .020-in. clearance while table is manually rotated.

h. Run a final drive system check as follows:

   Recheck locked zero position of potentiometer control.

   Push the stop buttons to disengage drive motor and motor clutch.

   Engage power main to table.

   Set Kinatrol cabinet handle to the on position to allow the electronic tubes to warm up (2 to 5 minutes) until an audible click is heard from Thyratron control timer.

Engage table motor and wait for a second audible timer click (2 to 5 minutes).

Engage motor clutch.

After Thyratron tubes light up, slowly and continuously turn control potentiometer until approximately 3700 counts are attained. The coarse tachometer indicator will read 16.0 rpm at 3700 counts.

Under normal startup conditions, the speed control feedback system will hunt for 20 to 30 minutes until the motor and its associated mechanical parts reach a stable operating temperature.

IMPORTANT

Lock potentiometer as soon as the desired setting is attained. Maintain a current range of 7 to 10 amperes to the drive motor when accelerating or decelerating the spin table. At initial startup, a transient surge in current will occur which is normal in the range of 15 to 20 amps for a short time interval of perhaps five to ten seconds. After 3700 ±30 counts are attained, observe both dial indicators and record the deflections.

i. Allow spintable to run for about one hour then record 50 consecutive readings of the electronic counter without touching the controls. At this time the readings should remain scattered around the nominal setting ±five counts.

j. Bring the table to rest as follows:

Disengage motor clutch

Stop motor

Turn Kinatrol cabinet switch to off position

Disengage table power main switch

Return control pot to zero and lock in place

APPENDIX D
SPINCAST MOLD SCRIBING PROCEDURE

APPENDIX D

SPINCAST MOLD SCRIBING PROCEDURE

In preparation for electroforming, two circular grooves were cut into the epoxy surface near the inner and outer periphery of the spincast mold (Figure D-1). During the electroform process the grooves formed a rigid lip at the inner and outer rim of the male master. The object of the lip was to prevent liquid from seeping beneath the deposited nickel surface since this might indelibly stain the electroformed surface.

Two very faint lines (ghost lines) were also scribed on the epoxy surface to delineate the inner and outer periphery of the working surface of the mirror and to establish permanent reference circles percisely concentric to the mold axis.

The reference circles would replicate on both the male master and the female mirror facilitating orientation of the mirror relative to its true axis anytime during or subsequent to final fabrication.

All scribed and grooved circles were generated by turning the mold in place on the spincast table to ensure concentricity to the paraboloidal axis of the cast epoxy surface. Specifically ground, hardened trammel points were used to cut the grooves while the light ghost line was made with a 3/32 in. diameter soft-steel rod which had a conically ground, dull, rounded point. The same tool post setup and tool rake angle (Figure D-1) were used to generate both the ghost lines and the grooves.

Since percise concentricity was desired and since the measured diametral lengths did not have to be extremely accurate, the following scribing procedure was employed. A light base reference circle was scribed near the center of the mold.

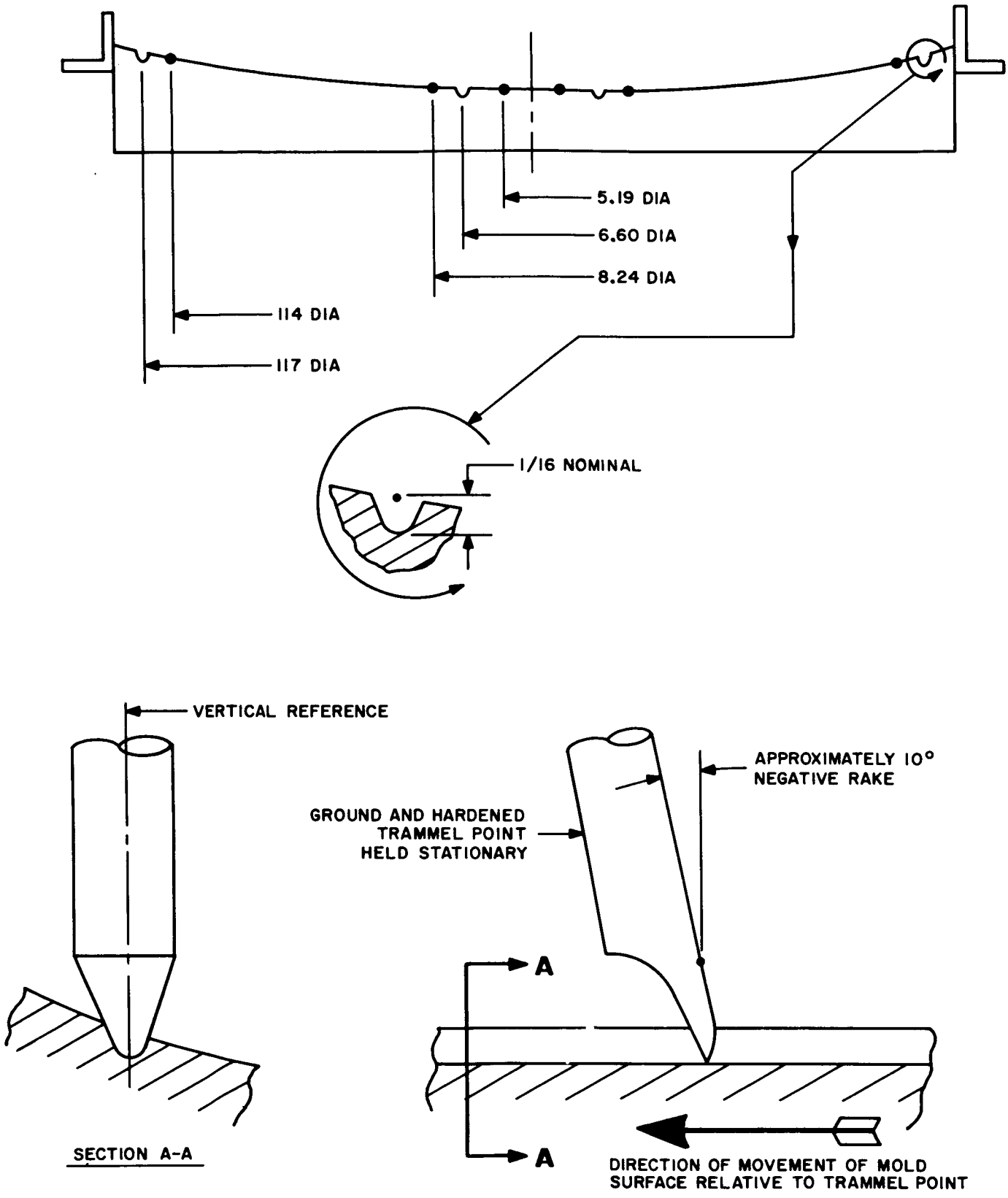

Figure D-1. Scribing of Spincast Mold

This was then determined to be 5.19 inches in diameter, and all subsequent measurements were made from it. A plumb bob was suspended from a long wooden 2 x 4 placed across a great circle diameter of the mold. Diametral distances were measured along the 2 x 4 from the 5.19-inch base circle. They were then transferred to the mold surface by means of the plumb bob. The grooving tool, held by a stationary tool post, was lowered directly over the diametral locations marked on the surface of the mold.

Cutting action was obtained by manually rotating the mold very slowly (approximately 1/2 rpm). Rotational speed was varied as the cumulative depth of cut increased and tool chatter was minimized by varying the rotational speed of the mold in accord with the cumulative depth of cut. The grooving tool was adjusted manually to remove .005 inch of material for every three revolutions of the mold.

The light ghost circles were scribed during a single revolution of the mold. An ambient temperature was maintained between 90 and 95^{o}F throughout all scribing and grooving operations on the final spincast coat. During scribing of the eighth coat, however, the temperature was maintained at 74^{o}F.

APPENDIX E
STRUCTURAL ANALYSIS OF SPINCAST SUPPORT STRUCTURE

APPENDIX E

STRUCTURAL ANALYSIS OF SPINCAST SUPPORT STRUCTURE

E.1 LOADS

Before Separation of Male Master

a. Epoxy: .5 in. thick, 90 lb/cu ft $\frac{90 \times 1/2}{12}$ = 3.75 lbs/sq ft

b. Nickel: .375 in. .3 lb/cu in 16.20 lb/sq ft

c. Male Back-up Structure: 1600 lb total weight,

78.5 sq ft total area $\frac{1600}{78.5}$ = 20.40 lb/sq ft

d. Total Unit Weight: 40.35 lb/sq ft
or 0.28 psi

E.2 HANDLING CONDITION

Load on structure = 3.75 lb/sq ft + female mold back-up structure weight (approx. 25 lb/sq ft)

= 30 lb/sq ft
at 6 g = 180 lb/sq ft or 1.25 psi

E.3 ALLOWABLE STRESSES AND DEFLECTIONS

a. Static deflection limit on structure: one minute of arc under 40 lb/sq ft during and after electroforming.

b. Epoxy stress limit: 2000 psi under 180 lb/sq ft handling condition.

E.4 DEFLECTION ANALYSIS

Reference: "Anisotropic Plates" by S.G. Lekhnitski, A.I.S.I. Translation from the Russian.

Sect. 54. Bending of a Circular Plate with Curvilinear Anisotropy

Case of Supported Edge: (p. 199) (Uniform Loading)

$$w = \frac{q\,a^4}{8\,(9-K^2)D_r}\left[\frac{(3-K)\,(4+K+\nu_\theta)}{(1+K)\,(K+\nu_\theta)} - \frac{4\,(3+\nu_\theta)}{(1+K)\,(K+\nu_\theta)}\left(\frac{r}{a}\right)^{K+1} + \left(\frac{r}{a}\right)^4\right]$$

where

$$K = \sqrt{D_\theta/D_r}\,, \quad D_r = \frac{E_r\,h^3}{12\,(1-\nu_r\,\nu_\theta)}\,, \quad D_\theta = \frac{E_\theta\,h^3}{12\,(1-\nu_r\,\nu_\theta)}\,.$$

$$Mr = \frac{q\,(3+\nu_\theta)\,a^2}{2\,(9-K^2)}\left[\left(\frac{r}{a}\right)^{K-1} - \left(\frac{r}{a}\right)^2\right]$$

$$M_\theta = \frac{qK^2\,a^2}{2\,(9-K^2)}\left[\frac{(3+\nu_\theta)\,(1+K\nu_r)}{K+\nu_\theta}\left(\frac{r}{a}\right)^{K-1} - (1+3\,\nu_r)\left(\frac{r}{a}\right)^2\right]$$

where

a = radius

and

q = uniformly distributed load.

E.4.1 "EFFECTIVE" THICKNESS

E.4.1.1 Radial Direction

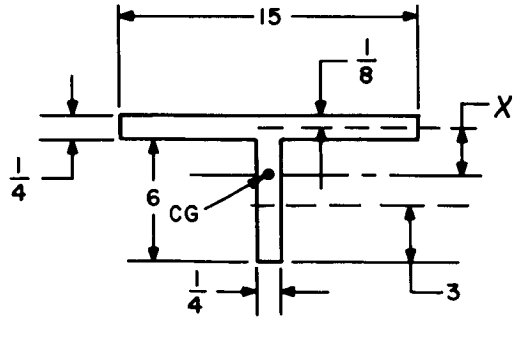

Centroid of section

15(.25) = 3.75, 6(.25) = 1.50

3.75 x = 1.50 (3.125-x)

5.25 x = 4.69

3.125-x = 2.232

x = 0.893 in.

Moment of Inertia

$$I = \frac{15\ (.25)^3}{12} + \frac{.25\ (6)^3}{12} + 3.75\ (.893)^2 + 1.50\ (2.232)^2 = 14.9\ \text{in.}^4$$

$$(h_e)^3_R = \frac{12I}{b} = \frac{12(14.9)}{15} = 11.9\ \text{in.}^3$$

E.4.1.2 Tangential Direction

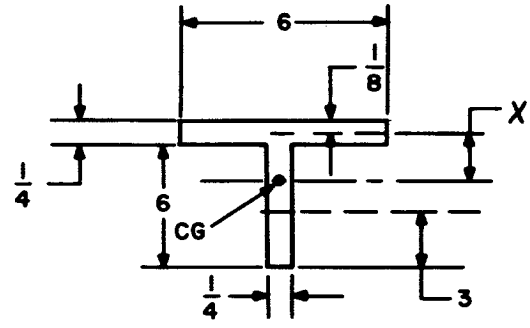

Centroid of section

$1.50\ (x) = 1.50\ (3.125 - x)$

$3.125 - x = 1.562$

$x = 1.563$ in.

Moment of Inertia

$$I = \frac{6\ (.25)^3}{12} + \frac{.25\ (6)^3}{12} + 2\left[1.50\ (1.563)^2\right] = 11.8\ \text{in.}^4$$

$$(h_e)^3_T = \frac{12I}{b} = \frac{12\ (11.8)}{6} = 23.6\ \text{in.}^3$$

E.4.2 "EFFECTIVE" RIGIDITY, using $E = 10 \times 10^6$ psi for aluminum

$$D_r = \frac{(10 \times 10^6)\ (11.9)}{12\ (1 - 0.3^2)} = 10.9 \times 10^6\ \text{psi}$$

$$D_\theta = \frac{(10 \times 10^6)\ (23.6)}{12\ (1 - 0.3^2)} = 21.6 \times 10^6\ \text{psi}$$

$$K = \sqrt{\frac{21.6 \times 10^6}{10.9 \times 10^6}} = 1.41$$

K = ratio of radial to tangential rigidity

E.4.3 NORMAL DEFLECTION, w

$$w = q\left[\frac{(60)^4}{8\,(9-1.41^2)\,(10.9 \times 10^6)}\left[\frac{(3-1.41)\,(4+1.41+0.3)}{(1+1.41)\,(1.41+0.3)}\right.\right.$$

$$\left.\left. - \frac{4\,(3+0.3)}{(1+1.41)\,(1.41+0.3)}\left(\frac{r}{a}\right)^{2.41} + \left(\frac{r}{a}\right)^4\right]\right]$$

$$w = q\,(.0212)\left[2.18 - 3.20\left(\frac{r}{a}\right)^{2.41} + \left(\frac{r}{a}\right)^4\right]$$

$$\frac{dw}{dr} = q\,(.0212)\left[-3.20\,(2.41)\left(\frac{r}{a}\right)^{1.41}\left(\frac{1}{a}\right) + 4\left(\frac{r}{a}\right)^3\left(\frac{1}{a}\right)\right]$$

$$\frac{dw}{dr} = q\,(.0212)\left[-0.120\left(\frac{r}{a}\right)^{1.41} + 0.667\left(\frac{r}{a}\right)^3\right]$$

$$w = q\left[0.0462 - 0.0678\left(\frac{r}{a}\right)^{2.41} + 0.0212\left(\frac{r}{a}\right)^4\right]$$

$$\frac{dw}{dr} = q\left[-0.00274\left(\frac{r}{a}\right)^{1.41} + 0.00141\left(\frac{r}{a}\right)^3\right]$$

$$w_{max} = 0.0462\,q \quad \text{at } r = 0$$

$$\left(\frac{dw}{dr}\right)_{max} = 0.00133\,q \quad \text{at } r = a$$

For 40 lb/sq ft (q = .28 psi):

$$w_{max} = 0.0129 \text{ in.}$$

$$\left(\frac{dw}{dr}\right)_{max} = 0.00037 \text{ equals } 1.28 \text{ minutes}$$

E.5 STRESS ANALYSIS

E.5.1 PLATE

Reference: "Formulas for Stress & Strain" by R.J. Roark (3rd Edition)

Table X Formulas for Flat Plates

Case 13 Outer Edge Supported. Uniform load over entire actual surface.

$$\sigma_{max} = \frac{3q}{4mt^2(a^2-b^2)}\left[a^4(3m+1)+b^4(m-1)-4m\,a^2b^2-4(m+1)\,a^2b^2\ln\left(\frac{a}{b}\right)\right]$$

$$w_{max} = \frac{3q(m^2-1)}{2m^2Et^3}\left[\frac{a^4(5m+1)}{8(m+1)}+\frac{b^4(7m+3)}{8(m+1)}-\frac{a^2b^2(3m+1)}{2(m+1)}+\frac{a^2b^2(3m+1)}{2(m-1)}\ln\left(\frac{a}{b}\right)\right.$$

$$\left.-\frac{2\,a^2b^4(m+1)}{(a^2-b^2)(m-1)}\left(\ln\frac{a}{b}\right)^2\right]$$

where:

q = uniform load (psi)

m = inverse of Poisson's ratio

t = plate thickness (in.)

a = outer radius (in.)

b = inner radius (in.)

E = modulus of elasticity (psi)

w = deflection (in.)

σ = stress (psi)

$$\sigma = \frac{3\,(1.27)}{4(3)\,(.25)^2\,(3519)} \left[(60)^4\,(10) + (9)^4\,(2) - 12\,(60)^2\,(9)^2 - 16\,(60)^2\,(9)^2 \ln\left(\frac{60}{9}\right) \right]$$

σ_{max} = 10,500 psi (aluminum 1/4" plate under full 6g load)

This corresponds to

$$\left[\frac{0.5 \times 10^6}{10 \times 10^6} \times 10{,}500 \right] = 525 \text{ psi in the epoxy}$$

E.5.2 MAIN CHANNELS (12 x 5 x 1/2)

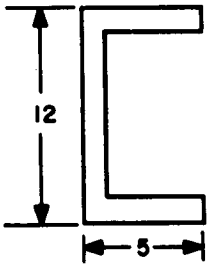

$$I = (.5)\,\frac{(11)^3}{12} + 2\left[5\frac{(.5)^3}{12} + (5)\,(.5)\,(5.75)^2 \right]$$

$$I = 55.5 + 2\,(0.052 + 82.7) = 221 \text{ in.}^4$$

Simply Supported Beam - Uniform Loading

$$w_{max} = \frac{5}{384}\,\frac{PL^3}{EI} \qquad P = \text{Total Load}$$

Total Area = $\pi\,(5)^2$ = 78.5 sq ft

Total Load = (78.5) (180 lb/sq ft) = 14,100 lb (under 6g)

14,100 ÷ 3 = 4,700 lb load per support channel

$$w_{max} = \frac{5}{384}\,\frac{4700\,(114)^3}{(10 \times 10^6)\,(221)} = 0.041 \text{ in.}$$

$$M_{max} = \frac{PL}{8} = \frac{4700\ (114)}{8} = 67,000 \text{ in. lb}$$

$$\sigma = \frac{Mc}{I} = \frac{(67,000)\ (6)}{221} = 1,820 \text{ psi}$$

E.6 CONCLUSION

Since the modulus of elasticity of the epoxy is only five percent that of aluminum, the epoxy stresses due to the channel beam action are less than 100 psi, hence VERY SAFE.

APPENDIX F
STRESS ANALYSIS OF COPPER ANODE RINGS FOR ELECTROFORMING OF MALE MASTER

APPENDIX F. STRESS ANALYSIS OF COPPER ANODE RINGS FOR ELECTROFORMING THE MALE MASTER

The 5-ft diameter ring is critical, because it is the biggest one supported at 4 points only. (See Figure 6.2-1.)

Take 80 lb/ft as a conservative value for anode weight plus ring weight.

Ref: Roark "Formulas for Stress and Strain" 2d Edition, p. 149

M_o = bending moment at quarter (support) points

T_{45} = torsional moment midway between support points

W = load per length

R = radius

$$M_o = W R^2 \left[\frac{\sin\frac{\theta}{2} - \frac{\theta}{2}\cos\frac{\theta}{2}}{\sin\theta/2}\right]$$

$$M_o = W R^2 \left[\frac{.707 - \frac{1}{2}\frac{\pi}{2}.707}{.707}\right] \quad \text{for } \theta = 90^o$$

$$= 80\,(2.5)^2 \left[.155\right]$$

$$= 78 \text{ ft-lb}$$

$$M_{45} = W R^2 \left[.09\right] = 80\,(2.5)^2 = 45 \text{ ft-lb}$$

$$T_{45} = -M_o \sin\alpha + \frac{WR^2}{2}(1-\cos\alpha) + WR^2(\alpha - \sin\alpha) \quad \left[\alpha = 45^o\right]$$

$$= W R^2 \left[-.707\left(1-\frac{\pi}{4}\right).707 + \frac{1}{2}\frac{\pi}{2}(1-.707) + \left(\frac{\pi}{4} - .707\right)\right]$$

$$= 80\,(2.5)^2 \left[.205\right]$$

$$= 102.5 \text{ ft-lb}$$

Maximum stress occurs at 45°, midway between support points.

$$\sigma = \frac{Mc}{I} = \frac{32\ M}{\pi d^3} = \frac{32 \times 45}{\pi (1.5)^3}\ 12 = 1630 \text{ psi}$$

$$\tau = \frac{Tc}{J} = \frac{16\ T}{\pi\ d^3} = \frac{16 \times 102.5}{\pi (1.5)^3}\ 12 = 1850 \text{ psi}$$

$$\sigma_{max} = \frac{\sigma}{2} \pm \left[\left(\frac{\sigma}{2}\right)^2 + (\tau)^2\right]^{1/2}$$

$$= \frac{1630}{2} \pm \left[\left(\frac{1630}{2}\right)^2 + (1850)^2\right]^{1/2}$$

$$= 815 \pm \left[2000\right]$$

$$= 2815 \text{ psi} \quad \text{SAFE}$$

APPENDIX G
VIBRATION INVESTIGATION

APPENDIX G

VIBRATION INVESTIGATION

Four successive spincast coats (numbers 2 through 5) had exhibited radial lines and concentric rings of discoloration. Both of these characteristics created noticeable distortions in the cast surface. Vibration of the spintable and the mold as a result of dynamic imbalance, table alignment, or worn bearings could be a possible contributor to these surface imperfections. A vibration test was therefore performed on the spintable to evaluate its dynamic characteristics and to compare these with similar measurements made on the table on 31 May 1961.

Velocity pickups were mounted at the top rim of the mold at the 10-ft diameter, and at the upper rim of the spintable at the 8-ft diameter. Each of these two locations had vertical, tangential, and radial pickups. Their arrangement is shown in Figure G-1. The assembly was dynamically balanced with lead shot to compensate for the integrated power-amplifier package. Balancing was accomplished to within .001-in. vertical and .004-in. radial which is equivalent to the dial indicator readings obtained on the 5th pour at 16 rpm. The transducers used were of the velocity type, manufactured by C.E.C., Model 4-102A in order to obtain the necessary sensitivity required. Recordings were made on a C.E.C. Model 124 direct readout oscillograph. The overall system sensitivity which includes transducers, amplifiers and galvanometers was .002 inches per second at maximum gain setting.

Since measurements were made of the spinning mass, the recorder was placed in the center of the mold cover to allow it to be turned on and off, and the amplifiers

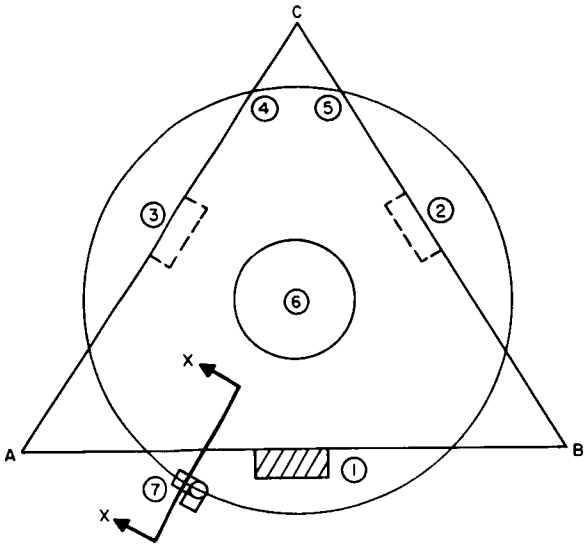

(1) 85-LB AMPLIFIER LOCATED AT CENTER OF SIDE A-B.

(2) 90-LB LEAD SHOT LOCATED IN CENTER CAVITY OF SUPPORT STRUCTURE CHANNEL.

(3) 90-LB LEAD SHOT LOCATED IN CENTER CAVITY OF SUPPORT STRUCTURE CHANNEL.

(4) 15-LB LEAD SHOT LOCATED BETWEEN BRACKET AND CORNER OF SUPPORT STRUCTURE.

(5) 15-LB LEAD SHOT LOCATED BETWEEN BRACKET AND CORNER OF SUPPORT STRUCTURE.

(6) 25-LB OSCILLOGRAPH RECORDER LOCATED AT CENTER OF SPINTABLE.

(7) VELOCITY PICKUPS.

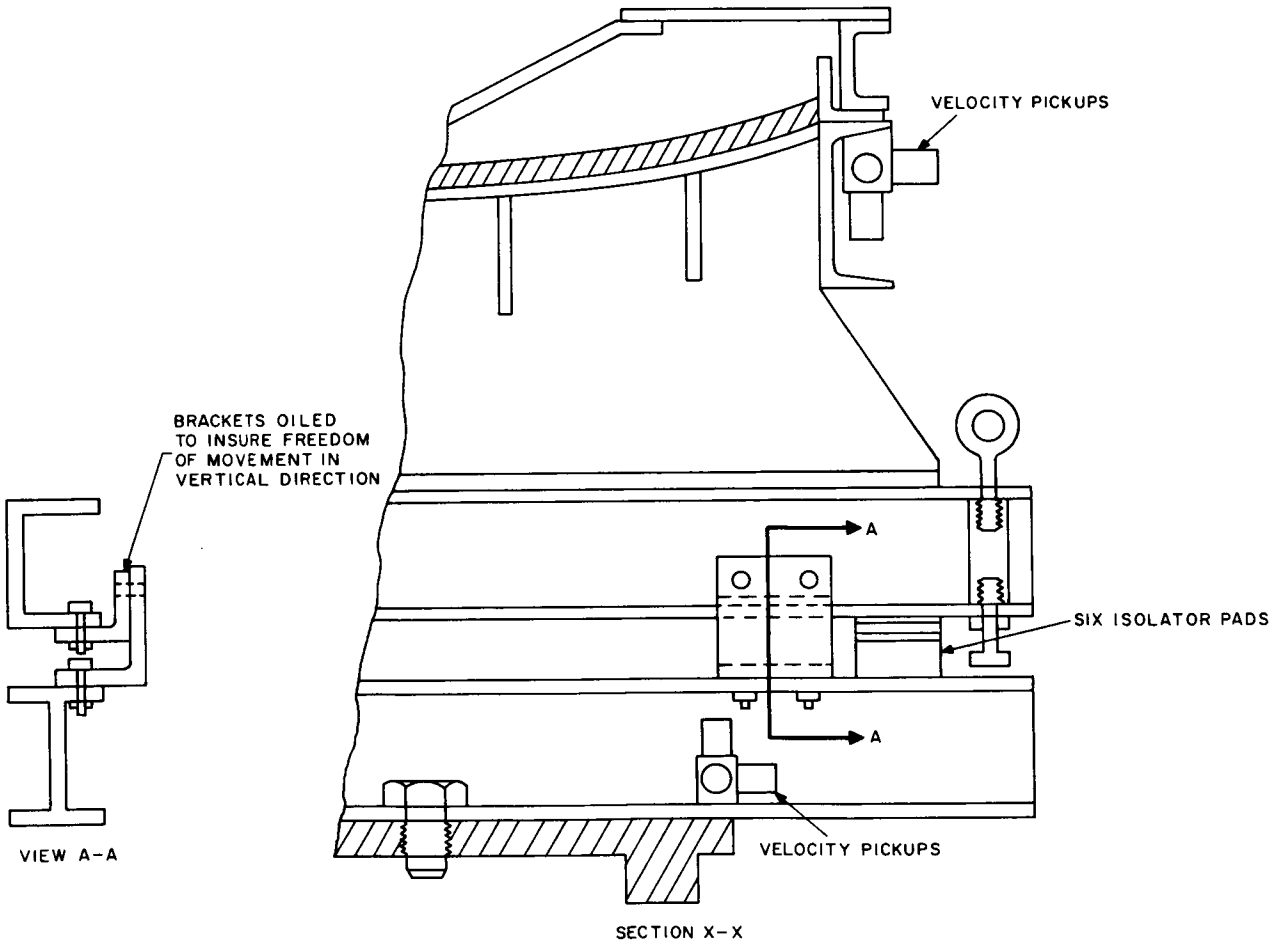

Figure G-1. Component Location for Spintable Vibration Measurements

were placed on the table. This created an unbalance in the system which was corrected by placing shot bags on the table until the unbalance was equal to that when the actual castings were made.

Power was supplied to the recording equipment by slip rings mounted on the main support shaft. The velocity pickups were mounted in a triaxial configuration on the top rim of the mold at 10-ft diameter and on the upper rim of the spin table at 8-ft diameter. Each of these locations had a transducer mounted vertically, radially and tangentially.

The following readings were taken:

1. Steady state 16 rpm (3.752 seconds per revolution Potentiometer setting 754)
2. During speed variation from 16 to 16 1/2 rpm and from 16 to 15 1/2 rpm

   16.5 rpm (3.640 potentiometer setting 775)

   15.5 rpm (3.870 potentiometer setting 734)
3. Steady State
   a) 10 rpm (6.000) potentiometer setting 473)
   b) 20 rpm (3.000) potentiometer setting 926)
4. Two radial and two vertical dial indicators located 90 degrees apart were also recorded at the time of vibration readings.
5. All of the above readings were recorded with outboard rubber dampers in place. From previous run on 1/22/63 the outboard dampers reduced radial dial indicator deflection from .0043 max. to .0004 max. Radial indicators are accurate to .0001.
6. Outboard dampers were removed and readings were also taken at steady state conditions at 16 rpm before and after additional grease was applied to the table shaft lower bearing.
7. With the spintable at rest the system natural frequency was estimated by measuring the vibrations caused when striking the table with a rubber mallet in an upward vertical direction at:
   a) the lower flange of the mold channel at the 10 foot diameter
   b) the bottom rim of the spintable at its eight foot diameter

Both mold and table rims were struck diametrically opposite to the velocity pickups. The outboard dampers were removed before these readings were taken.

The first series of runs were made without modification to the system, i.e., under the same conditions that existed when the castings were made. Recordings were taken at 10 rpm, 16 rpm, and 20 rpm steady state and during changes from 16 to 15.5 rpm and 16.5 rpm. All data was recorded with the outboard dampers installed except at 16 rpm where a second record was made with the outboard dampers removed.

It was noted from the records that the mold consistently exhibited frequencies of approximately 45 cps vertically and between 8 to 13 cps radially and tangentially. In an endeavor to determine the origin of this excitation, the resonant frequencies of the table and mold were found by striking each with a rubber hammer and recording the die-away frequencies. This information showed that the exciting frequencies were not those of the natural frequencies of the table or mold. It was then decided to run a vibration check on the bearings and to determine the mold-cover frequencies. As a result of these tests, it was determined that the lower frequencies from 8 to 13 cps were generated in the bearings and the higher frequency of approximately 45 cps was generated in the mold cover.

After analysis of the data it was decided to try to isolate the 45 cps frequency through the use of 6 isolation points located approximately 18 inches in from the corner points of the triangular structure connecting the mold to the table. Four layers of 5/16 inch isomode pad 3 x 3, separated by a .032-inch aluminum plate, providing about .25 inch static displacement were used at each point. The corresponding natural frequency of the suspension system was 6 cps.

After completing a run with the centering pin still in place, it was noted from the records that the frequencies and amplitudes on the mold were approximately the same and that the isolation system was ineffective because the centering pin provided a mechanical coupling between the table and the mold.

With the centering pin removed, another run was made and the records showed that the vertical frequency of 45 cps was effectively isolated. The vertical frequency was changed to approximately 13 cps which was generated by the bearings. However, it was noted that the tangential frequency of the mold changed from approximately 13 cps to 30 cps. This can be explained as a torsional resonance of the mold due to the coupling between the triangular structures by the clip angles.

Complete results of all runs are shown in Tables G-1 through G-6.

TABLE G-1. SPINTABLE VIBRATION RESULTS (WITH DAMPERS)

Table Speed (rpm)	Vibration Data			Pickup Location	Pickup Direction	Remarks
	Frequency (cps)	Displacement (μ in. D.A.)	Acceleration (g, O-P)			
10	11.0	307	.0019	Mold	RAD	
	8.6	559	.0021		TANG	
	11.2	355	.0023		VERT	Without
	45.0	116	.0120		VERT	Isomodes
	75.0	6	.0017	Table	RAD	
	8.1	279	.0009		TANG	
	11.2	247	.0016		VERT	
	95.0	27	.0126		VERT	
10	11.7	250	.0017	Mold	RAD	
	11.0	286	.0018		TANG	
	42	54	.0048		TANG	With Isomodes.
	42	126	.0113		VERT	Centering Pin
	50	12	.0015	Table	RAD	Installed
	8.2	284	.0010		TANG	
	50	54	.0069		VERT	
16	10.4	282	.0016	Mold	RAD	
	12	348	.0025		TANG	
	45	150	.0150		VERT	Without
	73	21	.0057	Table	RAD	Isomodes
	13.8	92	.0009		TANG	
	95	48	.0223		VERT	

TABLE G-1. SPINTABLE VIBRATION RESULTS (WITH DAMPERS)(Continued)

Table Speed (rpm)	Vibration Data			Pickup Location	Pickup Direction	Remarks
	Frequency (cps)	Displacement (μ in. D.A.)	Acceleration (g, O-P)			
16	10.5	152	.0009	Mold	RAD	
	50	40	.0050		RAD	
	13	274	.0023		TANG	With Isomodes.
	50	140	.0178		VERT	Centering Pin
	50	22	.0028	Table	RAD	Installed
	13.2	140	.0012		TAN	
	50	74	.0094		VERT	
16	11.1	288	.0018	Mold	RAD	
to	11.9	358	.0026		TANG	
15.5	45.0	238	.0246		VERT	Without
	95.0	13	.0060	Table	RAD	Isomodes
	13.3	79	.0007		TANG	
	95.0	25	.0117		VERT	
16	10.4	272	.0015	Mold	RAD	
to	12.5	264	.0021		TANG	
16.5	45.0	158	.0163		VERT	Without
	74.0	18	.0050	Table	RAD	Isomodes
	13.9	102	.0010		TANG	
	95.0	38	.0175		VERT	
20	9.8	299	.0015	Mold	RAD	
	65.0	47	.0102		RAD	
	33.0	196	.0109		TANG	Without
	52.0	140	.0194		VERT	Isomodes
	95.0	20	.0092	Table	RAD	
	30.0	104	.0048		TANG	
	95.0	76	.0351		VERT	
20	10.3	208	.0012	Mold	RAD	
	35	154	.0097		TANG	
	35	176	.0111		VERT	With Isomodes.
	90	14	.0057	Table	RAD	Centering Pin
	35	71	.0045		TANG	Installed
	90	52	.0218		VERT	

TABLE G-2. SPINTABLE VIBRATION RESULTS (WITHOUT DAMPERS)

Table Speed (rpm)	Vibration Data			Pickup Location	Pickup Direction	Remarks
	Frequency (cps)	Displacement (μ in. D.A.)	Acceleration (g, O-P)			
10	12.2	132	.0010	Mold	RAD	Centering
	12.2	320	.0024		TANG	Pin
	30	158	.0072		TANG	Retracted
	30	100	.0046		VERT	
	30	32	.0015	Table	RAD	Without
	12.2	152	.0012		TANG	Isomodes
	30	66	.0030		TANG	
	30	128	.0059		VERT	
10	7.8	314	.0010	Mold	RAD	Centering Pin
	8.2	428	.0015		TANG	Retracted,
	30	146	.0067		TANG	
	12.4	162	.0013		VERT	Isomodes
	30	100	.0046		VERT	Installed,
	35	24	.0015	Table	RAD	
	8.2	268	.0009		TANG	Mold
	30	56	.0026		TANG	Cover
	35	70	.0043		VERT	Removed
16	17.5	86	.0013	Mold	RAD	Centering Pin
	30	140	.0064		TANG	Retracted,
	12.8	208	.0017		VERT	Isomodes
	35	24	.0015	Table	RAD	Installed,
	13	136	.0012		TANG	Mold Cover
	40	72	.0059		VERT	Removed.
16	18.7	78	.0012	Mold	RAD	Centering Pin
	30	164	.0075		TANG	Retracted,
	13.5	184	.0017		VERT	Isomodes
	31	36	.0018	Table	RAD	Installed.
	13.3	106	.0010		TANG	
	30	112	.0052		TANG	
	37	118	.0083		VERT	
16	18.2	86	.0015	Mold	RAD	Centering Pin
	30	140	.0065		TANG	Retracted,
	13.6	264	.0025		VERT	Isomodes
	30	30	.0014	Table	RAD	Installed
	13.1	140	.0012		TANG	
	33	132	.0074		VERT	

TABLE G-2. SPINTABLE VIBRATION RESULTS (WITHOUT DAMPERS) (Continued)

Table Speed (rpm)	Vibration Data			Pickup Location	Pickup Direction	Remarks
	Frequency (cps)	Displacement (μ in. D.A.)	Acceleration (g, O-P)			
16	19.5	104	.0020	Mold	RAD	Centering Pin
	17.7	198	.0032		TANG	Retracted,
	42	150	.0135		VERT	Without
	75	20	.0055	Table	RAD	Isomodes
	16.6	90	.0013		TANG	
	70	56	.0141		VERT	
16	50	26	.0033	Mold	RAD	
	13.1	214	.0019		TANG	With Isomodes,
	42	172	.0150		VERT	Centering Pin
	60	20	.0037	Table	RAD	Installed
	13.3	138	.0012		TANG	
	50	78	.0099		VERT	
16	18.9	130	.0024	Mold	RAD	Bearings
	13.3	237	.0021		TANG	Repacked,
	45.0	154	.0160		VERT	Without
	45.0	18	.0019	Table	RAD	Isomodes
	13.6	77	.0007		TANG	
	95.0	32	.0147		VERT	
16	18.9	145	.0026	Mold	RAD	
	75.0	29	.0084		RAD	
	17.4	210	.0033		TANG	
	45.0	228	.0236		VERT	Without
	75.0	18	.0051	Table	RAD	Isomodes
	13.3	43	.0004		TANG	
	95.0	17	.0078		TANG	
	95.0	43	.0198		VERT	

TABLE G-3. SPINTABLE BEARING VIBRATION CHECK (WITHOUT DAMPERS)

Table Speed (rpm	Vibration Data: Frequency (cps)	Displacement (μ in. D.A.)	Acceleration (g, O-P)	Pickup Location	Pickup Direction	Remarks
10	8.2	78	.0003	Upper Bearing	RAD	Not Isolated with Isomode
	No Measurable Vibration				TANG	
	No Measurable Vibration				VERT	
	8.2	162	.0006	Lower Bearing	RAD	
	8.1	140	.0005		TANG	
	No Measurable Vibration				VERT	
16	No Measurable Vibration			Upper Bearing		Not Isolated with Isomode
	12.4	54	.0004	Lower Bearing	RAD	
	8.4	54	.0003		TANG	
	No Measurable Vibration				VERT	
20	16.6	26	.0004	Upper Bearing	RAD	Not Isolated with Isomode
	No Measurable Vibration				TANG	
	No Measurable Vibration				VERT	
	11.9	56	.0004	Lower Bearing	RAD	
	7.95	116	.0004		TANG	
	15.6	22	.0003		VERT	

TABLE G-4. IMPACT ON MOLD

Freq. No. 1 (cps)	Freq. No. 2 (cps)	Pickup Location	Pickup Direction
365	19.6	Mold	RAD
400	26.7		TANG
308	19.5		VERT
218	80	Table	RAD
368	228		TANG
216	71		VERT

TABLE G-5. COVER FREQUENCIES DUE TO IMPACT

23 cps 48.6 cps 50 cps 89 cps 430 cps	Accelerometer in Center
38 cps 101 cps 116 cps	Accelerometer on Outer Panel
25.6 cps 152 cps 202 cps	Accelerometer on Outer Panel IXI Aluminum Bar Taped Across Panel

TABLE G-6. DIAL INDICATOR READINGS

Indicator No.	Dial Indicator Readings - Maximum per Revolution			
	With Outboard Dampers			Without Dampers
	RPM			RPM
	10	16	20	16
1 Vertical	.0002	.0004	.0004	.0008
3 Radial	.0004	.0008	.0007	.0025
2 Vertical	.0001	.0002	.0002	.001
4 Radial	.0004	.0008	.0007	.003

Note: Indicators No. 1 and 3 were at same location, 2 and 4 were at same location and 90^{o} away from 1 and 3.
Indicators 1 and 2 read in .001 increments.
Indicators 3 and 4 read in .0001 increments.

Since the spintable bearings are a possible source of excitation for the rotating system, the bearing vendor (SKF Industries, Inc., Philadelphia, Pa.) was consulted; his conclusions were:

a. The capacity of the bearings is greatly in excess of the load applied.

b. The estimated 1000 hours of total spintable operation would not produce any noticeable wear in the bearings.

c. Based on a summary of the GE vibration data, the bearings in the spintable are sound.

The vendor suggested that we measure the actual run-out of the table spindle. He pointed out that this run-out is largely determined by the spherical roller bearing, not the thrust bearings (see Figure 5.2-1). The radial tolerances of this bearing are listed below for both standard and Class C-2 grades.

Bearing Class	Radial Looseness (inch)	Maximum Run-out (inch)	Maximum Total Radial Play (inch)
Standard	.0058-.0087	.0020	.0107
Class C-2	.0035-.0060	.0020	.0080

The vendor stressed, however, that it was unlikely that the total maximum radial play was actually present in the spindle, and it was suggested that the actual value be measured and that the bearings be preloaded by a few thousand pounds in order to eliminate any radial motion of the upper thrust bearing. In this manner it may be possible to have all the radial load (which should be small) carried by the two thrust bearings and have the spherical roller bearing coast along.

The alignment and run-out of the spintable shaft was checked. The spintable shaft was aligned in a vertical plane within .002 full indicator reading (FIR) run-out for one full 360^{o} revolution. Repeat measurements were made with a precision machinist's level (.0005 in. per foot graduations) placed at the outer periphery of the 8-foot table diameter.

The runout of the spintable shaft as measured near the sliprings with a dial indicator was .0003 FIR maximum.

Thus, there was no need to follow SKF's suggestion and increase the bearing preload. Based on vibration and run-out data and the vendor's evaluation it was decided to leave the bearings unchanged. The possibility of bearing excitations causing vibrations of the rotating system, however, was not ruled out.

Consideration of the formation of radial ripples in the spin castings beads leads immediately to consideration of torsional oscillation or flow characteristics since either vertical or radial excitation would result in circumferential waves. Flow characteristics would result in spiral waves as the fluid flows out from the center of the mold, but the deviation due to spurious forces of the waves from pure radial motion would be slight at the rotational speeds used in the spincasting process. The primary effort undertaken was to see if a standing wave could be generated in a circular enclosure due to a rotational oscillation of the mold. This is analogous to the wave in a rectangular enclosure such as a cake pan if the pan is caused to oscillate along its long axis.

Summary of the data obtained from velocity pickups mounted on the mold and on the spintable indicated strong tangential velocity oscillation at 13 cps for the 16 RPM spintable speed. This fostered an effort to see if an expression for a standing wave could be found which would show a correlation with the 13 cps velocity variation; i.e.,

$$\frac{\text{circumferential velocity}}{\text{wave length}} = 2\pi f \text{ or some integral multiple of } 2\pi f.$$

Before analytical expression could be developed, it was demonstrated experimentally that radial waves could be formed by introducing a tangential excitation. No further analytical effort was expended to obtain a correlation between wave length and excitation frequency because it was concluded that the possibility of wave formation resulting from high frequency rotational speed variations had been adequately substantiated.

Considering that the tangential oscillations caused the radial waves observed in the castings, two forms of solution were possible: 1) revise the mold configuration so that the observed wave lengths cannot be supported or 2) reduce or eliminate the excitation.

The first approach was indicated by the feeling that, if the continuity of the circular path in which the waves are formed were broken up, the waves could not be supported. This approach was rejected because it would likely lead to extensive and time consuming experimentation to arrive at a suitable mold shape.

The second solution appeared more feasible. Elimination of the excitation was first considered. Examination of the test data indicated that the frequency of the significant excitation was approximately 13 cps at 16 rpm, and 8 cps at 10 rpm. One would expect that at 20 rpm the excitation would appear at about 16 cps; however, there appeared a doubling of the frequency to the neighborhood of 32 cps at 16 rpm. The nature of the measured response indicated that it was not a torsional structural mode of the system. If it were one would expect that, when any excitation was present near the natural frequency of the system, a large response would be exhibited but the level of response would be significantly reduced at off-resonance conditions. The data indicated no significant change in response level over the range of frequencies observed. The conclusion was drawn that the excitation was delivered by mechanical operation of the system not significantly amplified by the structure. The possible sources appeared to be (1) the bearings, (2) the speed reduction system or (3) the motor.

Test results from the bearings indicated measurable but very low motion in the tangential direction. Only the 8 cps component showed in the tangential direction at any speed. No other frequency component was measurable. This appeared to eliminate the bearings as a possible source of excitation.

The drive motor was reasonably well isolated from the actual rotating mass by a belt and was therefore unlikely as the source of the troublesome excitation.

The probably source was the speed reduction system. To eliminate excitation from this source would require an extensive experimental program and a possible change in the mechanism itself. Additional torsional flexibility between the speed reducer

and the table or a revision of the drive system to drive through a belt selected for isolation characteristics might have helped. However, work on these lines would be both time-consuming and expensive. The most straightforward approach was to attempt to reduce the effective speed fluctuation by significantly increasing the rotatory moment of inertia of the rotating system. Thus although the exciting forces remain at the same level, the resulting motion is reduced in level due to the increase in inertia.

It was therefore decided to mount a four-truss, 30-foot structure onto the spintable which would increase the rotatory moment of inertia of the assembly by eight. This structure had been used to support the female masters for the GE space simulator mirrors during spincasting. It was thus readily available.

The JPL master and its support structure was removed from the spintable, the truss structure was mounted on the spintable, and the 9-1/2-foot master and support structure mounted on it. Details of the mounting system are shown in Figure 5.2-12. Vibration measurements were repeated after this installation was completed.

The overall vibration level on the mold was improved. The 7.6 cps radial response was eliminated. The 13 cps tangential vibration noted on the original configuration was also eliminated and replaced by a 40 cps response. Not only is the tangential change of response an improvement on the basis of amplitude of vibration, but also on the basis of duration of time occurrence. Where the 13 cps vibration was essentially continuous, the 40 cps response existed generally less than 0.5 second at a given time. The vertical response of the mold was unchanged. The amplitude of vibration of the table was improved with exception of the radial response which remained the same.

As a result of the overall improvement of the mold vibration amplitude and especially the elimination of the tangential 13 cps, there was a high probability that additional spincastings could be formed without radial ripples.

APPENDIX H
OPTICAL INSPECTION DATA THIRD AND EIGHTH SPINCAST COAT

APPENDIX H

THIRD AND EIGHTH SPINCAST COAT OPTICAL INSPECTION DATA

Tables H-1 and H-2 show the optical inspection data of the third spincast pour. Tables H-3 through H-7 show the optical inspection data for the eighth spincast pour before and after thermal curing.

TABLE H-1. OPTICAL INSPECTION OF THIRD SPINCAST COAT (RETICLE READINGS)

Angular Station		Telescope Number							
		1	2	3	4	5	6	7	8
A-1	X	120	80	49	50	55	54	50	50
	Y	18	50	44	85	45	45	49	45
A-2	X	120	76	51	52	55	53	52	48
	Y	20	50	40	82	44	44	44	40
A-3	X	120	82	53	52	55	53	53	47
	Y	20	48	40	80	43	43	45	43
A-4	X	120	90	51	50	57	55	53	49
	Y	20	50	40	82	44	45	46	40
B-1	X	120	88	50	49	55	53	50	49
	Y	20	50	45	85	49	50	53	51
B-2	X	120	87	46	45	51	46	45	40
	Y	20	51	45	85	46	49	47	45
B-3	X	110	83	45	45	49	47	45	40
	Y	20	49	40	83	44	43	45	42
B-4	X	120	88	46	45	51	49	47	45
	Y	20	49	38	77	37	40	41	40
C-1	X	120	88	49	47	55	53	49	49
	Y	20	50	40	80	38	40	40	37
C-2	X	120	88	51	50	55	54	54	47
	Y	20	50	40	80	43	44	45	40
C-3	X	120	90	52	55	55	55	55	48
	Y	20	51	45	85	45	46	50	45
C-4	X	120	90	51	51	56	54	50	47
	Y	20	51	47	85	48	50	50	46

Notes: For locations of measured points see Figure 5.5-4.
For general arrangement of inspection system see Figure 5.5-5.

TABLE H-2. OPTICAL INSPECTION OF THIRD SPINCAST COAT.
SLOPE ERRORS (SECONDS OF ARC)

Angular Station	Telescope Number							
	1	2	3	4	5	6	7	8
A-1	-	-	25	0	35	35	0	25
A-2	-	20	50	28	38	34	22	51
A-3	-	14	53	10	43	38	29	38
A-4	-	50	50	15	46	35	25	50
B-1	-	40	25	5	25	15	15	6
B-2	-	35	32	25	20	20	29	56
B-3	50*	16	56	27	30	38	45	64
B-4	-	40	63	47	65	50	47	56
C-1	-	40	50	29	65	52	50	65
C-2	-	40	50	25	43	30	32	52
C-3	-	50	27	25	35	32	25	26
C-4	-	50	16	5	31	20	0	25

*Approximate reading

MEDIAN: 35

Notes: For locations of measured points see Figure 5.5-4.
For general arrangement of inspection system see Figure 5.5-5.

TABLE H-3. OPTICAL INSPECTION OF EIGHTH SPINCAST COAT BEFORE THERMAL CURE. RETICLE READINGS

Angular Station		Telescope Number 1	2	3	4	5	6	7	8
A-1	X	56	60	55	55	52	48	48	48
	Y	42	46	43	44	50	52	52	56
A-2	X	55	52	52	51	49	48	48	46
	Y	45	46	46	53	50	50	49	49
A-3	X	52	52	50	46	48	48	50	48
	Y	47	46	45	42	43	44	44	42
A-4	X	52	50	52	54	52	51	55	52
	Y	46	48	46	46	45	45	42	38
B-1	X	52	52	52	52	53	55	56	54
	Y	44	48	49	46	50	54	52	52
B-2	X	50	50	48	48	48	46	46	44
	Y	44	45	48	47	50	54	52	52
B-3	X	52	50	47	47	44	42	44	43
	Y	44	44	42	41	42	44	43	42
B-4	X	55	56	54	55	54	53	53	50
	Y	41	40	39	36	40	38	36	34
C-1	X	58	62	60	60	57	59	58	56
	Y	40	40	40	40	44	45	46	42
C-2	X	60	62	56	58	54	54	51	46
	Y	40	42	42	42	48	47	46	47
C-3	X	62	64	56	60	57	56	56	56
	Y	42	45	44	41	43	43	42	38
C-4	X	62	64	60	65	63	62	60	58
	Y	45	48	45	45	50	50	44	44

Notes: For locations of measured points, see Figure 5.5-4.
For general arrangement of inspection system, see Figure 5.5-5.

TABLE H-4. OPTICAL INSPECTION OF EIGHTH SPINCAST COAT BEFORE THERMAL CURE. SLOPE ERRORS (SECONDS OF ARC)

Angular Station	Telescope Number							
	1	2	3	4	5	6	7	8
A-1	47	50	43	40	5	14	14	26
A-2	35	22	22	16	5	7	11	21
A-3	16	22	25	40	36	31	30	36
A-4	17	5	21	28	27	26	47	56
B-1	31	14	11	17	15	32	26	21
B-2	25	25	14	17	10	24	22	32
B-3	26	30	38	47	50	50	43	53
B-4	52	54	57	70	20	62	72	80
C-1	62	71	67	67	43	47	45	46
C-2	67	63	46	50	22	24	22	24
C-3	69	70	42	63	50	46	46	63
C-4	65	72	52	80	65	60	56	50

MEDIAN: 35

Notes: For locations of measured points, see Figure 5.5-4.
For general arrangement of inspection system, see Figure 5.5-5.

TABLE H-5. OPTICAL INSPECTION OF EIGHTH SPINCAST COAT AFTER THERMAL CURE. (RETICLE READINGS)

Angular Station		Telescope Number							
		1	2	3	4	5	6	7	8
A-1	X	50	50	59	53	50	45	44	50
	Y	45	50	49	50	50	51	52	54
A-2	X	48	47	44	48	45	39	33	43
	Y	40	43	42	43	44	43	42	44
A-3	X	45	48	48	47	48	43	37	45
	Y	38	38	35	35	37	32	28	27
A-4	X	50	50	50	53	53	47	47	51
	Y	35	37	33	33	35	32	28	25
B-1	X	35	50	50	54	52	48	49	51
	Y	48	37	35	38	39	40	40	43
B-2	X	49	49	46	49	44	40	36	45
	Y	33	36	36	41	43	42	42	42
B-3	X	50	49	44	44	45	38	35	47
	Y	32	33	32	33	34	33	28	32
B-4	X	52	52	50	52	52	45	43	50
	Y	32	32	29	28	30	27	24	28
C-1	X	55	58	57	57	55	48	50	53
	Y	34	33	31	33	37	37	35	36
C-2	X	59	58	55	57	50	44	44	52
	Y	36	37	38	38	40	38	40	41
C-3	X	59	58	56	56	59	49	48	62
	Y	37	43	48	40	42	37	34	33
C-4	X	55	56	55	58	57	50	50	62
	Y	42	48	44	45	46	44	40	40

Notes: For locations of measured points, see Figure 5.5-4.
For general arrangement of inspection system, see Figure 5.5-5.

TABLE H-6. OPTICAL INSPECTION OF EIGHTH SPINCAST COAT AFTER THERMAL CURE. RAW MEASURED SLOPE ERRORS (SECOND OF ARC)

Angular Location	Telescope Number							
	1	2	3	4	5	6	7	8
A-1	25	0	7	15	0	26	32	20
A-2	51	38	50	36	38	66	94	46
A-3	64	61	76	77	66	96	128	117
A-4	75	65	85	87	77	91	111	126
B-1	76	65	75	63	56	51	50	35
B-2	85	70	72	45	46	64	80	47
B-3	90	85	95	91	83	104	133	91
B-4	90	90	105	110	100	117	134	140
C-1	83	93	101	91	42	66	75	72
C-2	83	76	65	68	50	66	58	46
C-3	79	52	32	58	60	65	81	104
C-4	47	51	39	47	40	30	50	78

MEDIAN: 66

Notes: For locations of measured points, see Figure 5.5-4.
For general arrangement of inspection system, see figure 5.5-5.

TABLE H-7. OPTICAL INSPECTION OF EIGHTH SPINCAST COAT AFTER THERMAL CURE
ADJUSTED SLOPE ERRORS (SECONDS OF ARC)

Angular Location	Telescope Number							
	1	2	3	4	5	6	7	8
A-1	35	60	55	63	60	68	74	80
A-2	11	27	32	26	32	55	82	42
A-3	20	5	15	18	7	42	78	58
A-4	16	7	26	32	25	32	51	66
B-1	86	7	16	25	16	11	10	27
B-2	25	10	18	15	35	49	68	28
B-3	30	25	39	35	28	60	86	32
B-4	33	33	45	52	43	59	76	50
C-1	42	52	53	47	30	7	16	22
C-2	51	45	30	40	11	25	27	21
C-3	50	51	61	36	54	5	20	70
C-4	36	61	42	57	57	30	11	66

MEDIAN: 35

Notes: For locations of measured points, see Figure 5.5-4.
For general arrangement of inspection system, see Figure 5.5-5.

APPENDIX J
FINAL (10TH) SPINCAST COAT OPTICAL INSPECTION DATA

APPENDIX J

FINAL (10th) SPINCAST COAT OPTICAL INSPECTION DATA

Tables J-1 through J-5 show the data for the first and second optical inspections of the final spincast coat.

TABLE J-1. FIRST OPTICAL INSPECTION OF FINAL SPINCAST COAT RETICLE READINGS

Angular Station		Telescope Number							
		1	2	3	4	5	6	7	8
A-1	X	24	53	38	60	54	52	54	60
	Y	50	50	56	51	56	52	56	54
A-2	X	23	50	33	51	48	47	54	53
	Y	57	56	55	53	61	59	60	60
A-3	X	25	53	35	60	55	49	53	58
	Y	62	60	60	52	60	55	56	53
A-4	X	21	51	35	56	50	53	51	62
	Y	66	62	61	50	55	56	55	51
B-1	X	15	50	34	56	50	49	52	54
	Y	65	61	63	61	65	64	67	67
B-2	X	09	43	24	47	35	37	42	44
	Y	67	66	70	64	70	67	70	69
B-3	X	12	40	20	39	35	38	40	44
	Y	64	64	65	56	59	57	68	59
B-4	X	15	40	25	48	40	40	45	45
	Y	60	60	60	50	52	50	50	50
C-1	X	15	42	30	50	45	43	40	54
	Y	60	58	58	52	58	54	60	58
C-2	X	15	41	25	55	40	36	47	50
	Y	50	51	50	55	50	51	50	50
C-3	X	22	42	27	42	42	41	52	56
	Y	50	50	48	40	46	43	45	45
C-4	X	25	50	35	51	50	48	48	62
	Y	51	51	50	42	47	42	44	43

Notes: For locations of measured points, see Figure 5.5-4.
For general arrangement of inspection system, see Figure 5.5-5.

TABLE J-2. FIRST OPTICAL INSPECTION OF FINAL SPINCAST COAT. RAW MEASURED SLOPE ERRORS (SECONDS OF ARC)

Angular Location	Telescope Number							
	1	2	3	4	5	6	7	8
A-1	130	15	62	50	33	14	36	53
A-2	138	30	58	16	56	48	53	52
A-3	138	52	90	51	56	26	33	42
A-4	170	61	92	52	25	33	26	60
B-1	197	55	103	52	72	71	85	87
B-2	220	87	163	72	124	107	107	100
B-3	202	85	168	57	87	69	103	53
B-4	181	71	134	10	78	50	25	25
C-1	181	56	107	10	47	40	71	44
C-2	175	46	125	35	50	71	15	0
C-3	140	40	104	64	44	57	27	38
C-4	125	5	75	41	15	42	31	69

MEDIAN: 59

Notes: For locations of measured points, see Figure 5.5-4.
For general arrangement of inspection system, see Figure 5.5-5.

TABLE J-3. FIRST OPTICAL INSPECTION OF FINAL SPINCAST COAT. ADJUSTED SLOPE ERRORS (SECONDS OF ARC)

Angular Location	Telescope Number							
	1	2	3	4	5	6	7	8
A-1	95	63	20	94	18	54	60	90
A-2	95	40	45	47	39	29	63	59
A-3	90	58	40	93	68	35	55	82
A-4	115	54	43	73	40	55	45	103
B-1	142	47	53	74	60	53	75	80
B-2	174	50	105	47	86	60	106	66
B-3	155	41	120	15	38	5	61	18
B-4	137	22	97	42	32	32	34	34
C-1	137	10	61	45	18	11	22	61
C-2	139	25	90	82	32	39	39	50
C-3	105	30	85	80	50	65	66	70
C-4	89	47	46	83	60	76	65	119

MEDIAN: 59

Notes: For locations of measured points, see Figure 5.5-4.
For general arrangement of inspection system, see Figure 5.5-5.

TABLE J-4. SECOND OPTICAL INSPECTION OF FINAL SPINCAST COAT. RETICLE READINGS

Angular Station		Telescope Number							
		1	2	3	4	5	6	7	8
A-1	X	31	60	43	68	60	58	60	62
	Y	50	49	50	38	45	46	47	48
A-2	X	32	52	42	60	58	56	58	58
	Y	46	43	50	45	50	42	46	46
A-3	X	31	52	36	58	60	52	56	62
	Y	43	43	48	35	40	40	37	38
A-4	X	32	58	45	62	61	63	58	68
	Y	49	44	42	30	38	33	35	35
B-1	X	30	60	50	70	63	62	65	65
	Y	45	50	50	40	50	45	45	44
B-2	X	28	57	42	60	52	55	55	57
	Y	50	45	50	44	50	50	50	50
B-3	X	30	55	37	55	52	53	58	58
	Y	45	42	46	38	45	40	40	42
B-4	X	35	55	43	62	58	60	61	62
	Y	50	45	42	30	35	35	35	35
C-1	X	35	63	50	70	64	70	65	63
	Y	50	45	50	38	48	40	43	42
C-2	X	35	58	45	60	57	55	60	62
	Y	50	45	52	43	50	47	50	50
C-3	X	35	57	42	55	58	53	65	68
	Y	51	46	50	43	47	42	42	44
C-4	X	35	53	42	56	56	56	58	68
	Y	56	45	50	36	43	42	42	44

Notes: For locations of measured points, see Figure 5.5-4.
For general arrangement of inspection system, see Figure 5.5-5.

TABLE J-5. SECOND OPTICAL INSPTECTION OF FINAL SPINCAST COAT. ADJUSTED SLOPE ERRORS (SECONDS OF ARC)

Angular Location	Telescope Number 1	2	3	4	5	6	7	8
A-1	119	46	63	76	30	22	34	45
A-2	110	11	67	30	36	14	22	22
A-3	115	11	92	49	36	22	36	50
A-4	112	20	46	81	46	71	49	83
B-1	120	42	36	80	54	40	55	55
B-2	133	16	67	30	32	30	30	34
B-3	120	11	86	30	11	21	28	22
B-4	100	7	56	45	49	54	57	60
C-1	100	46	36	85	54	80	55	46
C-2	100	21	60	30	34	16	42	50
C-3	101	18	67	7	25	11	56	70
C-4	112	7	67	41	11	15	22	70

MEDIAN: 46

Notes: For locations of measured points, see Figure 5.5-4.
For general arrangement of inspection system, see Figure 5.5-5.

APPENDIX K
MIRROR OPTICAL INSPECTION DATA

APPENDIX K

MIRROR OPTICAL INSPECTION DATA

Tables K-1 through K-5 show the optical inspection data of the mirror.

TABLE K-1. OPTICAL INSPECTION OF MIRROR (RETICLE READINGS IN UNITS OF TEN DIVISIONS)

Angular Station		Telescope Number 1	2	3	4	5	6	7	8
A-1	X	5	3	5	5	1	-	-	-
	Y	1	5	5	4	2	-	-	-
A-2	X	0	3	4	4	2	5	-	-
	Y	3	8	6	5	5	7	-	-
A-3	X	-	5	5	5	3	-	-	-
	Y	-	5	6	5	5	-	-	-
A-4	X	-	5	4	-	6	9	-	-
	Y	-	5	10	-	7	5	-	-
B-1	X	-	5	5	5	1	0	-	-
	Y	-	5	5	5	5	2	-	-
B-2	X	2	4	4	4	2	1	-	-
	Y	8	6	6	6	7	8	-	-
B-3	X	2	4	3	3	3	0	-	-
	Y	4	6	7	7	8	7	-	-
B-4	X	0	5	4	5	5	1	-	-
	Y	2	4	4	3	2	1	-	-
C-1	X	1	4	6	5	6	3	-	-
	Y	3	4	5	4	2	0	-	-
C-2	X	2	5	5	5	5	5	-	-
	Y	6	7	7	7	8	10	-	-
C-3	X	0	4	4	4	2	1	-	-
	Y	10	9	9	7	7	5	-	-
C-4	X	3	3	4	4	3	4	-	-
	Y	6	6	7	6	5	5	-	-

NOTES: For locations of measured points see Fig. 5.5-4.
For general arrangement of inspection system see Fig. 5.5-5.
Where a dash appears in the table, the center of the filament image appeared to lie outside the field of the telescope eyepiece.

TABLE K-2. OPTICAL INSPECTION OF MIRROR

ADJUSTED SLOPE ERRORS FROM RETICLE READINGS (SECONDS OF ARC)

Angular Station	Telescope Number 1	2	3	4	5	6	7	8
A-1	210	50	50	70	210	---	---	---
A-2	220	130	50	0	100	110	---	---
A-3	---	50	70	50	50	---	---	---
A-4	---	50	250	---	140	250	---	---
B-1	---	50	50	50	150	250	---	---
B-2	180	50	50	50	140	210	---	---
B-3	110	50	110	110	160	220	---	---
B-4	250	70	50	110	160	250	---	---
C-1	180	50	100	70	180	250	---	---
C-2	110	110	110	110	160	250	---	---
C-3	320	200	200	100	140	150	---	---
C-4	70	110	100	50	50	---	---	---

For locations of measured points see Fig. 5.5-4.

For general arrangement of inspection system see Fig. 5.5-1.

TABLE K-3. OPTICAL INSPECTION OF MIRROR

RETICLE READINGS AND SLOPE ERRORS IN OUTER QUARTER

Angular Station	Telescope Station 7			Telescope Station 8		
	10X	10Y	Slope Error (sec)	10X	10Y	Slope Error (sec)
A-1.95	8	5	150	4	1	205
A-2	9	5	200	6	2	158
A-2.8	10	4	275	4	4	71
A-3	10	1	320	10	0	354
A-4**						
B-1.95				10	10	354
B-2				9	8	250
B-3.3	8	5	150	5	6	150
B-3.5	8	2	212	3	2	180
C-2.9				0	1	320
C-3.7				7	7	141
C-4	10+	5	250+	*0-10	4	50(?)

* Image appeared from x = 0 to x = 10 at y = 4

** Area of anode dropped on female master

For locations of measured points see Figs. 5.5-4 and 7.7-1.

TABLE K-4. OPTICAL INSPECTION OF MIRROR

(THEODOLITE READINGS)

Angular Station	Telescope Station 7			Telescope Station 8		
	Theodolite Inclination	Theodolite Azimuth	Slope Error	Theodolite Inclination	Theodolite Azimuth	Slope Error
A-1	34'10"	230°	17'5"	43'20"	250°	21'40"
A-2	8'	135°	4'	13'	160°	6'30"
A-3	14'30"	210°	7'15"	13'50"	225°	6'55"
A-4*	9'	315°	4'30"	24'30"	180°	12'20"
B-1	27'	190°	13'30"	31'	180°	15'30"
B-2	17'30"	170°	8'45"	8'10"	90°	4'5"
B-3	18'30"	135°	9'15"	18'40"	135°	9'20"
B-4	31'	195°	15'30"	39'30"	200°	19'45"
C-1	36'40"	185°	18'20"	36'	180°	18'
C-2	24'50"	140°	12'25"	17'50"	120°	8'55"
C-3	17'	190°	8'30"	17'	190°	8'30"
C-4	16'30"	170°	8'15"	2'10"	90°	1'5"

For locations of measured points see Figs. 5.5-4 and 7.7-1.

* Location of anode dropped on female master.

Zero azimuth indicates a radially outward slope error,
180° azimuth indicates a radially inward slope error.

TABLE K-5. OPTICAL INSPECTION OF MIRROR

ADJUSTED SLOPE ERRORS (MINUTES)

Angular Stations	Telescope Number							
	1	2	3	4	5	6	7	8
A-1	3.5	0.8	0.8	1.2	3.5	3.25*	17.1*	21.7*
A-2	3.7	2.2	0.8	--	1.7	1.8	4.0*	6.5*
A-3	4.75*	0.8	1.2	0.8	0.8	1.75*	7.25*	6.9*
A-4**	11.75*	0.8	4.2	5.75*	2.3	4.2	4.5*	12.3*
B-1	5.7*	0.8	0.8	0.8	2.5	4.2	13.5*	15.5*
B-2	3.0	0.8	0.8	0.8	2.3	3.5	8.75*	4.1*
B-3	1.8	0.8	1.8	1.8	2.7	3.7	9.25*	9.3*
B-4	4.2	1.2	0.8	1.8	2.7	4.2	15.5*	19.75*
C-1	3.0	0.8	1.7	1.2	3.0	4.2	18.3*	18.0*
C-2	1.8	1.8	1.8	1.8	2.7	4.2	12.4*	8.9*
C-3	5.3	3.3	3.3	1.7	2.3	2.5	8.5*	8.5*
C-4	1.2	1.8	1.7	0.8	0.8	0	8.25*	1.1*

MEDIAN: 2.7

Notes: For locations of measured points see Fig. 5.5-4.

For general arrangement of inspection system see Fig. 5.4-5.

* These readings have not been adjusted for errors in the lateral focal point location (Section 5.5.1 (F)).

**Area of anode dropped on female master.

APPENDIX L
MISCELLANEOUS DATA SHEETS

APPENDIX L

MISCELLANEOUS DATA SHEETS

A copy of the thermal log recorded during cure of eighth coat is shown below and in Table L-1.

June 6, 1963

0945 Temperature in tent is 93°F

1020 Sealed Tent

1045 Lighted Salamander

1315 Heard audible crack from mold (sounded like light hammer blow)
Opened hole in curtain. Saw no visible signs of damage.

1400 Temperature in tent is 114F and 118F

1420 Temperature in tent is 115F and 118F

1520 Reached 120F air temperature
Thermocouple average reading 115F

1640 Heard audible crack
No visible crack

1930 Secured all heat and fans. Temperature in tent 120F.
Maximum thermocouple reading 123F. Building temperature 101F.

TABLE L-1. RECORDED TEMPERATURES (°F) DURING THERMAL CURE OF EIGHTH COAT

Date	Time	Inside Tent	Room Temp.	Thermocouple #2 Epoxy	#5 Epoxy	#06 Structure
6/6/63	10 00	98	100	94	96	96
		102				
	12 00	109	100	104	102	107
		112				
	14 00	114	100	111	108	113
	15 20	120				
	16 00	120	100	117	113	122
	18 00	121	100	120	115	122
	20 00	121	101	120	115	120
		114				
	22 00	112	100	116	114	115
	24 00	108	100	112	111	111
6/7/63						
	02 00	105	99	109	109	109
	04 00	101	98	104	104	104
	06 00	98	97	100	100	100
	08 00	96	96	98	98	98

A copy of the log kept during Pour No. 9 is shown below:

6/17/63 1104 hours - started to pour epoxy into mold

1106 hours - short duration thyratron tube flicker noticed just after pour started.

1150 hours - stopped pouring at 1500 strokes or nearly 14 gallons (13 gallons are equivalent to 1/4 inch thickness)

1755 hours - spintable drive motor ammeter reading dropped to zero, spintable starts to slow down.

1757 hours - spintable stopped rotation completely.

1805 hours - after performing several circuit checks, a fuse in the main table power supply circuit was found blown and it was replaced.

1805-1810 - standard spintable start-up procedure was used to initiate rotation of table.

1810 hours - table was made to spin overspeed at 3600 counts (3.600 seconds per revolution). After the table stopped the epoxy had receded approximately 8" from the outer periphery thereby visibly exposing the light colored aluminum sub-surface. The overspeed technique was used to accelerate the epoxy flow and hasten a return to conditions of equilibrium.

1835 hours - thyratron tube flicker observed and ammeter needle began fluctuating rapidly at a total variation of one ampere with table speed setting remaining at 3.600 seconds per revolution. An adjustment of 10 small divisions was made to reduce the potentiometer setting, thereby slowing down the table speed. This setting was held for one minute until the fluctuation stopped; the table speed was then returned to 3.600 seconds per revolution.

1910 hours - visual observation showed that the epoxy had recovered the aluminum in the outer 8" periphery of the mold; therefore the table speed was reset to and maintained at 3.747 to 3.757 seconds per revolution, the standard setting

6/19/63 0730 hours - the spintable was stopped approximately 43 hours after pouring was completed. Throughout the curing time the room temperature varied between 70 to 78°F, and the relative humidity varied from 51 to 78%.

A copy of the log kept during Pour No. 10 is shown below:

6/20/63 Small spintable leveled to 0.0008" T.I.R. at 5' diameter. Large spintable was out of level 0.006" T.I.R., and one adjustment on Leg #3 improved shaft vertical alignment to 0.002" T.I.R. at 8' dia. (large mold truss was leveled to within ±0.010 at 4 optical buttons)

1430 hours - hardener test port weight checks: 48.3 - 48.4 - 48.3 - 48.1 grams

1700 hours - separate weight checks with both test ports pumping simultaneously. hardener: 48.4 - 48.2 grams, resin 319.7 - 318.9 - 318.8 grams

$$\text{ratio} = \frac{48.3}{318.9} \times 100 = 15.15\% = \frac{\text{hardener mix}}{\text{resin mix}}$$

Dispensed catalyzed resin weight checks grams total 367.0 - 366.2 - 363.7 - 366.3 - 366.9. At 366.5 grams per 10 strokes the dispensing ratio is 108 strokes per gallon.

2105 hours - after mechanically repairing the resin solenoid valve, pouring was started.

2114 hours - slowed pumping rate down to 10 strokes in 20 seconds to prevent overflow in mold funnel.

2115 hours - slowed pumping to 10 strokes in 24 seconds

2122 hours - side A-C closed at 390 strokes

2133 hours - 650 strokes dispensed

2137 hours - 733 strokes dispensed

2142 hours - 870 strokes dispensed

2145 hours - 6 of 8 plexiglass panels closed

2159 hours - 1160 strokes dispensed

2200 hours - 1200 strokes dispensed

2202 hours - entire surface completely closed

2204 hours - 1400 strokes dispensed, stopped pouring

Total weight check from head - 366.2 grams separate weight checks both ports pumping together resin - 320.4 grams
hardener - - 48.1 grams

Pour went very smoothly, no bubbles except at outer periphery (beyond 9 1/2' diameter) 6/22/63 at 1200 hours rotation was stopped and the mold cover was removed to inspect the surface.

Figures L-1a through L-1i are reproductions of the various data sheets for Pour No. 10.

Pour No. 10

CHECK SHEET
CURRENT TO DRIVE TABLE MOTOR

Date: 6/20/63 START

NOTE: Continuously observe current readings & record every one-half hour.

Ref: PIR #3630-206

TIME	AMPS	BY	TIME	AMPS	BY	TIME	AMPS	BY	TIME	AMPS	BY	TIME	AMPS	BY
2100	7	HR.	0630	7	HR	1630	6.8	R.D.	0300	7	H.R.			
2130	7	HR	0700	7	HR	1700	6.8	R.D	0330	7	NR			
2200	7	HR.	0730	7	H.S	1730	6.8	R.D.	0400	7	NR			
2230	7	HR.	0800	7	H.S	1800	6.8	R.D.	0430	7	H.R			
2300	7	HR	0830	7	E.A	1830	6.8	R.D.	0500	7	HR			
2330	7	HR.	0900	7	E.A	1900	6.5	R.D.	0530	7	HR			
2400	7	HR.	0930	6.8	H.S.	1930	6.8	R.D.	0600	7	HR			
0030	7	HR	1000	6.8	E.A	2000	6.9	HR	0830	7	H.R.			
0100	7	HR.	1030	6.8	H.S	2130	7	HR	0700	7	HR			
0130	7	HR	1100	6.8	E.A	2200	7	HR	0730	7	HR			
0200	7	HR.	1130	6.8	E.A	2230	7	HR	0800	7	E.A			
0230	7	HR	1200	6.8	R.D.	2300	7	HR.	0830	7	E.A			
0300	7	HR	1230	7.0	R.D.	2330	7	HR	0900	7	E.A			
0330	7	HR	1300	7.0	E.A	2400	7	HR	0930	7	E.A			
0400	7	HR.	1400	6.8	H.S	0030	7	HR	1000	7	E.A			
0430	7	HR	1430	6.8	E.A	0100	7	HR	1030	7	E.A			
0500	7	HR.	1500	6.9	H.S.	0130	7	HR	1100	7	E.A			
0530	7	HR	1530	6.8	H.S.	0200	7	HR	1130	7	E.A			
0600	7	HR.	1600	6.8	R.D.	0230	7	HR	1200					

Figure L-1a. Copy of Pour No. 10 Data Sheet

CHECK SHEET

Ten (10) Consecutive Electronic Counter Readings

Pour No. 10

Date: 6/30/63

PAGE 1 OF 2

Hourly Cycle

NOMINAL READING IS 3.752 SECONDS/REVOLUTION

TIME	READINGS OF LAST TWO DIGITS												OPERATOR
2100	50	48	46	50	48	47	48	48	48	48			H. ROSENTHAL
2200	51	49	57	49	58	51	51	50	56	51			H.R.
2300	50	57	53	51	52	47	54	57	49	50			H.R.
2400	48	50	49	49	53	49	51	47	52	45			H.R.
0100	52	52	52	50	49	50	50	48	51	49			H.R.
0200	49	47	49	48	47	50	48	49	50	45			H.R.
0300	51	54	50	49	47	48	49	51	53	51			H.R.
0400	49	51	48	52	52	54	53	54	54	53			H.R.
0500	50	50	52	50	51	55	55	57	51	53			H.R.
0600	54	52	53	54	47	52	47	57	47	50			H.R.
0700	NO READINGS - NOT COUNTING SINGLE REVOLUTION COUNTS AS TIMES IN AIR GAP												
0800	49	49	51	51	55	53	49	51	51	50			
0900	53	55	58	57	53	60	54	57	57	57			H.S
1000	52	48	49	46	45	49	43	45	47	48			E.A
1100	52	56	54	51	51	53	50	50	50	49			H.S
1200	54	57	51	55	54	52	51	50	51	52			R.D.
1300	48	53	51	52	51	47	52	48	50	51			E.A.
1400	48	51	53	57	51	51	52	48	49	46			H.S
1500	54	50	57	54	50	48	52	48	45	49			H.S
1600	52	51	51	50	52	52	49	52	51	49			R.D.
1700	56	58	57	53	55	54	54	55	53	53			R.D.
1800	56	55	51	49	53	52	55	54	51	54			R.D.

START POUR OF

TRIGGER LEVEL ADJ. AT 8:25. READING GOOD + STEADY AFTER ADJUSTMENT

ADJ PST AT 10:43

ADJ. PST AT 0900 HRS

PST ADJ AT 11.00

Ref: PIR 6630-206

Figure L-1b. Copy of Pour No. 10 Data Sheet

CHECK SHEET

Ten (10) Consecutive Electronic Counter Readings

Hourly Cycle

Pour No. 10

Date: 6/21/63 AND 6/22/63

PAGE 2 OF 2

TIME	READINGS												OPERATOR
1900	51	53	49	52	52	53	49	50	50	49			R.D.
2000	52	48	53	52	50	54	52	55	57	49			H.R.
2100	51	54	52	54	51	51	46	48	50	50			H.R.
2200	52	47	49	45	49	46	53	52	47	55			H.R.
2300	50	51	52	49	45	49	47	47	48	49			H.R.
2400	56	54	55	51	54	52	53	53	56	53			H.R.
0100	54	55	52	52	56	53	51	53	54	53			H.R.
0200	52	55	51	53	56	56	57	56	56	50			H.R.
0300	50	50	48	48	53	46	48	53	47	50			H.R.
0400	52	49	52	47	46	51	47	46	50	50			H.R.
0500	50	51	48	47	51	49	47	48	50	52			H.R.
0600	51	52	54	53	51	51	46	53	51	52			H.R.
0700	53	55	54	52	51	48	52	50	50	54			H.R.
0800	48	52	48	52	47	49	52	55	51	53			E.A.
0900	55	54	51	53	54	53	51	51	48	49			E.A.
1000	54	49	53	53	55	55	58	54	55	53			E.A.
1100	52	54	52	52	56	53	53	54	51	54			E.A.
1200													
1300													
1400													
1500													
1600													

Ref: PIR 6630-206

Figure L-1c. Copy of Pour No. 10 Data Sheet

Date: 6/20/63

POUR #10

PAGE 1 OF 4

CHECK SHEET - INDICATOR DEFLECTION

One-Half Hour Cycle

TIME:	2100	2130	2200	2230	2300	2330	2400	0030	0100	0130
INDICATOR #1	.0005	.001	.0005	.0005	.0005	.0005	.0005	.0005	.0004	.0005
INDICATOR #2	.0005	.0015	.0008	.0005	.0006	.0006	.0006	.0005	.0007	.0005
OPERATOR	HR.	HR.	HR.	HR	HR.	HR.	HR.	HR.	HR.	HR

TIME:	2100	2130	2200	2230	2300	2330	2400	0030	0100	0130
INDICATOR #3	.0017	.0015	.0013	.002	.0018	.002	.002	.0018	.0002	.0018
INDICATOR #4	.0016	.0015	.0015	.0015	.0015	.0015	.0015	.0014	.0015	.0014
OPERATOR	HR.	HR	HR	HR.	HR.	HR.	HR.	HR.	HR	HR.

TIME:	0200	0230	0300	0330	0400	0430	0500	0530	0600	0630
INDICATOR #1	.0005	.0005	.0004	.0005	.0004	.0004	.0004	.0004	.0004	.0004
INDICATOR #2	.0005	.0005	.0005	.0006	.0005	.0005	.0005	.0005	.0006	.0008
OPERATOR	HR	HR	HR.	HR	HR	HR	HR.	HR.	HR	HR.

TIME:	0200	0230	0300	0330	0400	0430	0500	0530	0600	0630
INDICATOR #3	0018	0018	0017	.0017	.0018	.0018	002	0018	.0018	.0015
INDICATOR #4	.0015	.0015	.0015	.0016	.0015	.0015	.0016	.0016	.0016	.0014
OPERATOR	HR	HR.	HR.	HR.	HR.	HR.	HR	HR	HR	HR.

NOTE: [illegible]

DEFLECTIONS ARE IN INCHES

Figure L-1d. Copy of Pour No. 10 Data Sheet

2/16

Date: 6/21/63

Room 10

PAGE 2 OF 4

CHECK SHEET - INDICATOR DEFLECTION

One-Half Hour Cycles

TIME:	0700	0730	0800	0830	0900	0930	1000	1030	1100	1130
INDICATOR #1	.0004	.0004	.0004	.0004	.0004	.0004	.0004	.0004	.0004	.0004
INDICATOR #2	.0008	.0007	.0007	.0007	.0007	.0007	.0007	.0006	.0006	.0006
OPERATOR	HR.	H S	E A	E A	E A	H S	E A	H S	E A	E A

TIME:	0700	0730	0800	0830	0900	0930	1000	1030	1100	1130
INDICATOR #3	.0015	0015	.0017	.0017	.0017	.0016	.0016	.0017	.0017	.0017
INDICATOR #4	.0014	0013	.0015	.0013	.0013	.0013	.0013	.0012	.0012	.0013
OPERATOR	HR.	H S	E A	E A	E A	H S	E A	H S	E A	E A

TIME:	1200	1230	1300	1330	1400	1430	1500	1530	1600	1630
INDICATOR #1	.0004	.0004	.0004	.0004	.0004	.0004	.0004	.0004	.0004	.0004
INDICATOR #2	.0006	.0006	.0006	.0006	.0007	.0007	.0007	.0006	.0006	.0006
OPERATOR	R.D.	R.D.	E A	H S	E A	E A.	E A	R.D.	R.D.	R.D.

TIME:	1200	1230	1300	1330	1400	1430	1500	1530	1600	1630
INDICATOR #3	.0018	.0017	.0017	.0018	.0018	.0018	.0017	.0018	.0017	.0017
INDICATOR #4	.0012	.0013	.0015	.0013	.0015	.0014	.0014	.0014	.0014	.0015
OPERATOR	R.D.	R.D.	E A	H S	E A	E A	E A	R.D.	R.D.	R.D.

NOTE: Recorded [illegible]

Figure L-1e. Copy of Pour No. 10 Data Sheet

Date: 6/21/63 AND 6/22/63

CHECK SHEET - INDICATOR DEFLECTION

Pour: 10

One-Half Hour Cycle

PAGE 3 OF 4

TIME:	1700	1730	1800	1830	1900	1920	2000	2030	2100	2130
INDICATOR #1	0004	.0004	.0004	.0004	.0004	.0004	.0004	.0004	.0004	.0004
INDICATOR #2	.0006	.0006	.0006	.0006	.0006	.0006	.0006	.0006	.0006	.0006
OPERATOR	R.D.	R.D.	R.D.	R.D.	R.D.	R.D.	H.R.	H.R.	H.R.	H.R.

TIME:	1700	1730	1800	1830	1900	1930	2000	2030	2100	2130
INDICATOR #3	.0018	.0017	.0018	.0017	.0015	.0018	.0018	.0018	.0018	.0018
INDICATOR #4	.0015	.0015	.0015	.0014	.0015	.0015	.0015	.0015	.0015	.0015
OPERATOR	R.D.	R.D.	R.D.	R.D.	R.D.	R.D.	H.R.	H.R.	H.R.	H.R.

TIME:	2200	2230	2300	2330	2400	0030	0100	0130	0200	0230
INDICATOR #1	.0004	.0004	.0004	.0004	.0004	.0004	.0004	.0004	.0004	.0004
INDICATOR #2	.0006	.0006	.0006	.0006	.0005	.0005	.0005	.0005	.0006	.0006
OPERATOR	H.R.	H.R.	H.R.	H.R.	H.R.	H.R.	H.R.	H.R.	H.R.	H.R.

TIME:	2200	2230	2300	2330	2400	0030	0100	0130	0200	0230
INDICATOR #3	.0018	.0018	.0018	.0019	.0019	.0018	.0018	.0019	.0018	.0018
INDICATOR #4	.0015	.0015	.0015	.0015	.0015	.0015	.0015	.0015	.0015	.0015
OPERATOR	H.R.	H.R.	H.R.	H.R.	H.R.	H.R.	H.R.	H.R.	H.R.	H.R.

NOTE: Recorded ...

Figure L-1f. Copy of Pour No. 10 Data Sheet

Date: 6/22/63

CHECK SHEET - INDICATOR DEFLECTION

POUR 10

One-Half Hour Cycle

PAGE 4 OF 4

TIME:	0300	0330	0400	0430	0500	0530	0600	0630	0700	0730
INDICATOR #1	.0004	.0004	.0004	.0004	.0004	.0004	.0004	.0004	.0004	.0004
INDICATOR #2	.0006	.0006	.0006	.0006	.0006	.0006	.0006	.0006	.0006	.0006
OPERATOR	HR.	HR	HR	HR	HR	HR	HR	HR	HR.	HR.

TIME:	0300	0330	0400	0430	0500	0530	0600	0630	0700	0730
INDICATOR #3	.0018	.0018	.0018	.0018	.0018	.0018	.0018	.0018	.0018	.0018
INDICATOR #4	.0014	.0015	.0015	.0015	.0015	.0015	.0015	.0015	.0015	.0015
OPERATOR	HR.	HR.	HR	HR.	HR.	HR	HR	HR	HR	HR

TIME:	0800	0830	0900	0930	1000	1030	1100	1130	1200	1230
INDICATOR #1	.0004	.0004	.0004	.0004	.0004	.0004	.0003	.0004		
INDICATOR #2	.0007	.0007	.0006	.0006	.0006	.0006	.0006	.0006		
OPERATOR	EA	EA	EA	EA	EA	EA	EA			

TIME:	0800	0830	0900	0930	1000	1030	1100	1130	1200	1230
INDICATOR #3	.0016	.0017	.0017	.0017	.0017	.0017	.0016	.0017		
INDICATOR #4	.0013	.0013	.0014	.0013	.0014	.0015	.0013	.0013		
OPERATOR	EA	EA	EA	EA	EA	EA	EA			

NOTE: Recorded read

Figure L-1g. Copy of Pour No. 10 Data Sheet

CHECK SHEET

(2) HOUR CYCLE

Pour No. 10

Date: 6-20-63 START

a. Oil level of table bearings.

b. Pit ventilation.

c. Drive motor tachometer generator belts, pulleys and general operation of motor components in the pit.

d. Location of the Korfund shock absorber springs within the retainer housings.

TIME	REMARKS	OPERATOR
2100	OK	HR.
2300	OK	HR.
0100	OK	HR
0300	OK	HR.
0500	OK	HR
0700	OK	HR
0900	OK	EA
1100	OK	HR.
1300	O.K.	R.D.
1500	OK	EA
1700	O.K.	R.D.
1900	O.K.	R.D.
2100	OK.	HR.
2300	OK	HR
0100	OK	HR.
0300	OK	HR.
0500	OK	HR
0700	OK	HR
0900	OK	EA
1100	OK	EA

Ref. Dia #0030-206

Figure L-1h. Copy of Pour No. 10 Data Sheet

CHECK SHEET

Pour No. 10

Wet & Dry Bulb - Temperatures & Relative Humidity

Date: 6/20/63

Every 4 HRS.

TIME	TEMPERATURES WET	DRY	REL. HUMIDITY	OPERATOR
2100	62	72	57 %	W. Rowland
0100	61	71	56 %	W. Rowland
0500	62	70	64 %	W Rowland
0900	62	70	64 %	H.L.
1300	62	71	61 %	H.L.
1700	62	70	64 %	R.D.
2100	58	70	49 %	W.R.
0100	57	69	47 %	WR
0500	57	69	47 %	WR
0900	58	68	55 %	E H
1200	SHUT DOWN 6/22/63 1200 HOURS Ed Howard			

Ref. PIR 6630-296

Figure L-1i. Copy of Pour No. 10 Data Sheet

DISTRIBUTION LIST

A. Abeshaus	U1211	A. Kirpich	U2513
G. Bainton	U8604	J. Kulp	CCIF 7527
R. Beaton	U3046	D. Lee	M2107
W. Beacraft	U2443	R. Leithiser	U2513
F. Blake	U2443	H. G. Lorsch (5)	U2612
M. Braun	CH-1931B	J. MacDonald	CH-1924
B. H. Caldwell	U3032B	W. M. Meyers	U2612
A. Christensen	U3228	J. May	U3032
I. M. Clausen	M-4292	C. B. Mayforth	U2612
J. Cooper	M9129	D. Nymoens	U3020
D. Cuthbert	CCIF 7240	G. F. Oberrender	U3231
R. Delzell	M2453	R. Passman	M3030
P. Dick	M2101	T. Petty, Jr.	M7211
J. Doman	U2513	E. Ray	M7038
J. Duryea	CH-6405B	T. D. Riney	M7023F
C. F. Foster	U8604	A. Ringwood	M2112
R. Fuse	U4239	R. E. Roach	U2612
A. Gaetjens	M2418	R. Roberts	CH-6000A
J. J. Guy (5)	U2450	J. Rossmeisel	M2418
K. Graf	M2408	J. Seiler	M2418
K. Hansen	U4448	L. Shenker	U8604
N. Hauft	U3228	H. Smith	M2453
S. Heiman	CH-5412	K. Stadthaus	U3210
J. Heyda	M7023F	F. J. Schmidt	CH-6405
R. Hockridge	U8604	D. Tecca	U3228
E. Howe	U3210	L. Tyrrell	U2513
W. Jolitz	M2418	C. Valori	M4428
P. Juneau	U8604	A. Watts	M4228
D. Kerr	M3094	R. Woodruff	M2432
W. Kinsey	U3032E	C. Zvanut	U3206

R. Wansor
General Electric Company
Defense Products Operation
6607 W. 80th Street
Los Angeles, California

J. B. McMahon, Contract Administrator (6 + 1 set tissues)
Jet Propulsion Laboratory
California Institute of Technology
4800 Oak Grove Drive
Pasadena, California

GENERAL ELECTRIC

A Department of the Missile and Space Division